Spectral Analysis for Stochastic Models of Large-Scale Complex Dynamical Networks

by

Víctor Manuel Preciado

Ingeniero Industrial, Universidad de Extremadura (1999)
Diploma de Estudios Avanzados, Universidad de Extremadura (2002)

Submitted to the Department of Electrical Engineering and Computer Science
in partial fulfillment of the requirements for the degree of

Doctor of Philosophy

at the

MASSACHUSETTS INSTITUTE OF TECHNOLOGY

September 2008

Author .....
Department of Electrical Engineering and Computer Science
August 8, 2008

Certified by .....
George C. Verghese
Professor
Thesis Supervisor

Accepted by .....
Terry P. Orlando
Chairman, Department Committee on Graduate Students

Spectral Analysis for Stochastic Models of Large-Scale Complex Dynamical Networks

by

Víctor Manuel Preciado

Submitted to the Department of Electrical Engineering and Computer Science
on August 8, 2008, in partial fulfillment of the
requirements for the degree of
Doctor of Philosophy

Abstract

Research on large-scale complex networks has important applications in diverse systems of current interest, including the Internet, the World-Wide Web, social, biological, and chemical networks. The growing availability of massive databases, computing facilities, and reliable data analysis tools has provided a powerful framework to explore structural properties of such real-world networks. However, one cannot efficiently retrieve and store the exact or full topology for many large-scale networks. As an alternative, several stochastic network models have been proposed that attempt to capture essential characteristics of such complex topologies. Network researchers then use these stochastic models to generate topologies similar to the complex network of interest and use these topologies to test, for example, the behavior of dynamical processes in the network.

In general, the topological properties of a network are not directly evident in the behavior of dynamical processes running on it. On the other hand, the eigenvalue spectra of certain matricial representations of the network topology do relate quite directly to the behavior of many dynamical processes of interest, such as random walks, Markov processes, virus/rumor spreading, or synchronization of oscillators in a network.

This thesis studies spectral properties of popular stochastic network models proposed in recent years. In particular, we develop several methods to determine or estimate the spectral moments of these models. We also present a variety of techniques to extract relevant spectral information from a finite sequence of spectral moments. A range of numerical examples throughout the thesis confirms the efficacy of our approach. Our ultimate objective is to use such results to understand and predict the behavior of dynamical processes taking place in large-scale networks.

Thesis Supervisor: George C. Verghese
Title: Professor

Acknowledgments

First of all, I would like to express my greatest gratitude to my advisor, George Verghese, for all he has taught me and so kindly shared with me during these years at MIT. His refreshing ideas, vast memory of references and alternative paths whenever I hit a wall have made a great difference in my growth as a researcher. Apart from his technical expertise, George is an example of integrity and ethics, blended with a sharp sense of humor. To him I will always be thankful for the time, effort, and attention he has dedicated to me.

Next, I thank my thesis committee members, Professors Pablo Parrilo and Devavrat Shah, for so generously sharing their insights with me. Apart from our interactions at a research level, I feel very fortunate to have had the chance to interact with both of them as a class student and a teaching assistant. To them, I would like to express my deepest appreciation.

Apart from the thesis committee, I have had the privilege to interact with a distinguished group of educators at MIT. Among them I would like to voice my admiration of Professors Al Oppenheim, Munther Dahleh, Vincent Blondel, Alex Megretski, Al Willsky, Sanjoy Mitter, and Jean-Jacques Slotine. Their teachings, inside and outside the classroom, have been a constant source of motivation.

I also had the chance to discuss my research with an outstanding group of colleagues at the Laboratory for Information and Decision Systems (LIDS) and the Laboratory for Electromagnetic and Electronic Systems (LEES). I would specially like to thank Bill Richoux, Laura Zager, Tushar Parlikar, Vivian Mizuno, Faisal Kashif, Julien Hendrickx, Alex Olshevsky, and Raj Rao.

Over these years, I have gained an outstanding group of friends. Zahi, Patrick, Zeina, Ali, Demba, Alaa... My experience at MIT would not have been as enjoyable without them.

I would like to thank my parents, Candido and Catalina, and my siblings, Miguel, Paloma, Maria, and Guadalupe, for their love and support during all these years.

Lastly, I would especially like to thank my wife Farah for her unconditional love,

cheerfulness, care, and support. Farah, you are the most important person and a true blessing in my life. Thank you for all the joy we share together.

Last, I gratefully acknowledge the financial support extended to me by the La Caixa Foundation in Spain. I also wish to thank the Air Force Office for Scientific Research for partial support of my research under the AFOSR multi-university research initiative on "Architectures for Secure and Robust Distributed Infrastructures." I also have benefited from a number of semesters of financial support from the Electrical Engineering and Computer Science Department, through teaching and research assistantships.

Contents

Chapter 1

Introduction

Research in complex networks has important applications in today's massive networked systems, including the Internet, the World-Wide Web (WWW), as well as social, biological and chemical networks. The availability of massive databases, and reliable tools for data analysis provides a powerful framework to explore structural properties of large-scale real-world networks.

A complex network, in the context of this thesis, presents the following structural properties [59]:

(i) Large size: ranging from thousands to millions of nodes.

(ii) Sparse structure: the average number of edges connected to a node is typically small in comparison with the size of the network.

(iii) Absence of symmetries and regularities: there is no small lossless representation of the network structure (i.e., regular rings and lattices are, for example, not "complex" in the context of this thesis).

In general, these properties foreclose the possibility of efficiently retrieving and/or storing the exact structure of a complex network. In many complex networks, it is often possible to gather a great deal of information by examining random samples of the graph topology. These are usually samples of local properties, such as the degree distribution (number of connections per node). Network researchers then use these samples to generate topologies similar to the original complex network [131], [192],

and use these to test, for example, the behavior of dynamical processes within the network [115].

Many dynamical processes on networks, such as random walks [9], Markov processes [41], virus/rumor spreading [35], and synchronization of oscillators [160], are interesting to study in the context of large-scale complex networks. In general, the empirical measurements from the network are loosely related to the behavior of the dynamical processes under study. In this thesis we are interested in studying network properties that are more directly related to the dynamical behavior on the network. Many of these characteristics are intimately related to the eigenvalue spectra of the underlying graph structure.

Spectral graph theory studies the eigenvalues of matrices that embody the graph structure. One of the traditional objectives in spectral graph theory is to deduce structural characteristics of a graph from such eigenvalue spectra. Traditional application of the study of the graph spectra can be found in chemistry (for example, in molecular stability [18]), nuclear physics (models of the atomic nucleus [30]), and quantum mechanics [45].

This thesis studies spectral properties of popular stochastic graph models proposed in recent years. In particular, we develop several methods to determine the spectral moments of these stochastic graph models. We also present a variety of techniques to extract relevant spectral information from a given sequence of spectral moments. Our final objective is to use these results to understand and predict the behavior of dynamical processes taking place in large-scale networks.

1.1 Organization and Contributions

Chapter 2 motivates the usage of spectral graph theory to study dynamical processes taking place in networks. In this thesis we pay special attention to three dynamical processes that are highly representative: virus spreading, decentralized consensus, and

synchronization of oscillators. We show how the spectra of the adjacency, Laplacian and Kirchhoff matrices determine the behavior of these dynamical processes in the network.

Chapter 3 reviews probabilistic graph models of relevance in today's network research. We classify these models into two different categories of stochastic networks: static (also called off-line) models, and dynamic (also called evolving or on-line) models. A static model is defined as a random graph ensemble with a fixed number of nodes. Different ensembles capture different structural properties observed in a real network.

As an alternative to static random graphs, we review dynamic random graph models. In these models, the number of nodes increases with time. The most popular model in this category is the preferential attachment model proposed by Barabási and Albert [24]. This model aims to represent the forces driving the generation process of a given complex graph that evolves over time.

In **Chapter 4** we study the spectrum of static random graphs. We pay special attention to a model proposed by Chung and Lu [55], that prescribes a given expected degree sequence on the random graph ensemble. We deduce, for the first time, analytical expressions for the expected spectral moments of the adjacency matrix of the Chung-Lu random graph model as a function of the given expected degree sequence.

In **Chapter 5** we present a variety of techniques to deduce spectral properties of relevance from a given set of spectral moments. First, we show how to use Wigner's high-order moment method [203], to deduce bounds on the support of a spectral distribution. Second, we propose several alternatives for fitting a piecewise-linear function that preserves a given finite sequence of spectral moments. Third, we show how to use semidefinite programming to deduce optimal bounds for several spectral properties.

Chapter 6 is devoted to study the spectral moments of dynamically evolving random graphs. The spectral moments of dynamic random graphs evolve as the graph

grows. We study the evolution of the expected spectral moments of the adjacency matrix as the network grows. This evolution can be analytically solved in the case of the Barabási and Albert model (linear preferential attachment).

In **Chapter 7** we apply some of the techniques developed in Chapters 4 and 5 to the analysis of the spectral properties of alternative matrix representations of the graph structure. In particular, we study the eigenvalue distribution of Laplacian and Kirchhoff matrices. We derive analytical expressions for the first three spectral moments of these matrices for our random graph models. We apply the techniques introduced in Chapter 6 to study implications of our results in the behavior of several dynamical processes.

Chapter 8 is dedicated to drawing conclusions and suggestions for future work. We include preliminary results concerning the problem of spectral design and the analysis of directed networks. We also include open questions for future research.

1.2 Notes on the Literature

The work presented in this thesis lies in the intersection of graph theory, probability, matrix analysis, and dynamical systems. We recommend the following books for a general treatment of each of these fields. For an introduction to graph theory, we recommend the books by West [202], or Diestel [67]. For rigorous treatments of probability theory, see the books by Grimmett and Stirzaker [94], Karr [109], and Gut [96]. For a classic matrix analysis text, we refer to the books by Horn and Johnson [99], [100]. For a graduate-level exposition on linear systems and control theory, see the books by Kailath [108], or Sontag [185].

The research presented in this thesis is mainly focused on the spectral/algebraic analysis of random graph models of complex networks. We recommend the following books and research monographs for a research-level exposition:

1. There is a large literature on algebraic aspects of spectral graph theory, documented in references such as by Biggs [32], or Cvétkovic, et al. [65]. A more recent title by Godsil and Royle [91], is rewarding. Above all, we note the monograph by Chung, *Spectral Graph Theory* [54], which includes an extensive coverage of (normalized) Laplacian matrices.

2. For an in-depth study of random graph theory, we cite a highly technical book by Bollobás [37]. A more gentle introduction to this field can be found in the book by Janson, Luczak and Ruciński [103]. We also make use of the probabilistic methods presented in the book by Alon and Spencer [14].

3. The field of complex networks has experienced an impressive growth in recent years. For an exposition from the physicists' point of view, we recommend the compilation of papers by Newman et al. [151], as well as the monograph by Dorogovtsev and Mendes [70]. Also, we must highlight the monograph by Chung and Lu entitled *Complex Graphs and Networks* [59], which is the basis of a substantial part of our research. A rigorous analysis of dynamic random graphs is presented in a recent book by Durrett [72].

Chapter 2

Spectral Analysis of Dynamical Processes in Networks

The eigenvalue spectra of a graph provide valuable information about the behavior of many dynamical processes running within the graph. In this chapter, we introduce examples of these dynamical processes and illustrate how spectral graph theory arises as a fundamental tool to study their behavior. For each process, we transform the set of equations governing its dynamical behavior into a form involving matrices representing the network structure. We conclude the analysis of each process by illustrating how the eigenvalues of these matrices relate to the dynamics in the network. Our final objective is to establish a clear connection between the dynamical behavior of the network and the spectral properties of the underlying graph.

In our exposition, we make use of several basic elements of spectral graph theory (see [32] and [54] for a thorough exposition).

2.1 Preliminaries: Spectral Graph Theory

We first introduce basic graph-theoretic notation (see [206] or [202] for graph-theoretic terminology and results). We consider simple undirected graphs $G = (V, E)$ with n nodes, where V denotes the set of nodes, $\{1, ..., n\}$, and E denotes the set of edges of

G. If $(i,j) \in E$ is an edge of G, we say that nodes i and j are adjacent, and represent this as $i \sim j$. The degree of i, denoted by $d_G(i)$ or d_i, is the number of nodes adjacent to node i in G. The degree sequence of G is given by $\mathbf{d}_G = \{d_G(i), i \in V\}$, where the sequence is usually given in monotonically non-increasing order. It is often convenient to represent the degree sequence as a degree distribution. The degree distribution of G is given by $\mathbf{r}_G = \{r_G(0), r_G(1), r_G(2), ...\}$, where $r_G(k)$ denotes the number of nodes with degree k in G (we also denote $r_G(k)$ by r_k).

It is often convenient to represent graphs via matrices. There are several choices for such a representation for a graph with n nodes or vertices. The adjacency matrix of an undirected graph G, denoted by $A_G = [a_{ij}]$, is an $n \times n$ matrix defined entry-wise as $a_{ij} = 1$ if nodes i and j are adjacent (i.e., connected by an edge), and $a_{ij} = 0$ otherwise; thus, A_G is symmetric for an undirected graph. In this thesis, we consider simple graphs with no self-loops; thus, we have that $a_{ii} = 0$ for all i.

The degree of node i, denoted by d_i, is the number of edges attached (or incident) to it. The degree can be written in terms of the adjacency entries as $d_i = \sum_j a_{ij}$. We can arrange the set of degrees on a diagonal matrix to yield the degree matrix, $D_G \triangleq diag(d_i)$.

The *Laplacian matrix* is defined in terms of the degree and adjacency matrices, D_G and A_G, as $\mathcal{L}_G = I_n - D_G^{-1/2} A_G D_G^{-1/2}$. The eigenvalue spectrum of the Laplacian matrix has applications in rapidly mixing Markov chains [8], [9], randomized approximation algorithms [197], and in the analysis of the dynamical behavior of many decentralized network algorithms.

The *Kirchhoff matrix* K_G of a graph G (also known as the combinatorial Laplacian) is defined as $K_G = D_G - A_G$ (this matrix was originally proposed by Gustav Kirchhoff in the context of the matrix tree theorem [112]). The Kirchhoff matrix, also called combinatorial Laplacian, arises in combinatorial problems [141], and in the analysis of random walks and electrical circuits [71]. The Kirchhoff eigenvalue spectrum contains useful structural information about, for example, the number of

spanning trees in G, or the stability of synchronization of a network of nonlinear oscillators [160].

We denote by $\{\lambda_i(A_G)\}_{i=1,...,n}$, $\{\lambda_i(\mathcal{L}_G)\}_{i=1,...,n}$, and $\{\lambda_i(K_G)\}_{i=1,...,n}$ the set of eigenvalues of the adjacency, Laplacian, and the Kirchhoff matrices, respectively (where the sequence of eigenvalues is ordered in non-increasing order, i.e. $\lambda_1 \leq \lambda_2 \leq ... \leq \lambda_n$). The following are some relevant properties concerning these eigenvalues [54]:

1. Both K_G and $\mathcal{L}_G$ have at least one eigenvalue at 0 (called the trivial eigenvalue) with associated eigenvectors $\mathbf{1} = [1, 1, ..., 1]^T$ and $\mathbf{d}^{1/2} = [d_1^{1/2}, d_2^{1/2}, ..., d_n^{1/2}]^T$, respectively. The multiplicity of the trivial eigenvalue equals the number of connected components of the graph G.

2. For undirected graphs, A_G, K_G and $\mathcal{L}_G$ are real symmetric matrices [32]. Consequently, all three matrices have all real eigenvalues and a full set of n real and orthogonal eigenvectors. Furthermore, K_G and $\mathcal{L}_G$ are positive semidefinite, so all their eigenvalues are non-negative.

3. All the eigenvalues of the Laplacian $\mathcal{L}_G$ fall into the interval $[0, 2]$. (This can be shown by applying Gershgorin's circle theorem to the rows of $\mathcal{L}_G$.) Similarly, the eigenvalues of the Kirchhoff matrix K_G fall within the interval $[0, 2\,d_{\max}]$, where $d_{\max} = \max_i d_i$.

2.2 Spectral Analysis of Dynamical Processes

In this section we study a series of dynamical processes run on networks. In these examples, the eigenvalue spectra of the underlying graph topology play a central role. Although we describe very specific processes, each one of them represents of a wide family of processes sharing a similar mathematical structure. We have chosen the following processes for our illustrations:

(i) virus spreading in a social network,

(ii) distributed consensus in a network of agents, and

(iii) synchronization of nonlinear oscillators connected via a network of 'resistors'.

We explicitly show how the eigenvalue spectra of respectively the adjacency, the Laplacian, and the Kirchhoff matrices are relevant in the analysis of the dynamics of these processes.

2.2.1 Virus Spreading

The spreading of a virus in human populations is closely related to the network of interactions within the population. In this section, we briefly review an automaton model for interactions of individuals that is well-suited for capturing a specific network of interactions among individuals. This model was proposed and analyzed in [200], where the authors established a connection between the existence of an epidemic outbreak and the eigenvalues of the adjacency matrix of social interactions. In this automaton model, each node represents an individual that is either infected or susceptible to infection. A virus can spread from one node to another only along the edges of G. This model involves several parameters. First, the infection rate β represents the probability of a virus at an infected node i spreading to another node j during a time step. Also, we denote by δ the probability of recovery of any infected node at each time step. For simplicity, we consider β and δ to be constants for all individuals in G.

We denote by $p_i[k]$ the probability that node i is infected at time k. The evolution of the probability of infection can be modeled using the following difference equation:

$$p_i[k+1] = [1 - \prod_{j \in \mathcal{N}_i} (1 - \beta p_j[k])] + (1 - \delta) p_i[k] \tag{2.1}$$

where $\mathcal{N}_i$ denotes the set of nodes adjacent to node i. Assuming that $\beta p_j[k] \ll 1$, the quantity $1 - \prod_{j \in \mathcal{N}_i} (1 - \beta p_j[k])$ can be approximated by $\sum_j \beta p_j[k]$. Thus, we

can linearize Eqn. (2.1) and write the resulting system of linear equations in matrix form as:

$$\mathbf{p}[k+1] = (\Delta + \beta A)\,\mathbf{p}[k], \tag{2.2}$$

where A is the adjacency matrix of the graph of interactions, $\Delta = diag(1-\delta)$, and $\mathbf{p}[k] = [p_1[k], p_2[k], ..., p_n[k]]^T$, where n is the number of nodes in the network. Thus, the largest eigenvalue of the matrix $(\Delta + \beta A)$ (denoted by $\lambda_{\max}(\Delta + \beta A)$) governs the spreading rate of the virus near a disease-free equilibrium. In particular, the condition for a small initial infection to die out is $|\lambda_{\max}(\Delta + \beta A)| < 1$. One can write this condition in terms of the maximum eigenvalue of the adjacency matrix as:

$$\lambda_{\max}(A) < \frac{\delta}{\beta}. \tag{2.3}$$

In conclusion, the spectral radius of the adjacency matrix of the social network determines whether or not an epidemic dies out in this model. There are other spreading processes that can be analyzed in a similar way [95], [41], [177].

2.2.2 Distributed Consensus

We illustrate the dynamics of a distributed consensus protocol by considering a network of n agents located at the nodes of a connected graph G. Associated with the i-th agent, there is a positive scalar variable, m_i (representing, for example, the temperature measured by a sensor). A consensus protocol aims to compute the average value of the set of n measurements, i.e., $\bar{x} = \sum_i m_i/n$. In a distributed consensus protocol, these agents can share information solely through the edges of G. In other words, none of the agents has access to the whole set of measurements. Under these constrains, the objective of the distributed consensus is to estimate the value of $\bar{x}$ in an iterative manner. Distributed consensus protocols have a broad range of applications including congestion control in communication networks [156], flocking of

dynamic agents [170], or formation control of unmanned vehicles, [153].

In this subsection, we discuss the specific case of a linear distributed consensus protocol in a bidirectional network with zero communication delay. This protocol is defined by the following set of linear discrete-time difference equations:

$$x_i[k+1] = \frac{1}{d_i} \sum_{j \in \mathcal{N}_i} \left(x_j[k] - x_i[k] \right), \text{ for } i = 1, 2, ..., n, \tag{2.4}$$

where d_i denotes the degree of node i. The initial conditions, $x_i[0]$ for $i = 1, ..., n$, are equal to the original set of distributed measurements, m_i. After a transient period, the iterated variables, $x_i[k]$, tend to the initial average value $\bar{x}$.

We can write the discrete-time Eqn. (2.4) in matrix form as:

$$\mathbf{x}[k+1] = \left(D^{-1}A \right) \mathbf{x}[k],$$

where $\mathbf{x}[k] = [x_1[k], x_2[k], ..., x_n[k]]^T$ and $D = diag(d_i)$. Thus, the dynamics of this linear protocol is ruled by the eigenvalues of $D^{-1}A$. For a connected graph, we have that $D^{-1}A\mathbf{1} = D^{-1}\mathbf{d} = \mathbf{1}$, where $\mathbf{1} = [1, 1, ..., 1]^T$ and $\mathbf{d} = [d_1, d_2, ..., d_n]^T$. Thus, the uniform vector $\mathbf{1}$ is an eigenvector of $(D^{-1}A)$ with associated eigenvalue 1 (which we denote as the trivial eigenvalue). Also, one can prove that for any set of initial conditions, $\{m_i : m_i \geq 0,\ i = 1, ..., n\}$, the iterations of the vector $\mathbf{x}[k]$ tend asymptotically to $\bar{x}\,\mathbf{1}$ if and only if the absolute value of the non-trivial eigenvalues of $D^{-1}A$ are all strictly less than 1. We can state this condition in terms of the eigenvalues of the Laplacian matrix, $\mathcal{L}_G$. First, we denote by σ_i and $\mathbf{u}_i$ the set of eigenvalues and eigenvectors of $(D^{-1}A)$, respectively (i.e., $(D^{-1}A)\,\mathbf{u}_i = \sigma_i\,\mathbf{u}_i$). For each eigenvector $\mathbf{u}_i$, we define a vector $\mathbf{v}_i = D^{1/2}\mathbf{u}_i$. We can then transform the

eigenvalue equation for $\mathbf{u}_i$ as follows:

$$\begin{aligned} D^{-1/2}A\,\mathbf{u}_i &= D^{-1/2}\sigma_i\,\mathbf{u}_i \\ D^{-1/2}AD^{-1/2}\,\mathbf{v}_i &= \sigma_i\,\mathbf{v}_i, \\ \left(I - D^{-1/2}AD^{-1/2}\right)\,\mathbf{v}_i &= (1-\sigma_i)\,\mathbf{v}_i, \\ \mathcal{L}_G\,\mathbf{v}_i &= (1-\sigma_i)\,\mathbf{v}_i, \end{aligned}$$

In other words, $\lambda_i \triangleq 1 - \sigma_i$, $i = 1, ..., n$, are the (real) eigenvalues of the (symmetric) Laplacian matrix, $\mathcal{L}_G$, with associated eigenvectors $\mathbf{v}_i$. Therefore, the condition $|\sigma_i| < 1$ for $i = 2, ..., n$ is equivalent to:

$$\lambda_i\left(\mathcal{L}_G\right) \in (0, 2)\,, \text{ for } i = 2, ..., n.$$

2.2.3 Synchronization of Nonlinear Oscillators

The phenomenon of synchronization of a network of identical oscillators has been thoroughly studied in many scientific fields [190], [161], [196]. In this section, we establish a connection between the stability of synchronization of a network of oscillators and the eigenvalue spectrum of the associated Kirchhoff matrix.

Several techniques have been proposed to analyze the synchronization of coupled oscillators. These include the master stability function approach [160] (extensively used in the physicist literature), passivity analysis [207], Lyapunov-based methods [208], and contraction analysis [182]. In [207], the author extends well-known results in control theory, such as the passivity criterion, the circle criterion, and a result on observer design of Lipschitz nonlinear systems, to global synchronization criteria on coupled arrays of identical nonlinear systems. In [182], the authors use partial contraction theory to derive sufficient conditions for global synchronization of a network of nonlinear oscillators. In this thesis we pay special attention to the master stability function approach [160]. As we explain below, this approach provides a criterion for

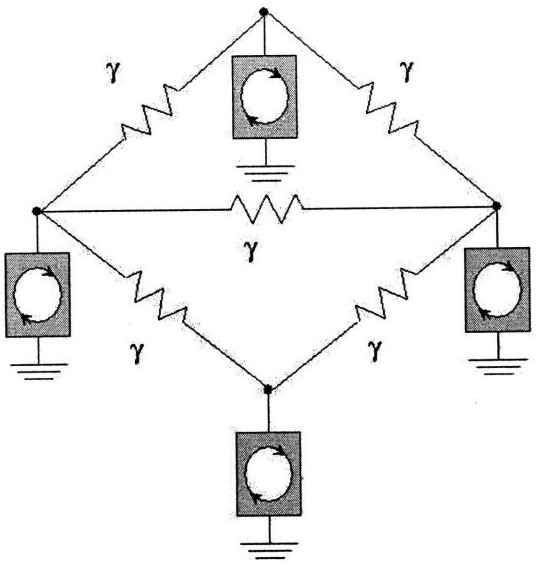

$$K_G = \begin{bmatrix} 2 & -1 & 0 & -1 \\ -1 & 3 & -1 & -1 \\ 0 & -1 & 2 & -1 \\ -1 & -1 & -1 & 3 \end{bmatrix}$$

Figure 2-1: A network of identical oscillators connected through identical resistors with admittance γ.

local stability of synchronization around the synchronization manifold based on the numerical computation of Lyapunov exponents. Even though quite different in nature, all these techniques note the key role played by the graph eigenvalue spectrum.

Consider a collection of n identical nonlinear oscillators, each one placed at the node of a graph G. Each oscillator is described by a d-dimensional system of first-order differential equations. We denote by $\mathbf{x}_i(t)$ the d-dimensional state vector associated with the oscillator in node i at time t. We shall usually drop the argument for notational simplicity, and simply write the state as $\mathbf{x}_i$. The dynamics of the i-th oscillator in isolation is described by the nonlinear differential equation $\dot{\mathbf{x}}_i = \mathbf{f}(\mathbf{x}_i)$. We now connect the collection of oscillators through a network of identical 'resistors' placed along the edges of the graph G. The set of differential equations describing the evolution of our network of oscillators is

$$\dot{\mathbf{x}}_i = \mathbf{f}(\mathbf{x}_i) + \gamma \sum_{j=1}^{N} a_{ij} \Gamma (\mathbf{x}_j - \mathbf{x}_i), \ 1 \leq i \leq n, \tag{2.5}$$

where the $d \times d$ real matrix Γ represents how states in neighboring oscillators are linearly combined through a link, the a_{ij} are the entries of the adjacency matrix A_G,

and the positive scalar γ can be interpreted as a global coupling strength. Since the degree $d_i = \sum_{j=1}^{n} a_{ij}$, we can rewrite Eqn. (2.5) as:

$$\begin{aligned} \dot{\mathbf{x}}_i &= \mathbf{f}(\mathbf{x}_i) + \gamma \left(\sum_{j=1}^{n} a_{ij} \Gamma \mathbf{x}_j - d_i \Gamma \mathbf{x}_i \right) \\ &= \mathbf{f}(\mathbf{x}_i) - \gamma \Gamma \sum_{j=1}^{n} k_{ij} \mathbf{x}_j, \end{aligned} \tag{2.6}$$

where the k_{ij} are the entries of the Kirchhoff matrix K_G, i.e., $k_{ii} = d_i$, and $k_{ij} = -a_{ij}$ for $j \neq i$.

We now analyze the dynamical behavior of Eqn. (2.6). We denote by $\phi(t; \mathbf{x}_0)$ the periodic solution to the ODE describing the isolated oscillator, $\dot{\mathbf{x}} = \mathbf{f}(\mathbf{x})$, with suitably chosen initial condition $\mathbf{x}(0) = \mathbf{x}_0$. Consider the dynamics of Eqn. (2.6) when $\mathbf{x}_i(0) = \mathbf{x}_0$ for all i. In this case, each oscillator in the network behaves as if in isolation, i.e., $\mathbf{x}_i(t) = \phi(t; \mathbf{x}_0)$ for $i = 1, ..., n$. We would like to answer the following question: Would the state vector of each oscillator, $\mathbf{x}_i(t)$, converge to the trajectory $\phi(t; \mathbf{x}_0)$ if we slightly perturb the initial conditions, $\mathbf{x}_i(0) = \mathbf{x}_0 + \varepsilon_i$, for $\|\varepsilon_i\|$ sufficiently small? We present the answer to this question next, referring to [160] for a detailed derivation.

We first define an error variable, $\eta_i(t) = \mathbf{x}_i(t) - \phi(t; \mathbf{x}_0)$, which represents the deviation of $x_i(t)$ from the periodic trajectory $\phi(t; \mathbf{x}_0)$. We assume these deviations are small. Assemble these vectors into the nd-dimensional vector $\eta(t) = \left[\eta_1^T(t), ..., \eta_n^T(t)\right]^T$. Now define the linear change of variables, $\xi := (V \otimes I)^{-1} \eta$, where V is the matrix that diagonalizes K_G, i.e., $\Lambda := diag(\lambda_i(K_G)) = V^{-1} K_G V$ (and $\otimes$ is the Kronecker product; see Appendix A for a brief review). It can then be shown that a linearized model for ξ can be written in terms of blocks of $d \times d$ matrices as

follows:

$$\dot{\xi} = \begin{bmatrix} \mathbf{Df}(t) - \gamma\lambda_1\Gamma & \mathbf{0} & \cdots & \mathbf{0} \\ \mathbf{0} & \mathbf{Df}(t) - \gamma\lambda_2\Gamma & \ddots & \mathbf{0} \\ \vdots & \ddots & \ddots & \vdots \\ \mathbf{0} & \mathbf{0} & \cdots & \mathbf{Df}(t) - \gamma\lambda_n\Gamma \end{bmatrix} \xi,$$

where $\mathbf{Df}(t)$ is the Jacobian of $\mathbf{f}(\mathbf{x})$ evaluated along the periodic trajectory $\phi(t; \mathbf{x}_0)$. The block diagonal structure of the above equation allows us to decouple this system of ODEs as follows:

$$\dot{\xi}_i = [\mathbf{Df}(t) + (\gamma\lambda_i)\,\Gamma]\,\xi_i, \text{ for } i = 1, 2, ..., n. \tag{2.7}$$

Observe that the d-dimensional ODE in Eqn. (2.7) is linear time-periodic (LTP). We want to study whether the dynamical evolution of each oscillator, $\mathbf{x}_i(t)$, tends to the stable orbit $\phi(t; \mathbf{x}_0)$. In other words, we want to study the stability of the LTP ODE's in Eqn. (2.7). This problem can be solved applying the theory of stability of periodic motions [77]. A classical criterion for the stability of Eqn. (2.7) is based on the maximal non-trivial Floquet exponent, a real number uniquely determined by the time-periodic matrix in (2.7), and measuring the maximum exponential rate of divergence of two solutions of Eqn. (2.7) with different, but close, initial conditions. For most LTP differential equations, the maximal Floquet exponent does not have a closed-form solution, although it can be efficiently approximated by numerical methods [50]. Based on the theory of LTP systems [77], the ODE in (2.7) is asymptotically stable if and only if the maximal non-trivial Floquet exponent is negative.

We now apply this result to a slightly modified version of Eqn. (2.7):

$$\dot{\xi} = [\mathbf{Df}(t) + \sigma\Gamma]\,\xi, \tag{2.8}$$

where we have substituted $\gamma\lambda_i$ in Eqn. (2.7) by σ. For a given value of σ, one can compute the maximum non-trivial Floquet exponent. The *Master Stability Function*

(MSF) proposed in [160] is defined as the maximal Floquet exponent of Eqn. (2.8) as a function of the real parameter σ. We denote this function by $F(\sigma)$. Again, one generally cannot derive an analytical expression for the MSF of an LTP differential equation, although in most cases one can approximate this function by numerical means at a set of points discretizing an interval of interest .

In the following example, we compute the MSF and illustrate how it can be used to analyze the stability of synchronization in a network of nonlinear oscillators. We study a network of Rössler[1] oscillators in our example.

Example Study the stability of synchronization of a ring of 6 coupled Rössler oscillators [173]. The dynamics of each oscillator is described by the following system of three nonlinear differential equations:

$$\begin{aligned} \dot{x}_i &= -(y_i + z_i), \\ \dot{y}_i &= x_i + a\, y_i, \\ \dot{z}_i &= b + z_i\,(x_i - c). \end{aligned}$$

The adjacency entries, a_{ij}, of a ring graph of six nodes are $a_{i,j} = 1$ if $j \in \{(i+1) \bmod 6, (i-1) \bmod 6\}$, for $i = 1, 2, ..., 6$, and $a_{ij} = 0$ otherwise. The dynamics of this ring of oscillators are defined by:

$$\begin{bmatrix} \dot{x}_i \\ \dot{y}_i \\ \dot{z}_i \end{bmatrix} = \begin{bmatrix} -(y_i + z_i) \\ x_i + a\, y_i \\ b + z_i\,(x_i - c) \end{bmatrix} + \gamma \sum_{j \in R(i)} \begin{bmatrix} 1 & 0 & 0 \\ 0 & 0 & 0 \\ 0 & 0 & 0 \end{bmatrix} \left(\begin{bmatrix} x_j \\ y_j \\ z_j \end{bmatrix} - \begin{bmatrix} x_i \\ y_i \\ z_i \end{bmatrix} \right) \tag{2.9}$$

where we have chosen to connect the oscillators through their x_i states exclusively. Our choice is reflected in the structure of the 3×3 matrix, Γ, inside the summation in Eqn. (2.9).

[1]The Rössler oscillator was proposed to model the kinematics of a type of chemical reaction and it is known to be one of the simplest systems able to present chaotic behavior.

Numerical simulations of an isolated Rössler oscillator unveil the existence of a periodic trajectory with period $T = 5.749$ when the parameters in Eqn. (2.9) take the values $a = 0.2$, $b = 0.2$, and $c = 2.5$ (see Fig. 2-2). We denote this periodic trajectory by $\phi(t) = [\phi_x(t), \phi_y(t), \phi_z(t)]$. In our specific case, the LTP differential equation (2.8) takes the following form:

$$\dot{\xi} = \left(\begin{bmatrix} 0 & -1 & -1 \\ 1 & a & 0 \\ \phi_z(t) & 0 & c \end{bmatrix} + \sigma \begin{bmatrix} 1 & 0 & 0 \\ 0 & 0 & 0 \\ 0 & 0 & 0 \end{bmatrix} \right) \xi, \tag{2.10}$$

where the leftmost matrix in the above equation represents the Jacobian of the isolated Rössler evaluated along the periodic trajectory $\phi(t)$, and the rightmost matrix represents Γ.

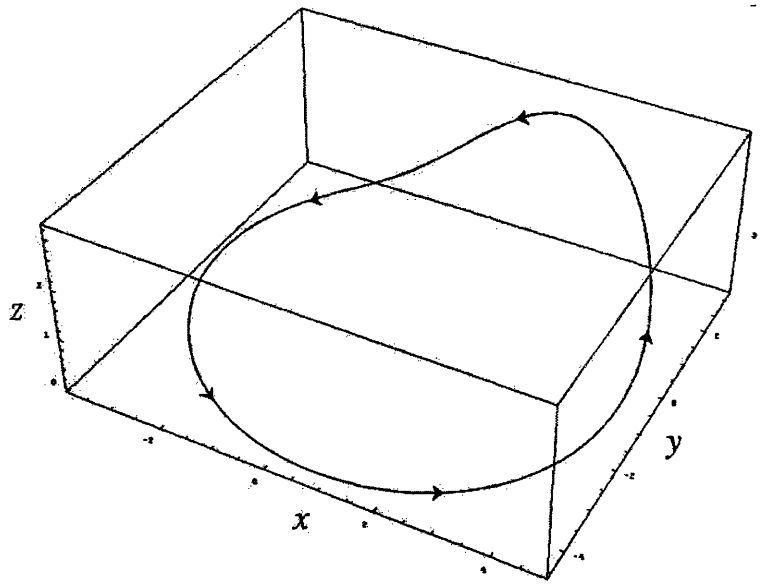

Figure 2-2: Periodic orbit of a Rössler oscillator in the x-y-z state space.

In Fig. 2-3, we plot the numerical values of the maximum Floquet exponent of Eqn. (2.10) for $\sigma \in [0, 15]$, discretizing at intervals of length 0.2. This plot shows the range in which the maximal Floquet exponent is negative. This range of stability is $S = (0, \sigma^*)$, for $\sigma^* \approx 4.7$. The MSF approach provides a criterion for local stability of the synchronization of the network of identical oscillators. This criterion,

introduced in [160], states that the synchronization is locally stable if the set of values $\{\gamma\lambda_i$, for $i = 1, ..., n\}$ lies inside the stability range, S. For the case of a 6-ring configuration, the eigenvalues of K_G are $0, 1, 1, 3, 3, 4$, so the set $\{\gamma\lambda_i$, for $i = 1, ..., n\}$ is $\{0, \gamma, \gamma, 3\gamma, 3\gamma, 4\gamma\}$. Therefore, we achieve stability for $\gamma \in (0, \sigma^*/\lambda_{\max}(K)) \equiv B$, where in our case $\sigma^*/\lambda_{\max}(K) \approx 1.175$.

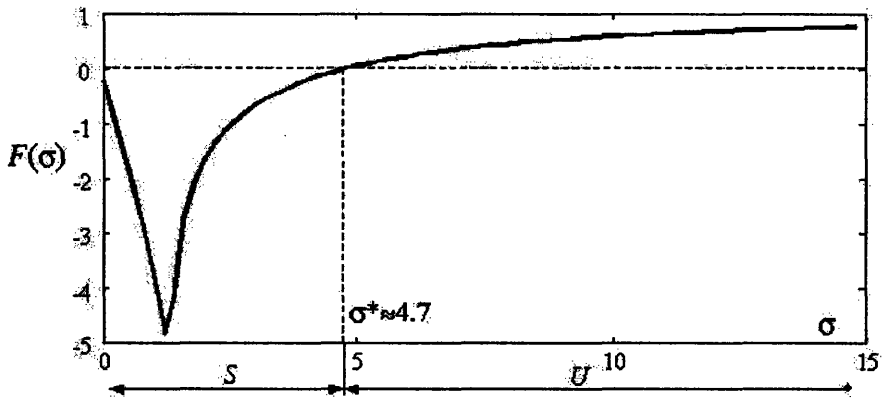

Figure 2-3: Numerical sweep of the maximal Floquet exponent in a periodic Rössler oscillator.

We now illustrate this result with several numerical simulations. First, we plot in Fig. 2-4 the temporal evolution of the x_i states of the 6-ring when $\gamma = 1.0$. Observe how, since $\gamma \in B$, we achieve asymptotic synchronization. On the other hand, if we choose $\gamma = 1.3 \notin B$, the time evolution of the set of oscillators does not converge to a common trajectory (see Fig. 2-5); instead, the even and odd nodes settle into two different trajectories

In conclusion, we can use the MSF, $F(\sigma)$, and the set of Kirchhoff eigenvalues, $\{\lambda_i(K_G)\}$, to study the stability of synchronization in networks of identical nonlinear oscillators. According to the MSF approach, the dynamics of the oscillator in isolation $\mathbf{f}(\mathbf{x})$, and the type of coupling Γ, define a region of stability, S. In most cases, this region, S, can be determined by numerical methods, independently of the graph topology. In order to achieve synchronization, the set $\{\gamma\lambda_i(K_G),\ i = 2, ..., n\}$ must lie in S.

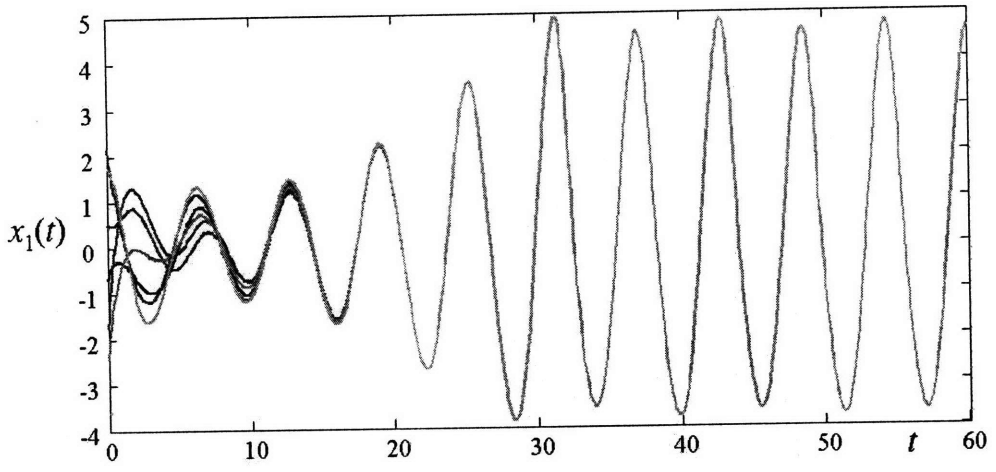

Figure 2-4: Temporal evolution of $x_i\,(t)$ in the ring, for $i = 1, 2, ..., 6$, with $\gamma \in B$.

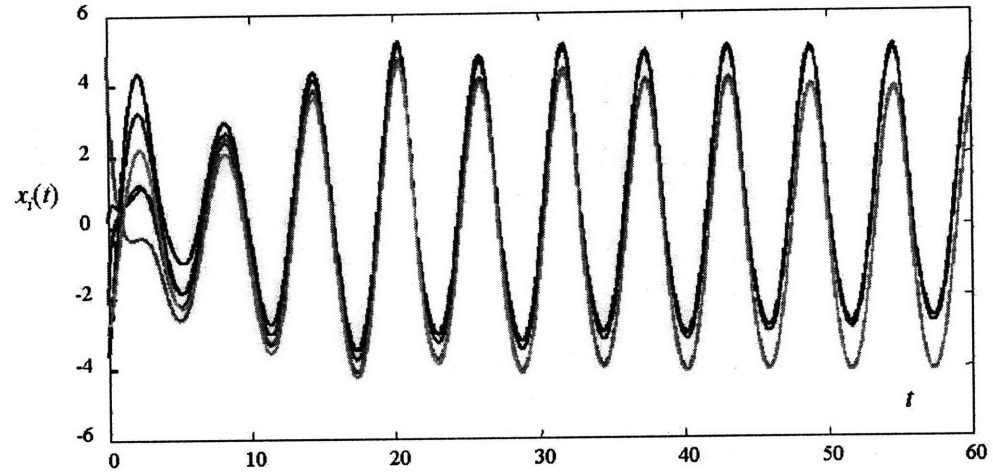

Figure 2-5: Temporal evolution of a ring of 6 Rösslers for $\gamma = 1.3 \notin B$.

2.3 Spectral Analysis of Structural Properties

Eigenvalue spectra are also related to structural properties of the graph. In this section we enumerate results relating structural properties of a graph to the eigenvalues of matrices representing the graph structure.

2.3.1 Graph Partitioning

Spectral methods have been widely used for graph bipartition [40]. To understand the basis of this method, it is useful to analyze the spectral properties of a graph, G_2, composed of two disjoint components. According to the properties introduced at the end of Section 2.1, G_2 has two zero Kirchhoff eigenvalues. In other words, the second-smallest eigenvalue of the Kirchhoff matrix, $\lambda_2(K_{G_2})$, is zero. Furthermore, the eigenvectors, $\mathbf{v}_2 = [v_1^{(2)}, ..., v_n^{(2)}]$, associated with $\lambda_2(K_G)$ satisfy $v_i^{(2)} = v_j^{(2)}$ when the nodes i and j are in the same component. This provides us with a clear criterion to partition the graph into two disconnected components.

Loosely speaking, a connected graph with a 'small' second-smallest Kirchhoff eigenvalue $\lambda_2(K_G)$ may be considered as being 'close' to separable into two disconnected components, and will therefore have a relatively 'clean' bipartition. Examination of any eigenvector associated with $\lambda_2(K_G)$ in this case will show entries clustered around one of two values, and this guides the bipartition. In general, the smaller the $\lambda_2(K_G)$, the smaller the relative number of edges whose removal is required to perform a bipartition.

The isoperimetric constant (also called Cheeger constant) of a graph is very relevant to graph bipartitioning. A graph bipartition is defined by a set of edges that, when removed, partitions the graph into two disconnected components, S_1 and S_2. We denote by $E(S_1, S_2)$ the set of edges involved in the partition. Considering all the possible bipartitions of the graph, the Cheeger constant, $h(G)$, is defined as:

$$h(G) := \min_{(S_1,S_2)} \frac{|E(S_1, S_2)|}{\min\{|S_1|, |S_2|\}}.$$

The Cheeger inequality relates the Cheeger constant and the second-smallest Laplacian eigenvalue as follows [54]:

$$2h(G) \geq \lambda_2(\mathcal{L}_G) \geq \frac{h^2(G)}{2}.$$

2.3.2 Matrix-Tree Theorem

The first articulation of a relationship between graph spectra and topological properties can be traced back to Gustav Kirchhoff's matrix-tree theorem [112], a classical result that provides the number of spanning trees in a graph.

Theorem 2.3.1 *Given a connected graph G with n vertices, let $0 < \lambda_2(K_G) \leq ... \leq \lambda_n(K_G)$ be the non-trivial eigenvalues of the Kirchhoff matrix of G. Then, the number of spanning trees of G is*

$$T(G) = \frac{1}{n} \prod_{s=2}^{n} \lambda_s(K_G).$$

As a conclusion, we have illustrated in this chapter how spectral graph theory arises as a fundamental tool to study graph structure as well as the dynamical behavior of many processes running within a network. We now turn to present several stochastic models of large-scale complex networks. Our final aim is to study the spectral properties of these models in order to predict the dynamical behavior of many processes taking place in complex networks.

Chapter 3

Stochastic Modeling of Large-Scale Complex Networks

In Chapter 2, we introduced several dynamical processes running on networks. We are interested in studying the behavior of these processes in large-scale complex networks. Recent mathematical work in network modeling has been driven by empirical observation; hence, we begin by presenting several popular network data sets. In order to extract valuable information, we also discuss common metrics quantifying network properties.

We then present several popular random graph ensembles to model complex topologies. We classify these stochastic graphs in two categories: static models and dynamic models. In a static model, the stochastic graph has a fixed number of nodes over which we define a random graph ensemble (i.e., a set of graphs with n nodes together with a probability distribution defined on them). In dynamic models, the number of nodes in the network varies over time, and edges are added (and/or deleted) according to a set of probabilistic rules, at each time interval.

There are many review articles [7], [123], [148], and books [133], [59], [72], on random graph models of complex networks. In this chapter, we cover some of the most popular of them. In later chapters, we deduce properties of the eigenvalue spectra of some of these stochastic models. We shall also analyze the behavior of

dynamical processes run on complex networks.

3.1 Complex Networks: Data Sets

Much of the recent mathematical work in network modeling has been driven by empirical observations in real networks. For example, the comparative analyses presented in the groundbreaking papers [201], [189], and [150] have inspired much of the recent work in the area. In this section, we briefly present some relevant data sets in order to motivate some of the random graph models of substantial impact in today's literature. Here, we divide our data sets into four categories: technological networks, information networks, social networks, and biological networks. (The boundaries of these categories are quite flexible, and it is possible to classify the same network into several categories.)

3.1.1 Technological Networks: The Internet

A technological network is an artificial infrastructure designed and constructed for the efficient distribution of a resource. We pay special attention to the distribution of information packets in the Internet at the level of Autonomous Systems (ASes). An AS is a group of routers under the control of a single entity. Examples of ASes are universities, research centers, or Internet Service Providers (ISP's). In this context, the nodes represent routers yielding the physical infrastructure of an ISP, and the edges represent communication links among ASes. Several useful sources of topological data can be found online. For example, an exhaustive source of topological data is publicly available at [47]. These data have been (and are still being) collected by CAIDA (the Cooperative Association for Internet Data Analysis). For example, in [48] we find a macroscopic snapshot of the IPv6 [1] Internet topology collected by CAIDA during the first week of January 2008 (source [47]). The snapshot reflects

[1] Many regions are starting to transition from IPv4 to Internet Protocol version 6 (IPv6) to satisfy the global need for a larger number of publicly accessible Internet addresses.

measurements from a total of 97 different IPv6 source addresses from 68 unique IPv6 prefixes and Autonomous Systems (ASes). The resulting IPv6-level graph contains 4,752 IPv6 addresses and 526 IPv6 prefixes.

Apart from studying the interconnections among Autonomous Systems in the Internet, one can analyze the internal structure of each AS. In this case, each node represents an individual router, and each edge represents a communication link between routers. ISP's generally regard their router-level topologies as confidential information; thus, we need tools to reverse-engineer their topology from externally available data. Several approaches have been proposed to estimate the topology of an ISP from external data. In this thesis, we use the (publicly available) reconstruction technique proposed in [187]. In Fig. 3-1, we represent the estimated topology of the high-speed core of a medium-sized European ISP (Tiscali, SpA). We shall use this topology as our test network for several experiments in this and later chapters.

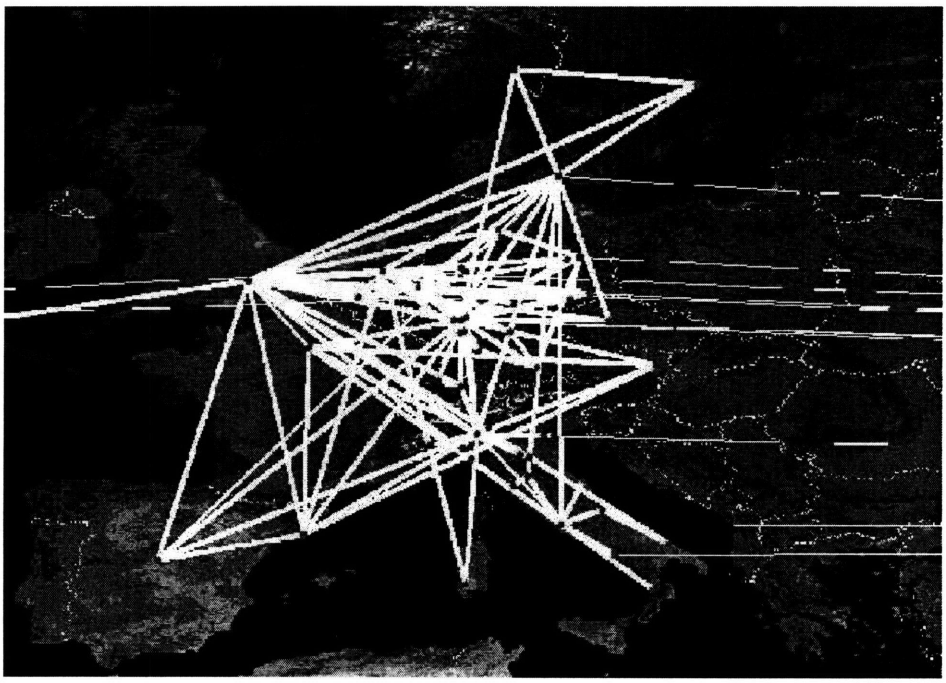

Figure 3-1: Graphical representation of the topology of the high-speed core of a medium size ISP (from [187]).

3.1.2 Information Networks: WWW and Peer-to-Peer

We consider two examples of information networks that use the Internet as their physical infrastructure: the World-Wide Web (WWW) and peer-to-peer networks. The Web graph has been the center of many studies since its appearance in the early 1990's. The works by Albert et al. [6], [25], Kleinberg et al. [113], and Broder et al. [44] provide a strong foundation for subsequent work in this direction.

Decentralized peer-to-peer systems (such as Gnutella or BitTorrent [171], [105]) represent a popular alternative for file-sharing applications. An important problem in the construction of a peer-to-peer network is the generation of a topology that enables efficient content searching. Partial views of the Gnutella topology are available at [125], although those topologies are limited to around 35,000 peers, and the accuracy of the data is questionable.

Figure 3-2: Partial topology of the Gnutella network from [http://home.comcast.net/].

3.1.3 Social Network: Cyber-Communities

In a social network, nodes represent individuals (or organizations) and the edges are a specific type of social relationship among them, such as friendship. A major problem in traditional studies of social networks is that they are often inaccurate and subjective [117]. In this context, the emergence of many online cyber-communities (such as MySpace, Facebook, or Yahoo! 360) provides valuable data to be exploited in social studies. Recent studies on the structure and evolution of some popular cyber-communities can be found in, for example [117], [51], or [2]. In this field, network theory represents a powerful tool, not only for the statistical characterization of these virtual contacts, but also to achieve a better knowledge of the processes forming such interactions.

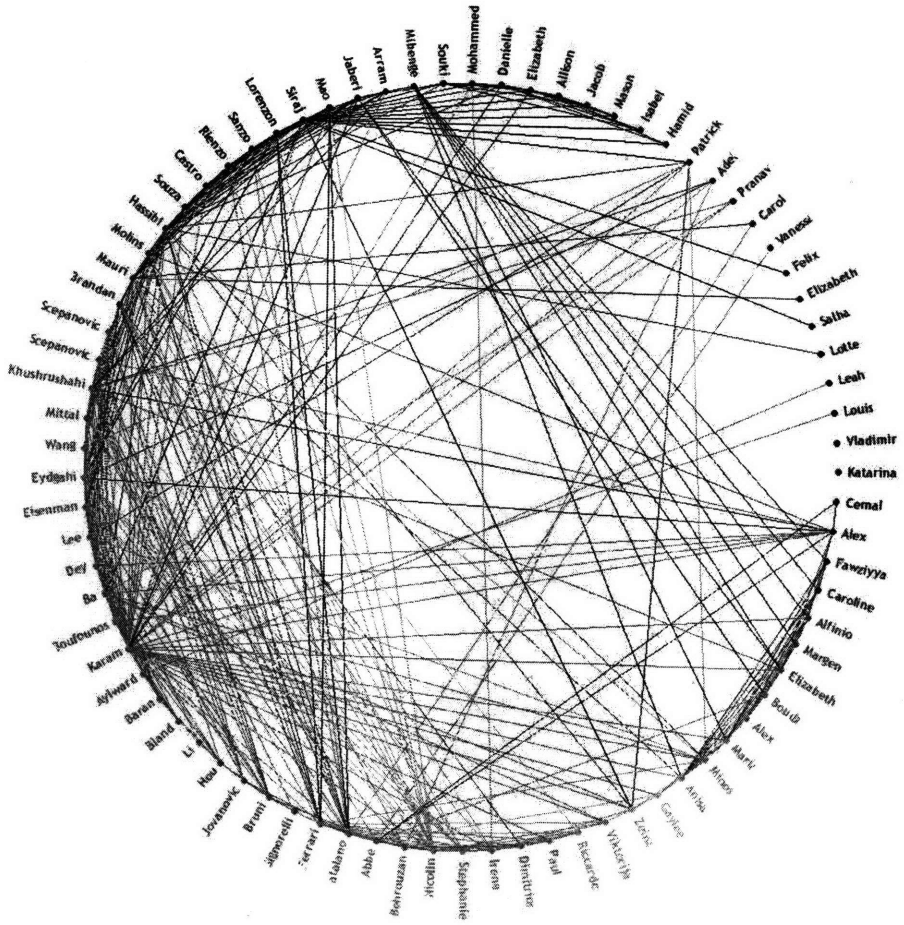

Figure 3-3: Connections among friends in www.facebook.com.

3.1.4 Biological Networks

A major challenge in the field of systems biology is to understand the principles behind the organization of various genetic and metabolic networks. In metabolic networks such as the E. coli metabolic networks (see [169]), the nodes represent metabolites and edges represent reactions among them. Other examples of biological networks are the yeast protein-protein networks (see [178]), and the yeast gene functional interaction network (see [193]).

3.2 Topological Metrics

Network researchers have at their disposal a large variety of metrics quantifying network properties. A wise selection of these metrics is key to the efficient extraction of relevant features for modeling of a real network. In the following subsections, we discuss the most common and useful graph metrics.

3.2.1 Degree Distribution

The degree distribution is probably the easiest metric to measure in a real-world network. This measurement can be presented either as a degree sequence, $(d_i)_{1\leq i\leq n}$, or as a degree distribution, $(r_k)_{1\leq k\leq M}$, where r_k represents the number of nodes with degree k. Many real-world networks present heavy-tailed degree distributions. Some of these distributions are believed to approximately follow a power-law (although such claims are often contested). A network presents a power-law degree distribution if the number of nodes with degree k is proportional to $k^{-\beta}$, for a positive parameter β.

3.2.2 Joint-Degree Distribution

Although the degree distribution is a very valuable network metric, it does not provide any information about the pattern of interconnections among nodes of different

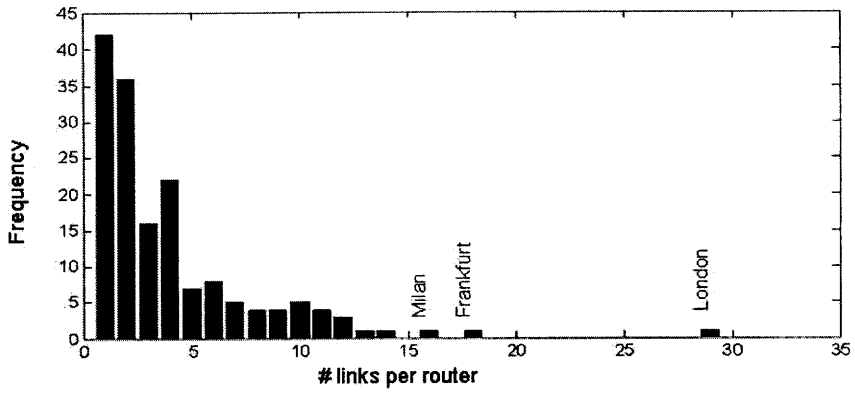

Figure 3-4: The above figure represents the estimated degree distribution of the high-speed core of a European ISP (Tiscali, SpA). (Estimation based on the publicly available data in [187].)

degrees. The joint-degree distribution is a network metric that provides information about this pattern.

Denote by $\mathcal{D}_k$ the set of nodes with degree k, and by $M_{k_1k_2}$ the total number of edges connecting nodes of degrees k_1 and k_2, i.e.,

$$\begin{aligned} M_{k_1k_2} &= \sum_{i\in\mathcal{D}_{k_1}}\sum_{j\in\mathcal{D}_{k_2}} a_{ij} \\ &= \sum_{i=1}^{n}\sum_{j=1}^{n} \mathbf{1}_{d_i=k_1}\mathbf{1}_{d_j=k_2}a_{ij}. \end{aligned} \tag{3.1}$$

We call the matrix $M = [M_{k_1,k_2}]$ the joint-degree matrix of G. The joint degree distribution (JDD) is defined as

$$J_{k_1k_2} = \frac{M_{k_1k_2}}{2E},$$

where E is the total number of edges in the graph.

The JDD in an indicator of correlations between nodes as a function of their degrees. For example, highly connected nodes in social networks tend to connect to nodes of high degree. This connectivity pattern is usually called assortative mixing [148]. On the other hand, in technological and biological networks nodes of high degree

tend to attach to nodes of low degree. This tendency is called disassortative mixing. One can detect these types of mixing using the so-called neighbor connectivity. The neighbor connectivity, $\bar{d}_k$, is defined as the average degree of the neighbors of a node with degree k, i.e.,

$$\bar{d}_k = \frac{\sum_{i \in \mathcal{D}_k} \sum_{j=1}^{n} a_{ij} d_j}{|\mathcal{D}_k|}.$$

If $\bar{d}_k$ is increasing with k, the network is assortative, since it shows that nodes of high degree connect (on average) to nodes of high degree. (Alternatively, if $\bar{d}_k$ is decreasing, the network is disassortative.) The neighbor connectivity of a graph can be plotted on a graph (see, for example, Fig. 3-5).

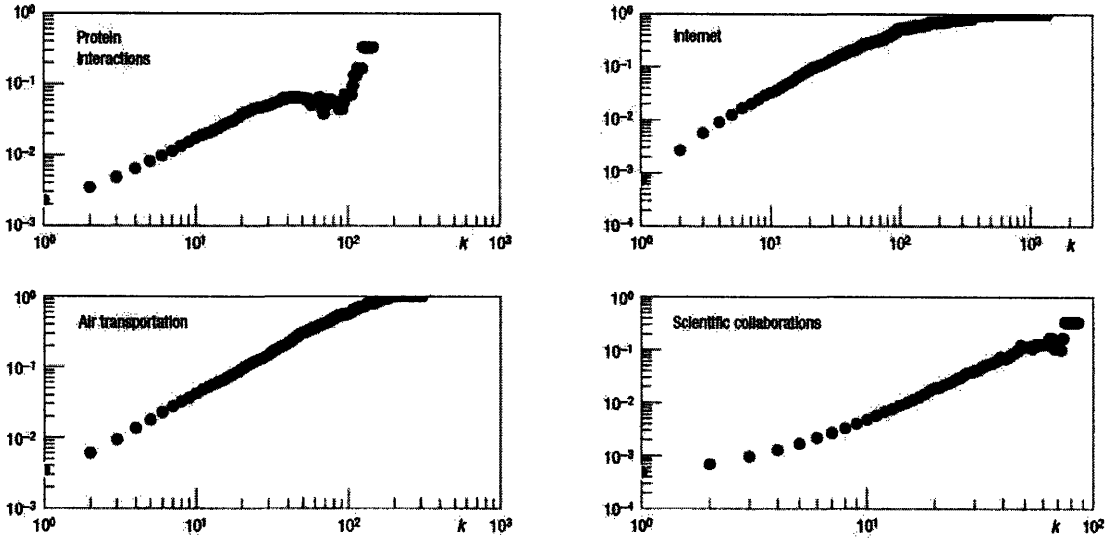

Figure 3-5: Assortative patterns in several real-world networks. Assortative mixing is defined as the tendency of high-degree nodes to link, on average, to high-degree nodes (from [61]).

3.2.3 Triangular Distribution

We now define several alternative distributions measuring the number of triangles in a given graph. The triangular coefficient, T_G, is the total number of triangles in the

graph G, i.e.,

$$T_G = \sum_{1 \leq i < j < k \leq n} a_{ij} a_{jk} a_{ki}.$$

The triangular-degree distribution, T_k, counts the number of triangles touching nodes of degree k. Lastly, the triangular distribution, T_{k_1,k_2,k_3}, counts the number of triangles connecting nodes of degrees k_1, k_2, and k_3.

3.2.4 Distance Distribution

The distribution of shortest paths between pairs of nodes in a network plays an important role in transportation and communication tasks. Consider a graph with one connected component. The distance l_{ij} between two nodes i and j is defined as the length of the shortest path between them. We define the distance matrix of the graph, $L_G = [l_{ij}]$, as the two-dimensional array containing the distances between every pair of nodes in the graph. The maximum value among the entries of L_G is called the diameter of the graph. (In the presence of several disconnected components, the above definitions are computed and listed per component.)

The following figure represents an estimate of the distribution of distances in the Internet, obtained by CAIDA in 1998. For this estimation, a host computer in Michigan measured the number of hops taken by information packets sent to about 13,900 destinations [49].

3.2.5 Betweenness Distribution

Most information networks use shortest-path routing to distribute packets of information. In this context, the number of shortest paths going through a node measures the relevance of a given node in the routing process. Betweenness is defined as the number of shortest paths passing through a given node under the assumption of uniform traffic (under this assumption, the same amount of information flows between

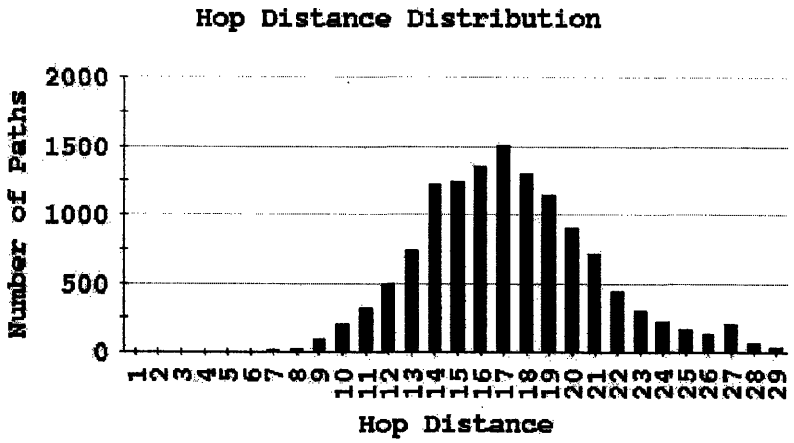

Figure 3-6: Histogram of the number of hops taken by information packets traveling from a host in Michigan to about 13,900 destinations (source [49]).

every pair of nodes in the network). Therefore, this metric measures the traffic load supported by a node.

For a graph with n vertices, the betweenness of node i is defined as:

$$B_i := \sum_{j \neq i} \sum_{k \neq i} \frac{\sigma_{jk}(i)}{\sigma_{jk}}$$

where σ_{jk} is the number of shortest paths from j to k, and $\sigma_{jk}(i)$ is the number of shortest paths from j to k passing through a node i.

We now comment on the process of retrieving the information needed to compute the various metrics above. In most complex networks, we do not have access to the complete topology. On the other hand, one can usually retrieve information about the topology of the neighborhood of a particular sampling node. The amount of information that can be extracted from each sampling node depends on the particular nature of the network under study. For example, in many online cyber-communities (such as Facebook), we can access information about our friends, as well as the list of friends of our friends. In other words, we have access to a second-order neighborhood. In this context, an important challenge is to infer global network properties from local samples of the topology.

We can classify the metrics presented in this section into two categories. First, we have metrics that can be estimated from local samples of the graph topology. In other words, we only need the topology of the neighborhood of a node to extract the corresponding sample information. The degree distribution, joint-degree distribution, and clustering distribution fall into this category. We denote this first category as local metrics. In the second category, we include metrics that require a complete knowledge of the graph topology for them to be computed. For example, in order to compute betweenness, one must first solve the shortest path problem for every pair of nodes in the network. Clearly, this task requires the knowledge of the whole graph topology. We denote this second category as global metrics.

3.3 Static Graph Models

In this section, we briefly introduce some of the most popular random graph models in the literature. (For a thorough survey, we direct the interested reader to the research monographs [72], [59], and surveys [70], [189].)

3.3.1 Erdös-Rényi Random Graphs

The systematic study of random graph models was initiated by Erdös and Rényi in 1959 with their seminal paper on random graphs [74]. Even though their model cannot typically replicate properties measured in real networks, the problems and techniques they introduced started a whole new branch of mathematical research. In the classical Erdös-Rényi (ER) model, the graph is generated by taking n nodes and connecting each pair of nodes by an edge with a fixed 'edge existence' probability p, independently of all other pairs of nodes. This random graph ensemble is denoted by $G_{n,p}$.

The main goal of the theory developed around this model is to determine the values of p at which relevant properties of the graph arise with high probability. In

many cases, these values of p are exactly solvable in the limit of large graph size. For example, if $np < 1$, then a graph in $G_{n,p}$ will almost surely have no connected components of size larger than $O(\log n)$; while if np tends to a constant $c > 1$, then a graph in $G_{n,p}$ will almost surely have a unique 'giant' component containing a positive fraction of the nodes. For large n, the graph presents a Poisson degree distribution. Thus, this model is inadequate to replicate non-Poissonian degree distributions observed in real-world networks. We shall examine an extension of this classical model in Section 3.3.3.

3.3.2 Small-World Model

The term *small-world effect* refers to the notion that any two people in the world can be related through a relatively short chain of acquaintances. Based on this observation, Watts and Strogatz proposed in [201] the small-world family of random graphs. These show the following apparently contradictory properties:

(i) most nodes are not neighbors of one another, and

(ii) most nodes can be reached from every other node by a small number of steps.

Watts and Strogatz proposed a model that takes a regular lattice and randomly rewires edges with a fixed probability p. As shown in Fig. 3-7 (b), the resulting architecture is intermediate between a regular lattice (achieved for $p = 0$) and a classical random graph (achieved for $p = 1$).

An exciting result observed in this model was the following: for small probability of rewiring, $p \ll 1$, the distribution of triangles is nearly the same as that of the regular lattice, but the average shortest-path length is close to that of classical random graphs. This property can be empirically observed in many real-world networks, such as the WWW and metabolic networks.

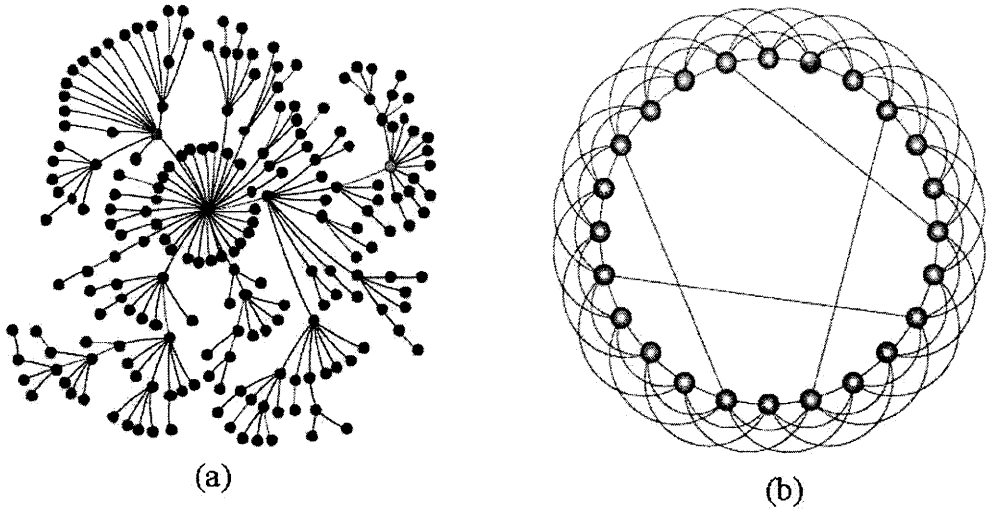

Figure 3-7: Examples of a power-law network and a small-world model, from [189].

3.3.3 Chung-Lu Random Networks

In the previous section, we have presented several network models that are useful to gain insight into some high-level properties observed in real networks (such as, for example, the origin of power-law degree distributions). In this section, we introduce a random graph ensemble able to replicate a given degree distribution.

We shall illustrate the use of this random graph ensemble with a specific real-world modeling problem. In particular, we shall model the topology of the optical high-speed core of a European ISP: *Tiscali S.p.A.* (one of the main European telecommunication companies). Since ISPs have economic incentives to maintain secrecy about their topologies, an active field of research is the development of techniques to estimate an ISP's topology based on externally available information. For example, Spring et al. developed a computational tool to estimate the topology of several ISP's from traceroute information [174]. In Fig. 3-8, we represent the estimate of the high-speed core of Tiscali using Rocketfuel.

We pay special attention to the random graph model proposed by Chung and Lu in [56]. In this model, we can prescribe a given expected degree sequence, $w_1, ..., w_n$, in a random graph ensemble with n nodes. This model is useful when we do not have

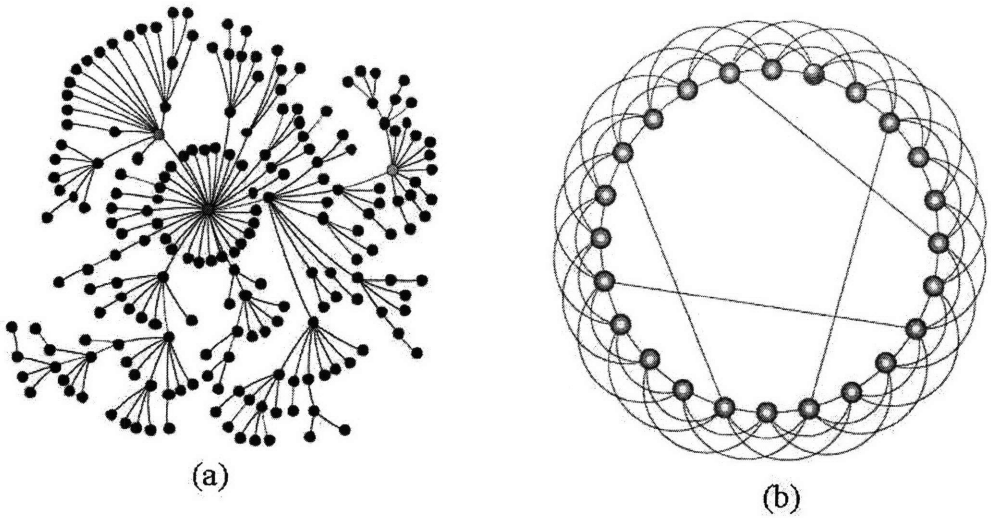

Figure 3-7: Examples of a power-law network and a small-world model, from [189].

3.3.3 Chung-Lu Random Networks

In the previous section, we have presented several network models that are useful to gain insight into some high-level properties observed in real networks (such as, for example, the origin of power-law degree distributions). In this section, we introduce a random graph ensemble able to replicate a given degree distribution.

We shall illustrate the use of this random graph ensemble with a specific real-world modeling problem. In particular, we shall model the topology of the optical high-speed core of a European ISP: *Tiscali S.p.A.* (one of the main European telecommunication companies). Since ISPs have economic incentives to maintain secrecy about their topologies, an active field of research is the development of techniques to estimate an ISP's topology based on externally available information. For example, Spring et al. developed a computational tool to estimate the topology of several ISP's from traceroute information [174]. In Fig. 3-8, we represent the estimate of the high-speed core of Tiscali using Rocketfuel.

We pay special attention to the random graph model proposed by Chung and Lu in [56]. In this model, we can prescribe a given expected degree sequence, $w_1, ..., w_n$, in a random graph ensemble with n nodes. This model is useful when we do not have

measure the average degree and impose this value on the ensemble. In particular, the estimated average degree of Tiscali's core is $\bar{w} = 4.0745$. Since we know that Tiscali's core has 161 high-speed routers, we can model this network with a random graph with $n = 161$ nodes and an edge existence probability equal to $p = \bar{w}/n = 0.0252$. In Fig. 3-9, we show one random realization of this graph, as well as histograms for the empirical eigenvalue distributions for the adjacency matrices of both the real Tiscali core and the random graph model. We observe that, as expected, the classical model is ill-suited to capture spectral properties of this ISP's core.

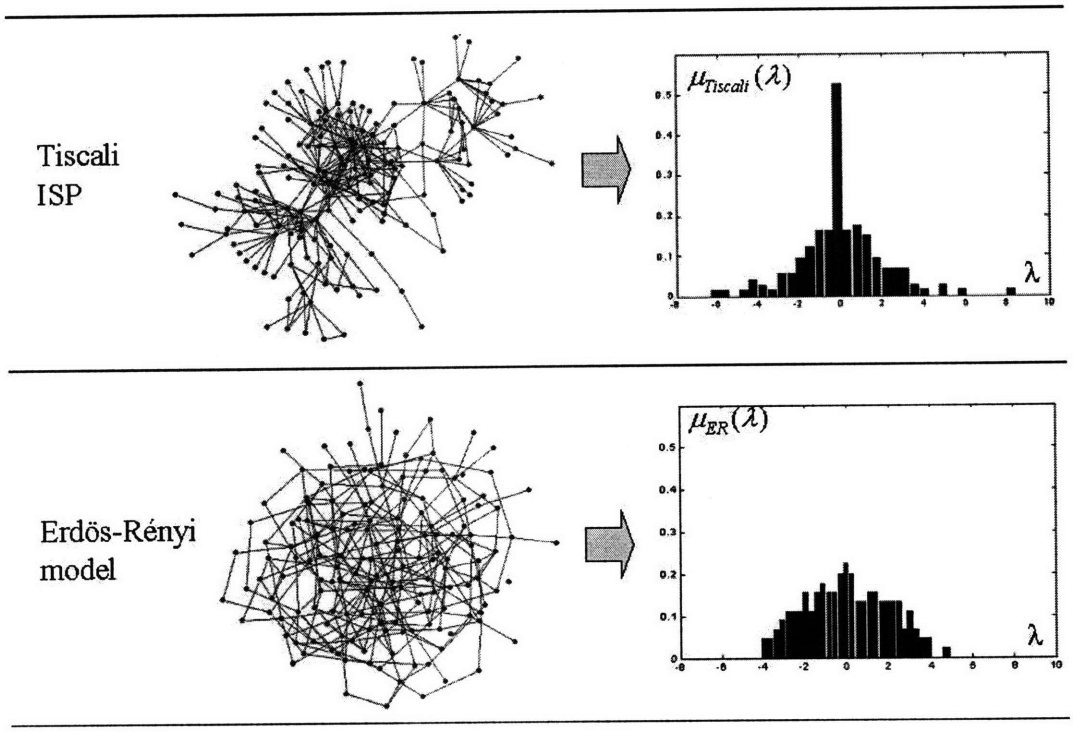

Figure 3-9: In this figure we compare the topology and the eigenvalue spectrum of a random realization of the classical ER model versus the graph representing Tiscali's high speed core.

In the following, we describe a random graph ensemble that allows for a more detailed description of the network topology. This model, proposed by Chung and Lu in [56], generalizes the classical ER model to prescribe a given expected degree sequence on it.

Due to the simplicity of sampling the degree distribution, several stochastic mod-

els aiming to replicate a given degree sequence have been proposed. The configuration model (first introduced by Bender and Canfield [28], and subsequently refined by Bollobás [37]) represents the most popular of this type of model. This model presents serious drawbacks on a theoretical level. Firstly, the probability of having multiedges increases dramatically as a function of the maximum degree. A series of (very restrictive) conditions on the degree sequence was proposed by Molloy and Reed [143] in order to avoid this effect. The second drawback is the presence of strong statistical dependencies among different edges. These dependencies complicate the mathematical analysis of this model.

In [56], Chung and Lu defined a random graph model in which one can prescribe a given expected degree sequence, $\{w_1, w_2, ..., w_n\}$, with $w_i > 0$ denoting the desired expected degree for node i. We shall assume the nodes are numbered so that $w_1 \geq w_2 \geq ... \geq w_n$. Many elaborate mathematical results concerning this model have already been published [56], [58]. This random graph is constructed by independently assigning edges between each pair of nodes (i, j), $1 \leq i < j \leq N$ with probabilities

$$p_{ij} := \mathbb{P}(a_{ij} = 1) = \rho w_i w_j, \text{ where } \rho = \left(\sum_k w_k \right)^{-1}. \tag{3.2}$$

For the expected degree sequence to be realizable, we need the condition $w_1^2 < \sum_k w_k$ (which ensures $p_{ij} \leq 1$). As a particular case, one can recover the classical Erdös-Rényi graph from a constant degree sequence, $w_i = \overline{w}$ for all i.

We now model the Tiscali core network using this random graph ensemble. First, we extract the sequence of degrees from the real network by counting the number of optical links attached to each high-speed router. In Fig. 3-10, we plot this sequence for the 161 high-speed routers in the network (ordered in non-increasing order). Next, we use this sequence to define a Chung-Lu random graph ensemble with 161 nodes. In the following figure, we show the topology of one random realization from this ensemble. We also plot the eigenvalue histograms for both the adjacency and Kirchhoff matrices. We observe how this model provides a surprisingly accurate description of Tiscali's

topology from a spectral point of view, including a good alignment between the spectral radius of the real and the random graph for both the adjacency and Kirchhoff matrices.

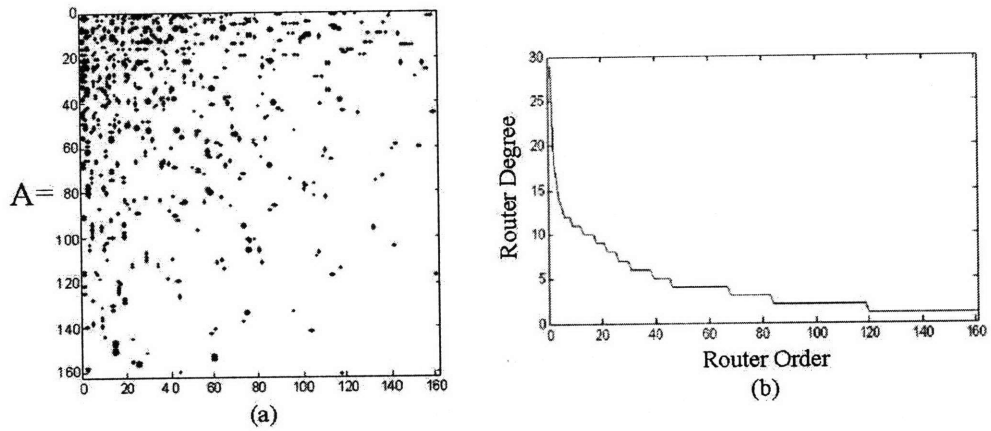

Figure 3-10: Structure of the adjacency matrix (a) and degree sequence (b) of Tiscali's core (161 nodes).

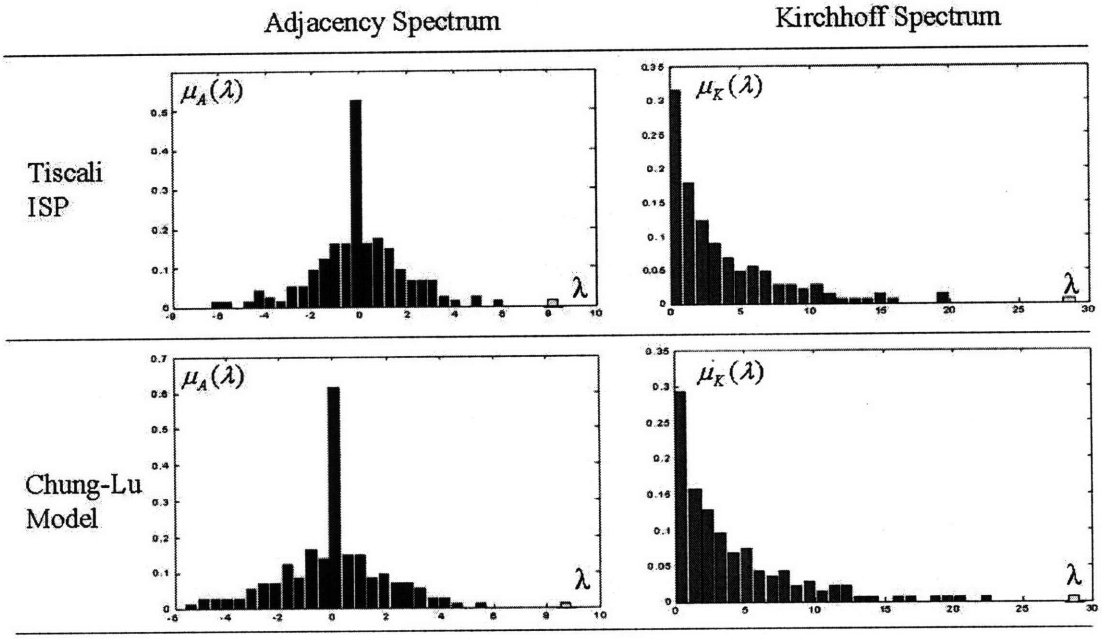

Figure 3-11: In this figure we compare the spectra of the adjacency and Kirchhoff matrices of a random realization of the Chung-Lu model versus the graph representing Tiscali's high speed core.

3.4 Dynamic Graph Models

In the previous section, we introduced a random graph model able to prescribe relevant empirical observations on a random graph ensemble. In contrast, there are other random graph models, called dynamic models, that aim to explain the developmental process of a complex network.

A network is named a power-law or scale-free if its degree distribution follows a power law (the number of vertices with degree k is proportional to $k^{-\beta}$ for some $\beta > 0$). The observation that many real networks approximate power-law distributions sparked the interest in such networks. Since then, several network models presenting power-law distributions have arisen. For example, the Yule process [211], was proposed in 1924 as a generative process for power laws. After Yule, this process has been reinvented several times under different names: the Gibrat's principle by Herbert Simon [101], the Matthew effect [135], Zipf's law [212] and, most recently, preferential attachment by Barabási and Albert [24].

The model proposed by Barabási and Albert has achieved great popularity in recent years, inspiring a long series of computational models aiming to explain the appearance of power laws. Among these models, we can cite the computational framework for the generation of synthetic topologies proposed by Medina et al. in [131]. In [3], Aiello et al. proposed a random graph model to generate massive graphs with a power-law degree sequence. Jin et al. developed *Inet*, [106], which is a computational framework aiming to generate synthetic topologies modeling the Internet.

The Barabási-Albert (BA) model has two fundamental ingredients:

(i) the sequential addition of nodes (in other words, the number of nodes in the BA network grows in time), and

(ii) the preferential attachment process: This ingredient causes new edges to attach to existing nodes of high degree with a higher probability than to nodes of low degree (in other words, "popularity is attractive").

We now quote part of the model description given by Barabási and Albert in [24]:

> "... starting with a small number m_0 of vertices, at every time step we add a new vertex with $m \leq m_0$ edges that link the new vertex to m different vertices already present in the system. To incorporate preferential attachment, we assume that the probability Π that a new vertex will be connected to a vertex i depends on the connectivity k_i of that vertex, so that $\Pi_i = k_i \Big/ \sum_j k_j$. After t steps the model leads to a random network with $t + m_0$ vertices and $m\,t$ edges."

This growth mechanism is called linear preferential attachment, and has been proved to yield a power-law degree distribution in the limit of large networks. (In Chapter 5, we shall give an in-depth analysis of several structural properties regarding this model.) Although the BA model represents a significant landmark in network modeling, it lacks the accuracy to describe many topological characteristics observed in real networks. For example, the degree distribution of the BA model is a power law with a fixed exponent ($\beta = 3$), while most real networks present a different exponent [150]. Also, the clustering coefficient and average path length are significantly smaller than those observed in real networks [39], [168].

Based on the work of Barabási and Albert, other dynamic models have been proposed. Relevant examples of dynamic models are the following:

1. Growth with nonlinear preferential attachment (proposed by Krapivsky et al. in [114]): In this extension of the BA model, the probability Π_i that a new node connects to an existing vertex v_i depends nonlinearly on the degree k_i of that vertex. In particular, the authors in [114] studied the case in which this probability is $\Pi_i \sim k_i^{\gamma}$, for some real $\gamma \geq 0$. Using a mean-field analysis of this model, different behaviors have been detected depending on the value of γ. In particular:

   - For $\gamma < 1$, the number of nodes with degree k varies as a "stretched exponential".

- For $\gamma > 1$, one node connects to a major portion of the network.
- For $\gamma = 1$, the degree distribution follows a power law.

2. Accelerated growth process (proposed by Dorogovtsev and Mendes in [68]): In many real networks such as the WWW, the Internet, or the collaboration network, the average degree of the network increases with time. In [68], the authors studied the possible consequences of this accelerated growth.

3. Preferential attachment with aging (proposed in [69]): In many real networks, the probability that a new node attaches to an older node depends on the age of the older node. For example, old papers are less likely to be cited. In [69], the authors analyzed the effect of aging on the structure of the network.

In the following chapters, we present an in-depth analysis of the spectral properties of stochastic graph models of relevance. Chapter 4 is devoted to the spectral analysis of static models, while Chapter 6 presents our results on dynamic networks.

Chapter 4

Spectral Analysis of Random Static Graphs

In this chapter we study the eigenvalue distribution of adjacency matrices associated with static random graphs. In particular, we study the random graph ensemble defined by Chung and Lu in [56]. This model allows us to prescribe a given expected degree sequence on the graph ensemble. We apply techniques from random matrix theory to study the adjacency matrix ensemble associated with this random graph.

A classical result in random matrix theory is the Wigner semicircle law [203]. This result states that the eigenvalue distribution of a random symmetric matrix with independent and identically distributed random entries on and above the diagonal (the other entries are fixed by the symmetry requirements) asymptotically follows a semicircular function as the number of nodes, n, goes to infinity. In [84], Füredi and Komlós extended Wigner's results to random symmetric matrices with independent entries presenting identical mean μ and variance σ^2 (although not necessarily the same distribution). They proved that, for $\mu \neq 0$, the largest eigenvalue λ_{max} asymptotically follows a normal distribution with expectation $n\mu$ and variance 2σ for large n. They also proved that, with probability tending to 1, as n increases

$$\max_{i>1} |\lambda_i| < 2\sigma\sqrt{n} + O(n^{1/3}\log n).$$

In this chapter, we study the spectral properties of the random adjacency matrix associated with the static Chung-Lu model. We derive closed-form expressions for the expected spectral moments of the random adjacency matrix as a function of the expected degree distribution. We also prove quadratic convergence of the random spectral moments to their expected values as the number of nodes in the graph grows. We illustrate our results with both analytical and numerical examples.

4.1 Notation and Useful Results

In this section we introduce basic graph-theoretic notation and results (see [206] for a complete exposition on graph-theoretic terminology and results). A closed walk of length L in a graph G, denoted by c_L, is an ordered sequence of nodes (possibly repeated), $c_L = \{i_1, i_2, ..., i_L, i_{L+1}\}$, such that $i_k \sim i_{k+1}$ for $k = 1, 2, ..., L$ and $i_1 \equiv i_{L+1}$. We denote by $C_L^{(n)}$ the set of all closed walks of length L on the complete graph (i.e.,with all possible edges present) with n nodes, K_n.

A tree is a connected graph in which any two vertices are connected by exactly one path. Whether or not a connected graph is a tree can be uniquely determined from its degree sequence or degree distribution. A connected graph, T, with $s+1$ nodes is a tree if and only if its degree sequence, $\mathbf{d}_T = \{d_T(1), ..., d_T(s+1)\}$, satisfies $\sum_{i=1}^{s+1} d_T(i) = 2s$, [188]. Similarly, a given degree distribution, $\{r_T(1), r_T(2), ..., r_T(s)\}$ is associated to a tree with $s+1$ nodes if and only if $\sum_{k=1}^{s} r_T(k) = s+1$ and $\sum_{k=1}^{s} k\, r_T(k) = 2s$. Consequently, we define the set of valid degree distributions for trees with s edges (and $s+1$ nodes) as:

$$\mathcal{F}_s := \left\{ \{r_1, r_2, ..., r_s\} \in \mathbb{N}^s : \sum_{k=1}^{s} r_k = s+1, \ \sum_{k=1}^{s} k\, r_k = 2s \right\}. \tag{4.1}$$

We now define two useful combinatorial structures: rooted trees and ordered rooted trees [188]. A rooted tree T is defined recursively, starting from a set of nodes $\{1, ..., n\}$, as follows:

(a) One node is assigned to be the *root* of T. We denote the root by $R(T)$.

(b) The remaining nodes are partitioned into $m \geq 1$ disjoint non-empty sets $T_1, ..., T_m$, each of which is a rooted tree (also called subtrees of the root).

The definition of an ordered rooted tree comes from replacing **(b)** in the above definition with:

(b') The remaining nodes are put into an ordered partition $(T_1, ..., T_m)$ of $m \geq 1$ disjoint non-empty sets $T_1, ..., T_m$, each of which is an ordered rooted tree.

One can use prefix notation to represent the structure of a ordered rooted tree [188]. In this notation, we represent a tree with root r and subtrees $T_1, ..., T_m$ as $r(T_1, ..., T_m)$. We can recursively apply prefix notation on the set of subtrees to obtain the final representation in prefix notation for a ordered rooted tree. Similarly, we define an ordered rooted forest as an ordered collection of ordered rooted trees (i.e., each connected component is an ordered rooted tree).

It is often convenient to describe the degree of a node in a rooted tree using the number of successors of the node (i.e., the number of branches growing from a given node). We call this quantity the δ-degree. The δ-degree of a node i, denoted by $\delta_T(i)$, satisfies:

$$\delta_T(i) = \begin{cases} d_T(i), & \text{for } i = R(T), \\ d_T(i) - 1, & \text{otherwise.} \end{cases}$$

Given an ordered rooted forest F, its δ-degree distribution is the sequence of integers $\rho_F = \{\rho_F(0), \rho_F(1), ...\}$, such as $\rho_F(k)$ counts the number of nodes in F with δ-degree equal to k. Given a sequence of nonnegative integers, $\rho = \{\rho_0, \rho_1, ...\}$, there exists an ordered rooted forest with s nodes and t components presenting a δ-degree distribution equal to ρ if and only if [188]: $\sum_i \rho_i = s$, and $\sum_i (i-1)\rho_i = -t$.

4.2 The Chung-Lu Model and its Random Adjacency Matrix

We now describe the random graph model introduced by Chung and Lu in [56]. This model allows one to prescribe a given sequence of expected degrees on a random graph with n nodes. We denote the prescribed sequence of expected degrees by $\mathbf{w} = (w_1, ..., w_n)$, $w_i > 0$, and the resulting graph ensemble by $\mathcal{G}_n(\mathbf{w})$. In this random graph, an edge joining nodes i and j appears, independently of the rest of edges, with probability:

$$p_{ij} := \mathbb{P}(i \sim j) = \rho w_i w_j, \tag{4.2}$$

where ρ is a normalizing factor defined as $\rho := (\sum_k w_k)^{-1}$. In order to guarantee $p_{ij} < 1$ for all $1 \leq i, j \leq n$, we assume $\max_i w_i^2 < \sum_j w_j$. One can easily check that the expectation of the degree of node i in this ensemble is:

$$\mathbb{E}[d_i] = \sum_j \mathbb{E}[a_{ij}] = \sum_j \mathbb{P}(i \sim j) = \sum_j \rho w_i w_j = w_i.$$

Notice that we recover the classical Erdös-Rényi random graph for $\mathbf{w} = (pn, pn, ..., pn)$.

For each graph in the Chung-Lu random graph ensemble, $G \in \mathcal{G}_n(\mathbf{w})$, we can associate an $n \times n$ adjacency matrix $A_n := A_n(G)$. Thus, we can associate a random ensemble of adjacency matrices to $\mathcal{G}_n(\mathbf{w})$. We denote this random matrix ensemble by $A_n(\mathbf{w})$. Furthermore, for each matrix in the ensemble, $A_n \in A_n(\mathbf{w})$, there is a corresponding set of n eigenvalues $\{\lambda_j(A_n)\}_{1 \leq j \leq n}$. Therefore, the random matrix ensemble $A_n(\mathbf{w})$ induces an n-dimensional joint probability density of eigenvalues. This density, called joint spectral density, is very difficult (if not impossible) to compute explicitly. (In [132], we find explicit solutions for a handful of random ensembles of matrices with i.i.d. Gaussian entries.)

In this chapter, we investigate the spectral density of the random adjacency matrix $A_n(\mathbf{w})$. Before studying the random adjacency matrix $\mathcal{G}_n(\mathbf{w})$, we introduce and study

a related class of random matrices in Section 4.4. Random matrices in this new class present zero-mean random entries with nonidentical variances distributed according to a particular pattern. To the best of our knowledge, spectral properties of random matrices with non-identical variances are unknown [23]. In this chapter, we provide a partial answer to this question. In later sections, we show how to apply the results in Section 4.4 to $\mathcal{G}_n(\mathbf{w})$.

Before we introduce the technical details, we motivate our approach with some numerical experiments in which we observe the behavior of spectral densities associated with random graphs of different sizes. In our first experiment, we consider a Chung-Lu random graph with 10 nodes and expected degree sequence $w_i = 10 - 4(i/10)$, $i = 1, 2, ..., 10$. (Notice that this sequence takes 10 equispaced samples of an affine function.) In the first row of Fig. 4-1, we plot the eigenvalue histograms of three empirical realizations of this random graph. We observe how, for all three realizations, the histogram of eigenvalues has approximately the same region of support and approximately the same shape. In a second experiment, we consider a Chung-Lu random graph with 100 nodes and expected degree sequence $w_i = 10 - 4(i/100)$, $i = 1, 2, ..., 100$. (This degree sequence is a more finely sampled version of the affine function used in the previous case.) In the second row of Fig. 4-1, we plot the eigenvalue histograms for three realizations of this random graph. The eigenvalue histograms in this case have supports that are even more closely aligned, and their shapes are remarkably similar. In our last experiment we increase the size of the random graph to 1000 nodes. We resample the same affine function yet more finely to obtain the expected degree sequence $w_i = 10 - 4(i/1000)$, $i = 1, 2, ..., 1000$. The third row in Fig. 4-1 shows the eigenvalue histograms of three realization of this random graph. In this final experiment, we can clearly observe a well-defined common shape for the three empirical eigenvalue histograms. Also, the shapes of the histograms are significantly smoother that the ones obtained in our second experiment.

In these numerical experiments, we observe how the eigenvalue histograms concentrate around a particular density as the graph grows. This density is called the

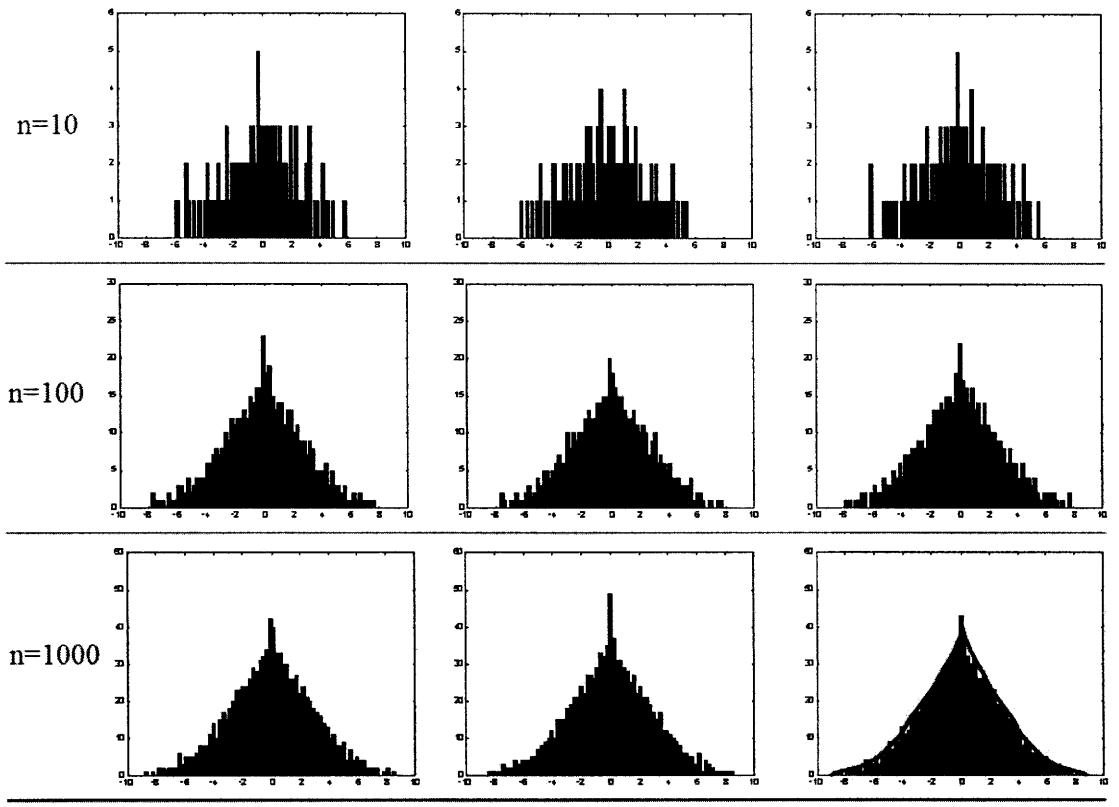

Figure 4-1: Eigenvalue histograms for three empirical realizations of $\mathcal{G}_n(\mathbf{w})$ with $w_i = 10 - 4(i/n)$, $i = 1, ..., n$, and $n \in \{10, 100, 1000\}$. Observe how the eigenvalue histograms concentrate around a limiting spectral density as n increases. We have include a sketch of this limiting density in the lower-right histogram.

limiting spectral density. The rest of this chapter is devoted to characterize this density, and study the convergence to this density, for random static graphs generated by the Chung-Lu model. We will do this by first examining another interesting class of random matrices in Section 4.4, then applying those results to the Chung-Lu model in Section 4.6.

4.3 The Method of Moments

In this thesis, we characterize a limiting spectral density using its sequence of moments. This 'method of moments' is extensively used in random matrix theory [103]. In the following subsection, we introduce definitions used in our derivations.

4.3.1 Basic Definitions and Notation

Consider an $n \times n$ real symmetric matrix A. Recall that $\{\lambda_i(A),\ i = 1, ..., n\}$ denotes the set of eigenvalues of A. We define the k-th spectral moment of A as

$$m_k(A) = \frac{1}{n}\sum_{i=1}^{n}[\lambda_i(A)]^k. \tag{4.3}$$

The k-th spectral moment associated with the random matrix ensemble $A_n(\mathbf{w})$ is a random variable. In this chapter we study the expectation and variance of the k-th spectral moment for all values of k. In particular, we derive closed-form expressions for the expected value of the spectral moments, $\mathbb{E}_{A\in A_n(\mathbf{w})}[m_k(A)]$, as a function of the expected degree sequence, $\mathbf{w} = (w_1, ..., w_n)$. These expressions are multivariate polynomials in the set of variables $\{W_1, ..., W_k\}$, where W_j is defined as:

$$W_j := \sum_{i=1}^{n} w_i^j. \tag{4.4}$$

(In other words, W_j is the j-th power sum of the given expected degree sequence $\mathbf{w}$.)

We also prove that the variances of the random spectral moments converge to zero as the graph grows (under some constrains in the expected degree sequence $\mathbf{w}$).

As mentioned earlier, we characterize the limiting spectral distribution using its sequence of moments, $\{m_k,\ k = 0, 1, 2, ...\}$. An arbitrarily specified sequence of moments does not necessarily have an associated spectral distribution. The problem of deciding whether or not a probability distribution matching a specified sequence of moments exists is called the classical moment problem [5], and our objective of reconstructing a spectral distribution from its moments can be discussed in this framework. We can find in the literature several sufficient conditions for the existence of a distribution that matches a specified sequence of moments. Especially useful if the following sufficient condition proposed by Carleman :

$$\sum_{s=1}^{\infty} m_{2s}^{-1/2s} = +\infty$$

With these basic definitions now introduced, we present the main ideas behind the method of moments applied to random graphs.

4.3.2 Graph-Theoretical Interpretation of the Spectral Moments

Consider a simple graph G, i.e., a graph with undirected (or equivalently, bidirectional) edges, and no self-loops. We denote by $A_G = [a_{ij}]$ the $n \times n$ adjacency matrix of G, and by λ_i, $i = 1, ..., n$, the eigenvalues of A_G. A closed walk of length k can be described as the (ordered) sequence of nodes visited by the walk, $\mathbf{c}_k = (i_1, i_2, ..., i_k, i_1)$, where nodes may repeat along the sequence. Associated with a walk $\mathbf{c}_k$, we define the function:

$$\omega_G(\mathbf{c}_k) = a_{i_1 i_2} a_{i_2 i_3} ... a_{i_k i_1}, \tag{4.5}$$

where a_{ij} is the (ij)-th entry of the adjacency matrix, A_G. The variable $\omega_G(\mathbf{c}_k)$ takes the value 1 if the closed walk $\mathbf{c}_k$ exists in G; otherwise, it takes the value 0. In other words, $\omega_G(\mathbf{c}_k)$ is the indicator function for the set of walks in G. Using this indicator function, we can count the number of closed walks of length k in G as:

$$\sum_{\mathbf{c}_k \in C_k^{(n)}} \omega_G(\mathbf{c}_k),$$

where $C_k^{(n)}$ is the set of possible closed-walks of length k in the complete graph with n nodes, K_n. ($C_k^{(n)}$ can also be described as the set of ordered sequences of k nodes, $(i_1, i_2, ..., i_k)$, chosen with replacement from the set $\{1, ..., n\}$.)

An interesting graph-theoretical interpretation of the spectral moments comes from the following two results:

(i) First, we have the following algebraic identity for the adjacency matrix:

$$\sum_{i=1}^{n} \lambda_i^k = tr\, A^k;$$

thus, the k-th spectral moment of A can be written as:

$$m_k(A) = \frac{1}{n} \mathrm{tr}\, A^k. \tag{4.6}$$

(ii) Also, we have the following result from algebraic graph theory [32]: The trace of A^k is equal to the number of closed walks of length k in G.

From (i) and (ii), we deduce that the k-th spectral moment of G is proportional to the number of closed walks of length k in G. Therefore, we can write the k-th spectral moment as:

$$m_k(A) = \frac{1}{n} \sum_{\mathbf{c}_k \in C_k^{(n)}} \omega_G(\mathbf{c}_k) = \frac{1}{n} \sum_{1 \le i_1, i_2, \ldots, i_k \le n} a_{i_1 i_2} a_{i_2 i_3} \ldots a_{i_{k-1} i_k} a_{i_k i_1}. \tag{4.7}$$

This formula allows us to transform the algebraic problem of computing spectral moments of the adjacency matrix into the combinatorial problem of counting closed walks in the graph. In a random graph ensemble, such as $A_n(\mathbf{w})$), the number of closed walks of length k is a random variable. In this chapter, we compute the expected value of the number of closed walks of length k in $A_n(\mathbf{w})$ and study its statistical convergence for asymptotically large graphs.

4.4 Eigenvalue Spectrum of Random Symmetric Matrices with Entries of Zero Mean and Non-identical Variances

In [84], Füredi and Komlós studied the limited distribution of eigenvalues of an ensemble of random symmetric matrices $\tilde{A}_n$ in which the upper-triangular entries, $\tilde{a}_{ij}$

for $1 \leq i < j \leq n$, are independent random variables with the same mean and variance, denoted by μ and σ^2, respectively. In particular, it was proven that for $\mu = 0$ the set of eigenvalues of $\widetilde{A}_n$, $\{\lambda_i(\widetilde{A}_n)\}_{1 \leq i \leq n}$, fulfills:

$$\max_{1 \leq i \leq n} |\lambda_i(\widetilde{A}_n)| = 2\sigma\sqrt{n} + O(n^{1/3} \log n), \tag{4.8}$$

with probability tending to 1 (under appropriate technical conditions).

For the Chung-Lu model, the (i, j)-th entry of the adjacency matrix, $a_{ij} = [A_n]_{ij}$, has mean and variance given by

$$E[a_{ij}] = Var[a_{ij}] = \rho w_i w_j. \tag{4.9}$$

In other words, the means, and similarly the variances, are non-identical across entries for the random adjacency matrix. Spectral properties of a random matrix ensemble with non-identical distribution for its entries was mentioned as one of the main open problems in random matrix theory in the review paper [23]. In this thesis we give a partial answer to this problem by studying the eigenvalue distribution of random matrices with a particularly interesting pattern of variances, specified in the next subsection. In Section 4.6 we then apply the results of the present section to the Chung-Lu model.

4.4.1 Asymptotic Behavior of Expected Spectral Moments for Zero-Mean, Rank-One-Variance Matrices

In this section, we introduce a new ensemble of random zero-mean symmetric matrices. This ensemble introduces the novelty of having random zero-mean entries with non-identical variances distributed in a particular pattern. We derive closed-form expressions for the expected spectral moments of this random matrix, $\widetilde{A}_n$. First, we define the ensemble:

Definition We define $\mathcal{A}_n(\sigma)$, with $\sigma = \{\sigma_i\}_{1\leq i\leq n}$, as the random ensemble of $n \times n$ real symmetric matrices, $\widetilde{A}_n = [\widetilde{a}_{ij}]$, with diagonal and upper-triangular entries being independent random variables satisfying the following conditions:

1. Uniformly bounded: $|\widetilde{a}_{ij}| \leq K$,

2. Zero mean: $\mathbb{E}[\widetilde{a}_{ij}] = 0$,

3. Rank-one pattern of variances: $Var[\widetilde{a}_{ij}] = \sigma_i\sigma_j$, where $\sigma = \{\sigma_i\}_{1\leq i\leq n}$ is a sequence of n non-negative numbers.

To the best of our knowledge, the distribution of eigenvalues of random matrices with entries presenting non-identical variances remains an open problem. The following two theorems state our main results in this direction. The corresponding proofs can be found at the end of this chapter, in Section 4.5.

Theorem 4.4.1 *Consider the random matrix ensemble $\mathcal{A}_n(\sigma)$ with $\sigma = (\sigma_1, \sigma_2, ..., \sigma_n)$. Denote*

$$\begin{aligned} \sigma_{\max} &= \max_i \sigma_i, \quad \sigma_{\min} = \min_i \sigma_i, \quad S_k = \sum_{j=1}^{n} \sigma_j^k, \\ \mathcal{F}_s &:= \left\{ \{r_1, r_2, ..., r_s\} \in \mathbb{N}^s : \sum_{k=1}^{s} r_k = s+1, \ \sum_{k=1}^{s} k\, r_k = 2s \right\}; \end{aligned}$$

Then, the even expected spectral moments of $\mathcal{A}_n(\sigma)$ are:

$$\mathbb{E}_{\widetilde{A}_n \in \mathcal{A}_n(\sigma)}[m_{2s}(\widetilde{A}_n)] = (1 + o(1))\, n^{-1} \sum_{(r_1,...,r_s)\in\mathcal{F}_s} 2\binom{s}{r_1, ..., r_s} S_1^{r_1} S_2^{r_2} ... S_s^{r_s}, \qquad (4.10)$$

provided that

$$\frac{s^6}{\sigma_{\max}^2} \left(\frac{\sigma_{\max}}{\sigma_{\min}}\right)^{2s} = o(n). \qquad (4.11)$$

Note that the set $\mathcal{F}_s$ was previously defined in Eqn. (4.1), and it represents the set of valid degree distributions for trees with s edges (and $s+1$ nodes). The set of nonnegative integers in $\mathcal{F}_s$ defines a base of monomials on the set of quantities $\{S_1, ..., S_s\}$. These monomials combine linearly, according to Eqn. (4.10), to yield the expected moments, $\mathbb{E}[m_{2s}(\widetilde{A}_n)]$. In other words, the even expected moments in Eqn. (4.10) are multivariate polynomial expressions in the quantities $\{S_1, ..., S_s\}$.

Regarding the odd expected spectral moments, we prove the following result:

Theorem 4.4.2 *Consider the random matrix ensemble $\mathcal{A}_n(\sigma)$ with $\sigma = (\sigma_1, \sigma_2, ..., \sigma_n)$ satisfying $n\,\sigma_{\max}^2 = o(1)$. Then, the odd expected spectral moments of $\tilde{A}_n \in \mathcal{A}_n(\sigma)$ are:*

$$\mathbb{E}_{\tilde{A}_n \in \mathcal{A}_n(\sigma)}[m_{2s+1}(\tilde{A}_n)] = o(1).$$

Proof (Proof in Appendix B.)

4.4.2 Closed-Form Expressions for Expected Spectral Moments

In this section, we provide explicit symbolic expressions for the multivariate polynomials in Eqn. (4.10). In Appendix C, we describe an algorithm to compute the exact polynomial expressions of the expected spectral moments in an efficient manner. The cost of computing the $2s$-th order spectral moment by this algorithm is the same as that of computing the set of integer partitions of $s+1$. Optimal algorithms to generate integer partitions work in $O(\mathcal{P}(N))$ time [213], where $\mathcal{P}(N)$ is the number of partitions of an integer N. Since the number of partitions fulfills $\mathcal{P}(N) = \Theta\left(N^{-1}\exp\left(N^{1/2}\right)\right)$ [17], the cost of computing the $2s$-th moment is $\Theta\left(s^{-1}\exp\left(s^{1/2}\right)\right)$.

We use the algorithm in Appendix C to compute the following symbolic multi-

variate polynomials for the first few even expected spectral moments of $\mathcal{A}_n(\sigma)$:

$$\begin{aligned}
\mathbb{E}_{\widetilde{A}_n \in \mathcal{A}_n(\sigma)}[m_2(\widetilde{A}_n)] &= (1+o(1))\frac{1}{n}\left(S_1^2\right), \\
\mathbb{E}_{\widetilde{A}_n \in \mathcal{A}_n(\sigma)}[m_4(\widetilde{A}_n)] &= (1+o(1))\frac{1}{n}\left(2S_1^2 S_2\right), \\
\mathbb{E}_{\widetilde{A}_n \in \mathcal{A}_n(\sigma)}[m_6(\widetilde{A}_n)] &= (1+o(1))\frac{1}{n}\left(2S_1^3 S_3 + 3S_1^2 S_2^2\right), \\
\mathbb{E}_{\widetilde{A}_n \in \mathcal{A}_n(\sigma)}[m_8(\widetilde{A}_n)] &= (1+o(1))\frac{1}{n}(2S_1^4 S_4 + 8S_1^3 S_2 S_3 + 4S_1^2 S_2^3), \\
\mathbb{E}_{\widetilde{A}_n \in \mathcal{A}_n(\sigma)}[m_{10}(\widetilde{A}_n)] &= (1+o(1))\frac{1}{n}(2S_1^5 S_5 + 10S_1^4 S_2 S_4 + 5S_1^4 S_3^2 \\
&\quad +20S_1^3 S_2^2 S_3 + 5S_1^2 S_2^4),
\end{aligned} \tag{4.12}$$

We illustrate the utility of these expressions in the following numerical example:

Example Consider a random ensemble of 500×500 symmetric matrices, $\mathcal{A}_{500}(\sigma)$, with random entries $\widetilde{a}_{ij}$ distributed according to a uniform distribution in the interval $[-w_{ij}, w_{ij}]$ (thus, the mean and variance of the (i,j)-th entry are $\mathbb{E}[\widetilde{a}_{ij}] = 0$ and $Var[\widetilde{a}_{ij}] = w_{ij}^2/3$). We can fit the pattern of variances $Var[\widetilde{a}_{ij}] = \sigma_i \sigma_j$ for a particular sequence $(\sigma_i)_{1 \le i \le n}$ using $w_{ij} = \sqrt{3\,\sigma_i \sigma_j}$. In this particular example, we study the spectral moments of $\mathcal{A}_{500}(\sigma)$ for the following affine sequence: $\sigma = \{\sigma_k = 10 - k/100,$ for $k = 1, 2, ..., 500\}$. We presents our results in Table 4.1. The second column of this table shows the values of the analytical expectation obtained from Eqns. (4.12). In the third column we list the corresponding empirical spectral moments from one realization of this random matrix (i.e., without averaging over multiple realizations). The last column represents the relative error between our analytical estimation and the empirical value. The small relative errors indicate that the random moments concentrate around the analytical expectations.

In the following subsection, we apply the results presented in Theorems 4.4.1 and 4.4.2 to study a classical result by Füredi and Komlós regarding the spectral moments of random matrices with entries having identical variances [84]. We then apply our results in Section 4.6 to study the eigenvalue distribution of random graphs with a given expected degree sequence, i.e., Chung-Lu graph.

$2s$-th order	Analytical Expectation	Numerical Realization	Relative Error
$m_2(\widetilde{A}_n)$	2.8088e+004	2.8024e+004	0.23 %
$m_4(\widetilde{A}_n)$	1.6363e+009	1.6237e+009	0.77 %
$m_6(\widetilde{A}_n)$	1.2075e+014	1.1870e+014	1.69 %
$m_8(\widetilde{A}_n)$	1.0040e+019	9.7485e+018	2.90 %
$m_{10}(\widetilde{A}_n)$	8.9736e+023	8.5881e+023	4.30 %

Table 4.1: Analytical expectations and numerical values for the even expected spectral moments of the random matrix defined in the example.

4.4.3 Spectral Moments for Identical Entries

The random matrix ensemble $\mathcal{A}_n(\sigma)$ generalizes the ensemble studied in [84]. We recover their results for the particular case of $\sigma_i = \sigma$ for all i. In this case, we have that $S_k = n\,\sigma^k$, and the expected even spectral moments from Theorem 4.4.1 become:

$$\begin{aligned}\mathbb{E}[m_{2s}(\widetilde{A}_n)] &= (1+o(1))\, n^{-1} \sum_{\mathbf{r}\in\mathcal{F}_s} 2\binom{s}{r_1,\ldots,r_s} \prod_{i=1}^{s} n^{r_i}\sigma^{i r_i} \\ &= (1+o(1))\, n^s\sigma^{2s} \sum_{\mathbf{r}\in\mathcal{F}_s} 2\binom{s}{r_1,\ldots,r_s}, \end{aligned} \tag{4.13}$$

where we have used $\sum_j r_j = s+1$ and $\sum_j j r_j = 2s$ (from the definition of the set $\mathcal{F}_s$) to derive the second equality. In Subsection 4.5.2, Corollary 4.5.6, we shall show that:

$$\sum_{\mathbf{r}\in\mathcal{F}_s} 2\binom{s}{r_1,\ldots,r_s} = \frac{1}{s+1}\binom{2s}{s}. \tag{4.14}$$

Thus, the moment sequence in Eqn. (4.13) becomes:

$$\mathbb{E}\left[m_{2s}(\widetilde{A}_n)\right] = (1+o(1))\, n^s\sigma^{2s}\frac{1}{s+1}\binom{2s}{s}. \tag{4.15}$$

We use the bound $\frac{1}{s+1}\binom{2s}{s} \leq 2^{2s}$ (proved in [198]), to deduce:

$$\mathbb{E}\left[m_{2s}(\widetilde{A}_n)\right] \leq \left(2\sigma\sqrt{n}\right)^{2s}.$$

We also have that $\mathbb{E}[\lambda_{\max}^{2s}(\widetilde{A}_n)] \leq \mathbb{E}[\sum_i \lambda_i^{2s}(\widetilde{A}_n)] = n\,\mathbb{E}\left[m_{2s}(\widetilde{A}_n)\right]$; thus, via Markov's inequality, one can prove the following (see [198] for a detailed derivation):

$$\mathbb{P}\left(\lambda_{\max}(\widetilde{A}_n) \geq 2\sigma\sqrt{n} + cn^{1/2-\delta}\log n\right) = o(1). \tag{4.16}$$

For $\delta = 1/6$, we recover a bound reminiscent of Füredi and Komlós' result in Eqn. (4.8).

In the following section, we provide the details concerning the proof of Theorem 4.4.1.

4.5 Proof of Theorem 4.4.1: Expected Spectral Moments of Even Order

In this section, we use the method of moments introduced in Section 4.3 to prove Theorem 4.4.1. According to Eqn. (4.7), the k-th expected spectral moment of a real symmetric $n \times n$ matrix, $\widetilde{A}_n = [\widetilde{a}_{ij}]$, can be written as:

$$m_k(\widetilde{A}_n) = n^{-1}\mathrm{tr}\,\widetilde{A}_n^k \tag{4.17}$$

$$= \frac{1}{n}\sum_{i_1,i_2,\ldots,i_k=1}^{n} \widetilde{a}_{i_1 i_2}\widetilde{a}_{i_2 i_3}\ldots\widetilde{a}_{i_{k-1} i_k}\widetilde{a}_{i_k i_1}, \tag{4.18}$$

The sequence of subindices in the above summation, $(i_1, i_2, ..., i_k, i_1)$, can be interpreted as a closed-walk of length k in the complete graph with n nodes, K_n. We denote the corresponding walk by $\mathbf{c}_k := (i_1, i_2, ..., i_k, i_1)$ (where we allow repeated nodes in $\mathbf{c}_k$). We denote by $\mathbf{c}_k(j)$ the j-th node visited by the walk $\mathbf{c}_k$. Associated with a specific closed walk $\mathbf{c}_k$, we define the following variable $\widetilde{\omega}(\mathbf{c}_k)$:

$$\widetilde{\omega}(\mathbf{c}_k) := \widetilde{a}_{i_1 i_2}\widetilde{a}_{i_2 i_3}\ldots\widetilde{a}_{i_{k-1} i_k}\widetilde{a}_{i_k i_1}, \tag{4.19}$$

We also denote by $C_k^{(n)}$ the set of all closed walks of length k in K_n. Thus, we can rewrite Eqn. (4.18) as:

$$m_k(\widetilde{A}_n) = \frac{1}{n} \sum_{\mathbf{c}_k \in C_k^{(n)}} \widetilde{\omega}(\mathbf{c}_k). \tag{4.20}$$

Denote by $\mathcal{E}(\mathbf{c}_k)$ the set of undirected edges in the closed walk $\mathbf{c}_k$ (independently of the direction it is used in the walk), i.e.,

$$\mathcal{E}(\mathbf{c}_k) = \{(i,j) : \mathbf{c}_k(s) = i \text{ (or } j) \text{ and } \mathbf{c}_k(s+1) = j \text{ (or } i),\ 1 \leq s \leq k-1\}.$$

We denote by $\mathcal{V}(\mathbf{c}_k)$ the set of nodes visited in $\mathbf{c}_k$. We also denote by m_{ij} the number of times that the edge (i,j) appears in the closed walk $\mathbf{c}_k$ (either as (i,j) or as (j,i)). Therefore, we can rewrite Eqn. (4.19) as:

$$\widetilde{\omega}(\mathbf{c}_k) = \prod_{(i,j) \in \mathcal{E}(\mathbf{c}_k)} \widetilde{a}_{ij}^{m_{ij}}. \tag{4.21}$$

Eqn. (4.20) involves a summation over the set of walks of k steps in K_n, $C_k^{(n)}$. It is useful to partition this set of closed walks, $C_k^{(n)}$, into subsets $C_{k,p}^{(n)}$ of closed walks of length k covering exactly p nodes, i.e.,

$$C_{k,p}^{(n)} \equiv \left\{ \mathbf{c}_k \in C_k^{(n)} \text{ s.t. } |\mathcal{V}(\mathbf{c}_k)| = p \right\}. \tag{4.22}$$

Using this partition, we have from Eqn. (4.20) that

$$m_k(\widetilde{A}_n) = \frac{1}{n} \sum_{p=1}^{k} \sum_{\mathbf{c}_k \in C_{k,p}^{(n)}} \widetilde{\omega}(\mathbf{c}_k). \tag{4.23}$$

Consider now a random matrix ensemble, $\mathcal{A}_n$. We can use (4.23) to compute the

expected spectral moments in the ensemble as

$$\mathbb{E}_{\widetilde{A}_n \in \mathcal{A}_n}[m_k(\widetilde{A}_n)] = \frac{1}{n} \sum_{p=1}^{k} \sum_{\mathbf{c}_k \in C_{k,p}^{(n)}} \mathbb{E}_{\widetilde{A}_n \in \mathcal{A}_n}[\widetilde{\omega}(\mathbf{c}_k)]. \tag{4.24}$$

We define

$$\mu_{k,p}(\mathcal{A}_n) := \frac{1}{n} \sum_{\mathbf{c}_k \in C_{k,p}^{(n)}} \mathbb{E}_{\widetilde{A}_n \in \mathcal{A}_n}[\widetilde{\omega}(\mathbf{c}_k)]. \tag{4.25}$$

Hence, we can rewrite (4.24) as

$$\mathbb{E}_{\widetilde{A}_n \in \mathcal{A}_n}[m_k(\widetilde{A}_n)] = \sum_{p=1}^{k} \mu_{k,p}(\mathcal{A}_n). \tag{4.26}$$

In the following, we prove that only a subset of walks in $C_{k,p}^{(n)}$ has a non-zero contribution to the summation (4.25). In particular, the set of walks presenting a non-zero weight is identified as follows:

$$\widehat{C}_{k,p}^{(n)} \equiv \left\{ \mathbf{c}_k \in C_{k,p}^{(n)} \text{ s.t. } m_{ij} \geq 2 \text{ for all } (i,j) \in \mathcal{E}(\mathbf{c}_k) \right\}. \tag{4.27}$$

In other words, $\widehat{C}_{k,p}^{(n)}$ is the subset of walks of $C_{k,p}^{(n)}$ in which each edge is used at least twice, regardless of the direction. In particular, we prove the following lemma:

Lemma 4.5.1 *For* $\mathbf{c}_k \in C_{k,p}^{(n)} \backslash \widehat{C}_{k,p}^{(n)}$, *we have:*

$$\mathbb{E}_{\widetilde{A}_n \in \mathcal{A}_n}[\widetilde{\omega}(\mathbf{c}_k)] = 0.$$

Proof Since $\mathbb{E}[\widetilde{a}_{ij}] = 0$, the expectation of $\widetilde{\omega}(\mathbf{c}_k)$ in Eqn. (4.21) is non-zero only if each edge appears in the walk $\mathbf{c}_k$ at least twice, i.e., $m_{ij} \geq 2$ for all $(i,j) \in \mathcal{E}(\mathbf{c}_k)$ (where m_{ij} is the multiplicity of the undirected edge (i,j) in the walk). Thus, $\mathbf{c}_k$ must be in $\widehat{C}_{k,p}^{(n)}$ for $\mathbb{E}[\widetilde{\omega}(\mathbf{c}_k)]$ to be non-zero.

This lemma implies that (4.25) can be redefined as:

$$\mu_{k,p}(\mathcal{A}_n) = \frac{1}{n} \sum_{c_k \in \widehat{C}_{k,p}^{(n)}} \mathbb{E}_{\widetilde{A}_n \in \mathcal{A}_n} \left[\widetilde{\omega}\left(\mathbf{c}_k\right) \right]. \tag{4.28}$$

In the next section, we analyze $\mu_{k,p}(\mathcal{A}_n)$ for different values of k and p. We shall show that for $k = 2s$ the above summation is dominated by the term $\mu_{2s,s+1}(\widetilde{A}_n)$. This term is associated with the set of closed walks of length $2s$ visiting $s+1$ nodes. We also show that these closed walks present a very particular structure. This structure is specially amenable to combinatorial analysis, which allows us to derive exact closed-form expressions for $\mu_{k,p}(\mathcal{A}_n)$.

4.5.1 Probabilistic Analysis of Closed Walks

In this subsection, we prove that for $k = 2s$ the term $\mu_{2s,s+1}(\mathcal{A}_n(\sigma))$ dominates the summation in Eqn. (4.26) for the random matrix $\mathcal{A}_n(\sigma)$ defined in Definition 4.4.1. As mentioned above, $\mu_{2s,s+1}(\mathcal{A}_n(\sigma))$ is related to closed walks of length $2s$ visiting $s+1$ nodes. These walks present a structure amenable to combinatorial analysis. In coming sections, we exploit the special structure of these walks to derive a closed-form expression for $\mu_{2s,s+1}(\mathcal{A}_n(\sigma))$.

First, from Eqn. (4.26) and for $k = 2s$, we have that:

$$\mathbb{E}_{\widetilde{A}_n \in \mathcal{A}_n}[m_{2s}(\widetilde{A}_n)] = \mu_{2s,s+1}(\mathcal{A}_n) + \sum_{p<s+1} \mu_{2s,p}(\mathcal{A}_n) + \sum_{p>s+1} \mu_{2s,p}(\mathcal{A}_n).$$

We prove that (under appropriate technical conditions) the term $\mu_{2s,s+1}(\widetilde{A}_n)$ dominates the above summation. Our result reads as follows:

Lemma 4.5.2 *Consider the random matrix ensemble $\mathcal{A}_n(\sigma)$ in Definition 4.4.1. The even expected spectral moments of $\mathcal{A}_n(\sigma)$ satisfy*

$$\mathbb{E}_{\widetilde{A}_n \in \mathcal{A}_n(\sigma)}[m_{2s}(\widetilde{A}_n)] = (1 + o(1))\ \mu_{2s,s+1}(\mathcal{A}_n(\sigma)),$$

if the sequence $\sigma = (\sigma_1, \sigma_2, ..., \sigma_n)$ *satisfies:*

$$\frac{s^6}{\sigma_{\max}^2}\left(\frac{\sigma_{\max}}{\sigma_{\min}}\right)^{2s} = o(n).$$

In order to prove the above lemma, we study the order of magnitude of $\mu_{2s,p}(\widetilde{A}_n)$ for different values of p. Specifically, we prove the following:

Lemma 4.5.3 *Consider the random matrix ensemble* $\mathcal{A}_n(\sigma)$ *in Definition 4.4.1. Then, for* $\mu_{k,p}(\mathcal{A}_n(\sigma))$ *in Eqn. (4.28), we have that:*

(i) $\mu_{2s,p}(\mathcal{A}_n(\sigma)) = 0$, *for* $p > s+1$.

(ii) $\mu_{2s,s+1}(\mathcal{A}_n(\sigma)) \geq n^s \frac{1}{s+1}\binom{2s}{s}\sigma_{\min}^{2s}$.

(iii) $\mu_{2s,p}(\mathcal{A}_n(\sigma)) = o(1)\mu_{2s,s+1}(\mathcal{A}_n(\sigma))$, *for* $p < s+1$,

if the sequence $\sigma = (\sigma_1, \sigma_2, ..., \sigma_n)$ *satisfies:*

$$\frac{s^6}{\sigma_{\max}^2}\left(\frac{\sigma_{\max}}{\sigma_{\min}}\right)^{2s} = o(n).$$

Proof (We include the proof of this lemma in Appendix D.)

Obviously, Lemma 4.5.2 is a direct consequence of Lemma 4.5.3. These lemmas allow us to approximate the even expected spectral moments of the random matrix ensemble $\mathcal{A}_n(\sigma)$ by $\mu_{2s,s+1}(\mathcal{A}_n(\sigma))$. Although we give a complete proof of Lemma 4.5.3 in Appendix D, we mention the main ideas behind our proofs in this section.

According to Eqn. (4.28), the computation of $\mu_{2s,s+1}(\mathcal{A}_n(\sigma))$ involves a summation over the set of closed walks $\widehat{C}_{k,p}^{(n)}$. Walks in $\widehat{C}_{k,p}^{(n)}$ are closed walks of length k, visiting exactly p nodes, and each edge in the walk is visited at least twice. As we prove in Appendix D, each walk $\mathbf{c}_k \in \widehat{C}_{2s,s+1}^{(n)}$ presents the following features:

1. Each edge in $\mathcal{E}(\mathbf{c}_k)$ is visited exactly twice (each time in a different direction).

2. Edges in $\mathcal{E}(\mathbf{c}_k)$ are distributed according to a tree-like structure with $s+1$ nodes (see Fig. 4-2 for an example of a walk in $\widehat{C}^{(n)}_{2s,s+1}$).

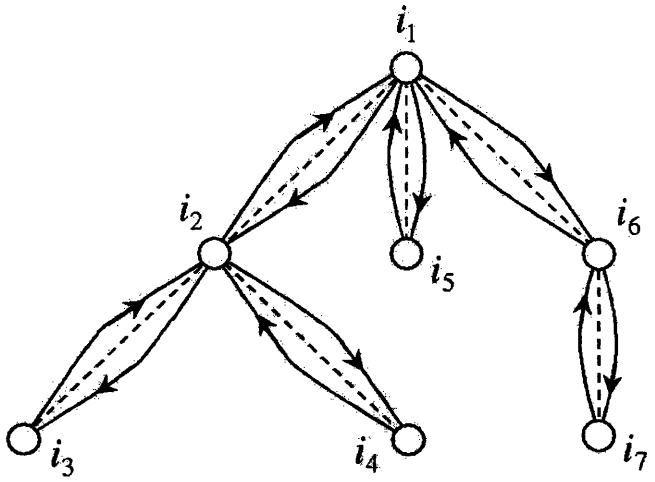

Figure 4-2: We represent a closed walk $\mathbf{c}_k$ of length 12 over 7 nodes in the dominant family of walks, $\widehat{C}^{(n)}_{2s,s+1}$. In this walk, we can observe the main features of this family: *(i)* the edges of the walk are distributed over an underlying tree, and *(ii)* each branch of the tree is visited exactly twice by the walk (each time in a different direction).

As we mentioned above, the edges of the walks in $\widehat{C}^{(n)}_{2s,s+1}$ (plotted as solid lines in Fig. 4-2) are confined to be in an underlying tree (plotted using dashed lines in Fig. 4-2). A walk $\mathbf{c}_k \in \widehat{C}^{(n)}_{2s,s+1}$ visits each branch in the underlying tree exactly twice, each time in a different direction. In Appendix D, we codify each walk in the dominant set $\widehat{C}^{(n)}_{2s,s+1}$ using its underlying tree.

Obviously, the underlying tree alone does not uniquely codify a closed walk $\mathbf{c}_k$. In order to have a unique codification for each walk, we must include two extra features to the codifying trees. First, we must indicate the starting node of the closed walk. We assign the starting node to be the root of the tree; hence, the codifying structure is a rooted tree. Apart from a starting node, we must also indicate the order in which the nodes in the tree are visited by the closed walk. We indicate this order by defining a total order over the set of $s+1$ nodes of the underlying tree. Thus, the codifying structure turns out to be an ordered rooted tree (ORT). (We provided a formal definition of this combinatorial structure in Section 4.1.) In Appendix D, we

define a bijection between the set of dominant closed walks, $\widehat{C}^{(n)}_{2s,s+1}$, and the set of ORTs with $s+1$ nodes chosen from the set $\{1,...,n\}$. This bijection allows us to count the number of closed walks in $\widehat{C}^{(n)}_{2s,s+1}$ by counting the number of ORTs spanning $s+1$ nodes chosen from the set $\{1,...,n\}$.

The following example illustrates how to codify the closed walk in Fig. 4-2 using an ORT:

Example Let us consider the walk represented in Fig. 4-2. The walk is defined by the following ordered sequence of nodes: $(i_1, i_2, i_3, i_2, i_4, i_2, i_1, i_5, i_1, i_6, i_7, i_6, i_1)$. (In Fig. 4-2, we represent each step in the walk with a solid directed arc.) We now illustrate the steps one can take to codify this walk using an ORT:

Step 1: We define the set of branches of the underlying tree, which we denote by $T_s(\mathbf{c}_k)$. These branches are represented by dashed lines in Fig. 4-2.

Step 2: The root of the ORT is defined by the starting node in the walk, i_1.

Step 3: The total order in the set of nodes is induced by the order in which nodes are visited by $\mathbf{c}_k$. Thus, the ordered set of nodes is: $(i_1, i_2, i_3, i_2, i_4, i_2, i_1, i_5, i_1, i_6, i_7, i_6, i_1)$. We can codify an ORT using, for example, prefix notation [188]. In particular, the ORT associated with the walk in Fig. 4-2 can be represented by the prefix code: $(i_1\,(i_2\,(i_3, i_4)\,, i_5, i_6\,(i_7)))$.

The features observed in the dominant walks, $\mathbf{c}_k \in \widehat{C}^{(n)}_{2s,s+1}$, allow us to rewrite $\mu_{2s,s+1}(\mathcal{A}_n)$ in a more convenient form. Since each edge in the closed walk $\mathbf{c}_k \in \widehat{C}^{(n)}_{2s,s+1}$ is visited exactly twice, we can write Eqn. (4.21) as:

$$\widetilde{\omega}\,(\mathbf{c}_k) = \prod_{(i,j)\in\mathcal{E}(\mathbf{c}_k)} \widetilde{a}^2_{ij}, \text{ for } \mathbf{c}_k \in \widehat{C}^{(n)}_{2s,s+1}.$$

We substitute the above expression in Eqn. (4.28) to derive:

$$\mu_{2s,s+1}(\mathcal{A}_n) = \frac{1}{n} \sum_{\mathbf{c}_k\in\widehat{C}^{(n)}_{2s,s+1}} \prod_{(i,j)\in\mathcal{E}(\mathbf{c}_k)} \mathbb{E}_{\widetilde{A}_n\in\mathcal{A}_n}[\widetilde{a}^2_{ij}], \tag{4.29}$$

where we have used independence of the random variables $\widetilde{a}_{ij}$ in order to shift the expectation inside the multiplication symbol.

We now translate Eqn. (4.29) into graph-theoretical terms. We denote by $\mathcal{T}_{s+1}$ the set of ORTs spanning $s+1$ nodes. Also, for a given ORT $\tau \in \mathcal{T}_{s+1}$, we denote by $\mathcal{E}(\tau)$ the set of branches in τ. Our translation of Eqn. (4.29) into graph-theoretical terms takes place in two steps:

1. First, consider a given walk $\mathbf{c}_k \in \widehat{C}_{2s,s+1}^{(n)}$, and denote by τ its underlying ORT. Since $\mathcal{E}(\mathbf{c}_k) \equiv \mathcal{E}(\tau)$, we can write the expectation of Eqn. (4.21) as:

$$\mathbb{E}_{\widetilde{A}_n \in \mathcal{A}_n}[\widetilde{\omega}(\mathbf{c}_k)] = \prod_{(i,j)\in\mathcal{E}(\tau)} \mathbb{E}_{\widetilde{A}_n \in \mathcal{A}_n}[\widetilde{a}_{ij}^2].$$

2. In the second step, we use the bijection between closed walks and ORTs described earlier in this section. This bijection associates each closed walk $\mathbf{c}_k \in \widehat{C}_{2s,s+1}^{(n)}$ to two ingredients: *(i)* a set of $s+1$ nodes chosen from $\{1,...,n\}$, and *(ii)* an ORT spanning those $s+1$ nodes (this ORT indicates the order in which those $s+1$ nodes are visited by the closed walk $\mathbf{c}_k$). Hence, we can substitute the summation over $\mathbf{c}_k \in \widehat{C}_{2s,s+1}^{(n)}$ in Eqn. (4.29) by the following double summation:

$$\mu_{2s,s+1}(\mathcal{A}_n) = \frac{1}{n} \sum_{1\le i_1,...,i_{s+1}\le n} \sum_{\tau\in\mathcal{T}_{s+1}} \prod_{(i,j)\in\mathcal{E}(\tau)} \mathbb{E}[\widetilde{a}_{ij}^2]. \tag{4.30}$$

In the following section, we exploit this graph-theoretical framework to deduce a closed-form expression (4.30) by combinatorial means.

4.5.2 Combinatorial Analysis of Dominant Closed Walks

In this section we derive an exact asymptotic expression for the even expected spectral moments, $\mathbb{E}_{\widetilde{A}_n \in \mathcal{A}_n(\sigma)}[m_{2s}(\widetilde{A}_n)]$. In our proof, we use several results regarding ordered rooted trees (ORTs) and ordered rooted forests (ORFs). Our first lemma allows us to

count the number of ORFs presenting a given δ-degree distribution, $\rho = (\rho_0, \rho_1, ..., \rho_m)$ (see Section 4.1 to review terminology).

Lemma 4.5.4 *Let* $\rho = (\rho_0, \rho_1, ..., \rho_s) \in \mathbb{N}^{s+1}$, *with* $\sum_i \rho_i = s$ *and* $\sum_i (1-i)\,\rho_i = t > 0$. *Then, the number,* $\mathcal{R}(\rho)$, *of ORFs (with* s *vertices and* t *components) with a* δ*-degree distribution* $\rho = (\rho_0, \rho_1, ..., \rho_m)$ *(i.e.* ρ_i *vertices have* i *successors) is given by:*

$$\mathcal{R}(\rho) = \frac{t}{s}\binom{s}{\rho_0, \rho_1, ..., \rho_m}.$$

Proof (The proof can be found in [188], lemma 5.3.10, with minor nomenclature modifications.)

The following lemma allows us to count the number of ORTs presenting a given degree sequence, $\mathbf{r} = (r_1, ..., r_e)$:

Lemma 4.5.5 *Let* $\mathbf{r} = (r_1, ..., r_s) \in \mathbb{N}^s$, *with* $\sum_i r_i = s + 1$ *and* $\sum_i i\,r_i = 2s > 0$. *Then the number* $\nu(\mathbf{r})$ *of ORTs (with* $s + 1$ *nodes) presenting a degree distribution* $\mathbf{r} = (r_1, ..., r_e)$ *is given by:*

$$\nu(\mathbf{r}) = 2\binom{s}{r_1, r_2, ..., r_s}.$$

Proof (Proof in Appendix E.)

Note that the first line in Lemma 4.5.5 indicates that $\mathbf{r}$ is a valid degree distribution for a tree with $s + 1$ nodes. We now use the above lemma to derive the following result:

Corollary 4.5.6 *Let* $\mathbf{r} = (r_1, ..., r_e) \in \mathbb{N}^e$. *Then,*

$$\sum_{\mathbf{r} \in \mathcal{F}_s} 2\binom{s}{r_1, ..., r_s} = \frac{1}{s+1}\binom{2s}{s},$$

where $\mathcal{F}_s$ *is the set of sequences of nonnegative integers defined in (4.1).*

Proof (Proof in Appendix E.)

In the rest of this section we use the above results to prove the following theorem:

Theorem 4.5.7 *Consider the random matrix ensemble $\mathcal{A}_n(\sigma)$, with $\sigma = \{\sigma_1, ..., \sigma_n\}$ (defined in Definition 4.4.1). Then, the term $\mu_{2s,s+1}(\mathcal{A}_n(\sigma))$ (defined in Eqn. (4.25)) is given by*

$$\mu_{2s,s+1}(\mathcal{A}_n(\sigma)) = n^{-1} \sum_{(r_1,...,r_s)\in\mathcal{F}_s} 2\binom{s}{r_1, r_2, ..., r_s} \prod_{j=1}^{s} S_j^{r_j},$$

where $\mathcal{F}_s$ is the set of sequences of nonnegative integers defined in (4.1), and $S_k = \sum_j \sigma_j^k$.

Proof For the random matrix $\widetilde{A}_n \in \mathcal{A}_n(\sigma)$, we have that $\mathbb{E}[\widetilde{a}_{ij}^2] = \sigma_i\sigma_j$. Therefore, from Eqn. (4.30), we have that:

$$\mu_{2s,s+1}(\mathcal{A}_n(\sigma)) = \frac{1}{n} \sum_{1\le i_1,...,i_{s+1}\le n} \sum_{\tau\in\mathcal{T}_{s+1}} \prod_{i\in\mathcal{E}(\tau)} \sigma_i\sigma_j. \tag{4.31}$$

For a given tree τ, one can easily prove that:

$$\prod_{(i,j)\in\mathcal{E}(\tau)} \sigma_i\sigma_j = \prod_{i\in\mathcal{V}(\tau)} \sigma_i^{d_\tau(i)},$$

where $\mathcal{V}(\tau)$ denotes the set of nodes in τ, and $d_\tau(i)$ is the degree of node i in τ. Thus, Eqn. (4.31) can be written as:

$$\mu_{2s,s+1}(\mathcal{A}_n(\sigma)) = \frac{1}{n} \sum_{\tau\in\mathcal{T}_{s+1}} \left(\sum_{1\le i_1,...,i_{s+1}\le n} \prod_{i\in\mathcal{V}(\tau)} \sigma_i^{d_\tau(i)} \right), \tag{4.32}$$

where we have interchanged the order of the summations in Eqn. (4.31).

We now analyze the summation inside the parenthesis in Eqn. (4.32). Consider an ORT τ with $s+1$ nodes and degree sequence $(d_\tau(1), ..., d_\tau(s+1))$. Then, the

term inside the parenthesis in Eqn. (4.32) can be rewritten as:

$$\begin{aligned}\sum_{1\leq i_1,\ldots,i_{s+1}\leq n}\prod_{i\in\mathcal{V}(\tau)}\sigma_i^{d_\tau(i)} &= \sum_{i_1=1}^{n}\sum_{i_2=1}^{n}\cdots\sum_{i_{s+1}=1}^{n}\sigma_{i_1}^{d_\tau(1)}\sigma_{i_2}^{d_\tau(2)}\ldots\sigma_{i_{s+1}}^{d_\tau(s+1)}\\ &= S_{d_\tau(1)}S_{d_\tau(2)}\ldots S_{d_\tau(s+1)}\\ &= S_1^{r_\tau(1)}S_2^{r_\tau(2)}\ldots S_s^{r_\tau(s)},\end{aligned} \tag{4.33}$$

where $S_k := \sum_i \sigma_i^k$, and $(r_\tau(1), r_\tau(2), ..., r_\tau(s))$ is the degree distribution of the underlying tree τ. Hence, we can rewrite Eqn. (4.32) as:

$$\mu_{2s,s+1}(\mathcal{A}_n(\sigma)) = \frac{1}{n}\sum_{\tau\in\mathcal{T}_{s+1}}\left(\prod_{j=1}^{s}S_j^{r_j}\right), \tag{4.34}$$

where, to simplify notation, we define $r_j = r_\tau(j)$.

Furthermore, denote by $\mathcal{T}_{s+1}(\mathbf{r})$ the subset of $\mathcal{T}_{s+1}$ consisting of ORTs with $s+1$ nodes presenting a given degree distribution $\mathbf{r} = (r_1, ..., r_s)$. Also, the set of all valid degree distributions for trees with $s+1$ nodes is given by $\mathcal{F}_s$ (defined in Section 4.1 ,Eqn. (4.1)). Therefore, we can partition the set $\mathcal{T}_{s+1}$ as:

$$\mathcal{T}_{s+1} \equiv \bigcup_{\mathbf{r}\in\mathcal{F}_s}\mathcal{T}_{s+1}(\mathbf{r}).$$

Using the above partition of $\mathcal{T}_{s+1}$, we can rewrite (4.34) as:

$$\mu_{2s,s+1}(\mathcal{A}_n(\sigma)) = \frac{1}{n}\sum_{\mathbf{r}\in\mathcal{F}_s}\sum_{\tau\in\mathcal{T}_{s+1}(\mathbf{r})}\left(\prod_{j=1}^{s}S_j^{r_j}\right). \tag{4.35}$$

Observe that the term inside the parenthesis in the above equation depends *exclusively* on the degree distribution of τ, i.e., $\mathbf{r} = (r_1, ..., r_s)$. Hence, we can move this term outside the second summation as follows:

$$\mu_{2s,s+1}(\mathcal{A}_n(\sigma)) = \frac{1}{n}\sum_{\mathbf{r}\in\mathcal{F}_s}\left(\prod_{j=1}^{s}S_j^{r_j}\right)\sum_{\tau\in\mathcal{T}_{s+1}(\mathbf{r})}1. \tag{4.36}$$

Finally, the last summation in Eqn. (4.36) counts the number of ORTs with a

given degree distribution $\mathbf{r}$, i.e., $|\mathcal{T}_{s+1}(\mathbf{r})|$. Lemma 4.5.5 provides us with a closed-form solution to this counting problem. Hence, using Lemma 4.5.5 in Eqn. (4.36), we have that:

$$\mu_{2s,s+1}(\mathcal{A}_n(\sigma)) = \frac{1}{n}\sum_{\mathbf{r}\in\mathcal{F}_s} 2\binom{s}{r_1,\ldots,r_s}\prod_{j=1}^{s} S_j^{r_j} \tag{4.37}$$

This concludes the proof of Theorem (4.5.7).

From Lemmas 4.5.7 and 4.5.2 the following expression for the even expected spectral moments is straightforward:

$$\mathbb{E}_{\widetilde{A}_n\in\mathcal{A}_n(\sigma)}[m_{2s}(\widetilde{A}_n)] = (1+o(1))\,\frac{1}{n}\sum_{\mathbf{r}\in\mathcal{F}_s} 2\binom{s}{r_1,\ldots,r_s}\prod_{j=1}^{s} S_j^{r_j}$$

(valid under the conditions of Lemma 4.5.2). This concludes the proof of Theorem 4.4.1.

We should also mention that the proof of Lemma 4.5.7 holds, with small variations, when the pattern of variances of $\widetilde{A}_n$ is $\mathbb{E}[\widetilde{a}_{ij}^2] = (1+o(1))\,\sigma_i\sigma_j$ (i.e., a small perturbation of the rank-one pattern defined in Definition 4.4.1). In this case, the final expression for $\mu_{2s,s+1}(\mathcal{A}_n)$ includes a small-order perturbation, i.e.,

$$\mu_{2s,s+1}(\mathcal{A}_n) = (1+o(1))\,n^{-1}\sum_{\mathbf{r}\in\mathcal{F}_s} 2\binom{s}{r_1,r_2,\ldots,r_s}\prod_{j=1}^{s} S_j^{r_j}.$$

Therefore, we can apply the expression in Theorem 4.4.1 to compute the even expected spectral moments of the centralized adjacency matrix $\widetilde{A}_n$ associated with a Chung-Lu random graph $\mathcal{G}(\mathbf{w})$.

4.6 The Eigenvalues of Chung-Lu Random Graphs with Given Expected Degree Sequence

In this section, we apply Theorems 4.4.1 and 4.4.2 to compute the expected spectral moments of the random adjacency matrix associated with the Chung-Lu model. Notice that this random adjacency matrix, denoted by $A_n(\mathbf{w})$, does not fulfill the conditions of applicability of Theorems 4.4.1 and 4.4.2. In this section, we present an approach that allows us to apply those theorems to $A_n(\mathbf{w})$.

First, we motivate our approach with the following numerical example. Consider a Chung-Lu random graph with an affine expected degree sequence: $w_i = 10 - 4i/500$, for $i = 1, 2, ..., 500$. In Fig. 4-3 (a) we plot one random realization of the empirical eigenvalue histogram of $A_n(\mathbf{w})$. From this figure, we draw the following observations:

(i) Most graph eigenvalues fall within a well-defined bulk.

(ii) The largest eigenvalue (spectral radius) is located outside this bulk.

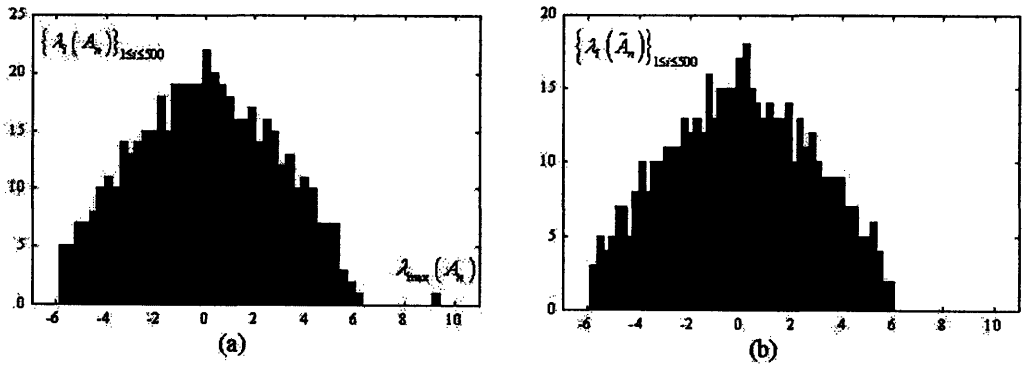

Figure 4-3: In (a) we plot the eigenvalue histogram of the adjacency matrix A_n for $n = 500$. We observe a bulk of 499 eigenvalues and one isolated maximum eigenvalue, $\lambda_{\max}(A_n)$. In (b) we represent the histogram for the centralized adjacency matrix $\widetilde{A}_n$.

In the following, we show that these observations are common to Chung-Lu random graphs with expected degree sequences satisfying certain technical conditions.

In our derivations, we use the following result by Chung et al. concerning the spectral radius of this random graph ensemble [58]:

Theorem 4.6.1 *Consider the Chung-Lu random graph ensemble* $\mathcal{G}_n(\mathbf{w})$ *with* $\mathbf{w} = (w_1, w_2, ..., w_n)$. *Define*

$$W_1 = \sum_{i=1}^{n} w_i, \text{ and } W_2 = \sum_{i=1}^{n} w_i^2. \tag{4.38}$$

Then the maximum eigenvalue of the adjacency matrix, $A_n := A_n(\mathbf{w})$, *satisfies:*

$$\lambda_{\max}(A_n) = (1 + o(1))\, W_2/W_1, \tag{4.39}$$

almost surely, assuming that:

$$W_2/W_1 > \sqrt{w_{\max}} \log n. \tag{4.40}$$

Under condition (4.40), we observe empirically that the eigenvector associated with $\lambda_{\max}(A_n)$ is highly concentrated around the vector $\mathbf{w} = (w_1, w_2, ..., w_n)$. This observation can be made plausible by analyzing the following equation:

$$A_n\, \mathbf{w} = \lambda \mathbf{w} + \varepsilon, \tag{4.41}$$

where we assume the vector ε is not collinear with $\mathbf{w}$. (Notice that if $\mathbf{w}$ were an eigenvector of A_n, the 'error' vector ε would be zero.) We have that the expectation of the left-hand side of (4.41) satisfies $\mathbb{E}[A_n\, \mathbf{w}] = \mathbb{E}[A_n]\, \mathbf{w} = \rho \mathbf{w}\mathbf{w}^T\mathbf{w} = (W_2/W_1)\, \mathbf{w}$. Hence, applying expectations to both sides of (4.41), we have that

$$(W_2/W_1)\, \mathbf{w} = \mathbb{E}[\lambda]\, \mathbf{w} + \mathbb{E}[\varepsilon].$$

This requires that either $\mathbb{E}[\varepsilon]$ is collinear with $\mathbf{w}$, or that

$$\begin{aligned} \mathbb{E}[\lambda] &= (W_2/W_1), \\ \mathbb{E}[\varepsilon] &= 0. \end{aligned}$$

Assuming the latter case, and noting that (W_2/W_1) is the asymptotic value for $\lambda_{\max}(A_n)$ in Theorem 4.6.1, we surmise that the eigenvector associated with $\lambda_{\max}(A_n)$ is highly concentrated around $\mathbf{w}$ under condition (4.40). We shall assume this in what follows, and our experiments based on this assumptions yield good results. A rigorous demonstration is left to future work.

In the following, we illustrate how to apply Theorem 4.4.1 in order to compute the expected spectral moments of a Chung-Lu graph satisfying Eqn. (4.40). The adjacency matrix $A_n(\mathbf{w})$ does not satisfy the conditions defining the class of matrices studied in Section 4.4.1; thus, Theorem 4.4.1 is not directly applicable. Specifically, there are two reasons for which the random adjacency matrix, $A_n(\mathbf{w})$, does not satisfy these conditions:

(R1) The mean of the random adjacency matrix $A_n(\mathbf{w})$ is

$$\mathbb{E}[A_n] = [\rho w_i w_j] = \rho \mathbf{w}\mathbf{w}^T,$$

where $\mathbf{w} = (w_1, w_2, ..., w_n)^T$ is a column vector. Thus, the entries have non-zero mean.

(R2) The random entries a_{ij} of A_n have variance

$$Var[a_{ij}] = \rho w_i w_j (1 - \rho w_i w_j).$$

This pattern of variances does not follow the rank-one pattern of variances described in the definition of $\mathcal{A}_n(\sigma)$.

In the following, we show how to overcome both *(R1)* and *(R2)*. To overcome *(R1)*, we remove the mean from the entries, a_{ij}, and study the effect of this removal

on the spectral moments. We term this process of average removal as *centralization.* The resulting matrix is

$$\widetilde{A}_n = A_n - \mathbb{E}[A_n] = [\widetilde{a}_{ij}],$$

which we call the centralized adjacency matrix. (Notice that the variance of the entries of $\widetilde{A}_n$ is still given by the expression in *(R2).*) Centralization of the adjacency matrix modifies the distribution of eigenvalues in an interesting manner. We illustrate the effects of centralization with a particular numerical example. Consider the expected degree sequence

$$w_i = 10 - 4i/500, \ i = 1, 2, ..., 500, \tag{4.42}$$

and its associated random adjacency matrix, $A_n(\mathbf{w})$. In Fig. 4-3 (b), we plot the histogram of the centralized adjacency matrix, $\widetilde{A}_n$. In this figure, we observe the following effects of centralization:

(E1) removal of the largest isolated eigenvalue, $\lambda_{\max}(A_n)$;

(E2) slight perturbation of the bulk of eigenvalues.

To understand why *(E1)* and *(E2)* hold for random adjacency matrices $A_n(\mathbf{w})$ with $\mathbf{w}$ satisfying Eqn. (4.40), we argue as follows. Assuming that, under the condition in Eqn. (4.40), the largest eigenvalue $\lambda_1 = \lambda_{\max}(A_n)$ has algebraic multiplicity 1, we can decompose $A_n(\mathbf{w})$ as

$$A_n(\mathbf{w}) = \sum_{i=1}^{n} \lambda_i \Phi_i = \lambda_1 \Phi_1 + \widehat{A}_n, \tag{4.43}$$

where

$$\Phi_1 = \mathbf{v}_1 \mathbf{v}_1^T / \left\| \mathbf{v}_1 \right\|^2,$$

and $\mathbf{v}_1$ is the eigenvector associated with λ_1. The matrix $\widehat{A}_n$ has the same eigenvalues as $A_n(\mathbf{w})$, except that the eigenvalue at λ_1 is replaced by an eigenvalue at 0. As we mentioned above, we also assume that the eigenvector $\mathbf{v}_1$ concentrates around $\mathbf{w}$ (under the condition in Eqn. (4.40)). Thus, we can approximate Φ_1 as

$$\Phi_1 \approx \mathbf{w}\mathbf{w}^T / \|\mathbf{w}\|^2 = \frac{W_1}{W_2}\mathbb{E}[A_n(\mathbf{w})].$$

This implies that

$$\lambda_1 \Phi_1 \approx \mathbb{E}[A_n(\mathbf{w})].$$

Substituting the above equation in (4.43), we find

$$A_n(\mathbf{w}) - \mathbb{E}[A_n(\mathbf{w})] \approx \widehat{A}_n.$$

In other words, under our stated assumptions, adjacency centralization removes the largest isolated eigenvalue and does not significantly perturb the bulk of eigenvalues.

Since the bulk of eigenvalues is only slightly perturbed, we can approximate the spectral moments of the bulk of eigenvalues of A_n using the spectral moments of $\widetilde{A}_n$. In Table 4.2, we compare the spectral moments of one random realization of the centralized adjacency matrix, $\widetilde{A}_n$, with the moments of the bulk of eigenvalues of the adjacency matrix, A_n, for $\mathbf{w}$ defined in Eqn. (4.42). We observe a remarkable matching in the even moments. We also observe odd moments are noticeably smaller than even moments (which indicates a tendency to an even symmetry in the distribution).

Since we know the location of the maximum eigenvalue (given by Theorem 4.6.1), we can quantify the effect of its removal on the spectral moments. In particular, one can easily prove that the effect on the k-th moment is to subtract $(1 + o(1))n^{-1}(W_2/W_1)^k$ from $m_k(A_n)$, i.e.,

$$m_k(A_n) \approx m_k(\widetilde{A}_n) + \frac{1}{n}\left(\frac{W_2}{W_1}\right)^k.$$

We include Table 4.3 to compare the numerical value of one random realization of the spectral moments of the adjacency, $m_k(A_n)$, to the moments of the approximation, $m_k(\widetilde{A}_n) + n^{-1}(W_2/W_1)^k$. We again observe a remarkable matching in the even moments. Odd moments are notably smaller than even moments (due to the asymptotic even symmetry in the bulk of eigenvalues).

k-th moment	m_k(Bulk of A_n)	$m_k(\tilde{A}_n)$	Relative Error
1	−0.0187	−0.0163	12.8%
2	7.7724	7.8148	0.54%
3	−0.5179	−0.3973	23.2%
4	133.4119	134.6208	0.90%

Table 4.2: Comparison of one numerical realization of the spectral moments of the bulk of eigenvalues of A_n to the moments of the centralized adjacency $\widetilde{A}_n$.

k-th moment	$m_k(A_n)$	$m_k(\tilde{A}_n) + n^{-1}(W_2/W_1)^k$	Relative Error
1	0.0000	0.0000	–
2	7.9480	7.9480	0.0004%
3	1.1280	0.6905	38.78%
4	148.8360	143.5001	3.58%

Table 4.3: Comparison of one numerical realization of the spectral moments of A_n to the moments of the centralized adjacency $\widetilde{A}_n$ including the correcting term $\frac{(W_2/W_1)^k}{n}$.

In the following, we use adjacency centralization to overcome the difficulty described in *(R1)*. In order to overcome *(R2)*, we must first study the pattern of variances of the (centralized) adjacency matrix, $\widetilde{A}_n$. The variances of the entries are

$$Var[\widetilde{a}_{ij}] = \rho w_i w_j (1 - \rho w_i w_j),$$

which do not follow the pattern in Definition 4.4.1. In this chapter, we are interested in studying bounded expected degree sequences, i.e., $w_i \leq D < \infty$. In this case, one can easily prove that $\rho w_i w_j = o(1)$; thus,

$$Var[\widetilde{a}_{ij}] = (1 + o(1))\rho w_i w_j.$$

In other words, the (centralized) adjacency matrix presents an 'almost' rank-one

pattern of variances. At the end of Subsection 4.5.2, we prove that Theorem 4.4.1 is also applicable to compute the expected spectral moments of $\widetilde{A}_n$ (even though the pattern of variances is not exactly a rank-one matrix). Therefore, we can compute the expected spectral moments of $A_n(\mathbf{w})$ by applying Theorem 4.4.1 with

$$\sigma = \sqrt{\rho}\mathbf{w}. \tag{4.44}$$

In Table 4.4, we compare the empirical spectral moments of one random realization of $\widetilde{A}_n(\mathbf{w})$, with $\mathbf{w} = (10 - 4i/500)_{i=1,2,...,500}$, and the analytical estimation obtained by using Theorem 4.4.1 with $\sigma = \sqrt{\rho}\mathbf{w}$. The relative errors in the last column are reasonably small, specially for small-order moments. We shall show, in the last section of this chapter, how these errors tend to zero for asymptotically large networks.

$2s$-th moment	$m_{2s}(\widetilde{A}_n)$	$\mathbb{E}[m_{2s}(\widetilde{A}_n)]$, for $n \to \infty$	Relative Error
2	7.9278	7.9960	0.86 %
4	135.7157	130.5387	3.81 %
6	3.0028e3	2.6848e3	10.59 %
8	6.5951e4	4.4678e4	32.32 %

Table 4.4: Comparison of one numerical realization of the even spectral moments of $\widetilde{A}_n$ to the analytical estimations from Theorem 4.4.1, with $\sigma = \sqrt{\rho}\mathbf{w}$.

In the following subsections, we apply the methodology introduced in this section to compute the expected spectral moments of two random graphs of special importance: random power-law graphs, and random graphs with exponential expected degree sequence.

4.6.1 Spectral Moments of Random Power-Law Graphs

Let us consider the random power-law graph proposed by Chung et al. in [58]. This random graph presents the following expected degree sequence: $w_i = c\,i^{-1/\beta-1}$, for $i = i_0, i_0+1, ..., i_0+n-1$. We can impose a prescribed maximum and average expected

degree, m and d, respectively, by choosing c and i_0 to be:

$$\begin{aligned} c &= \frac{\beta-2}{\beta-1} d n^{\frac{1}{\beta-1}}, \\ i_0 &= n\left(\frac{d(\beta-2)}{m(\beta-1)}\right)^{\beta-1}. \end{aligned}$$

In Figures 4-4 (a) and (b) we include the empirical eigenvalue histograms of A_{PL} and $\widetilde{A}_{PL} := A_{PL} - \mathbb{E}[A_{PL}]$, respectively. As we mentioned in the previous section, centralization of the adjacency matrix has the following effects:

(i) removal of the largest isolated eigenvalue;

(ii) slight perturbation of the bulk of the empirical eigenvalue histogram.

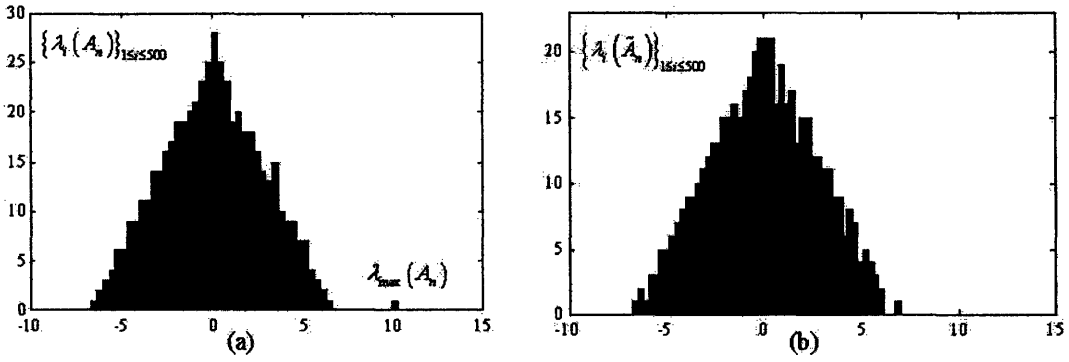

Figure 4-4: Fig. (a) represents the eigenvalue histogram of a random power-law network with $n = 500$, $\beta = 3.0$, $d = 10$, and $m = 20$. In Fig (b), we plot the histogram after adjacency centralization. We observe how the largest isolated eigenvalue is removed by centralization, while the bulk of eigenvalues is slightly perturbed.

We now apply Theorem 4.4.1, with $\sigma = \sqrt{\rho}\mathbf{w}$, to compute the even expected spectral moments of the random power-law graph. First, we must compute the power sum, W_k. We can use the following approximation for W_k:

$$\begin{aligned} W_k &= \sum_{i=i_0}^{i_0+n} w_i^k \approx \int_{i_0}^{i_0+n} c^k x^{-\frac{k}{\beta-1}}\, dx \\ &= \frac{\beta-1}{k+1-\beta}\left(\frac{\beta-2}{\beta-1}\right)^k d^k n\, \Gamma_k(\delta,\beta), \end{aligned}$$

where:

$$\begin{aligned} \Gamma_k(\delta,\beta) &= \delta^{\beta-1-k} - \left(1+\delta^{\beta-1}\right)^{\frac{\beta-1-k}{\beta-1}}, \\ \delta &= \frac{d(\beta-2)}{m(\beta-1)}. \end{aligned}$$

We use these expressions for the power sums, and use the identities $\sum_j r_j = s+1$ and $\sum_j j r_j = 2s$, to derive the following expressions for the expected spectral moments:

$$\mathbb{E}\left[m_{2s}(A_n)\right] = (1+o(1))\,\rho^s n^s \left(\frac{\beta-2}{\beta-1}d\right)^{2s} f_{2s}(\delta,\beta), \tag{4.45}$$

where

$$f_{2s}(\delta,\beta) = 2\sum_{\mathbf{r}\in\mathcal{F}_{2s}} \binom{s}{r_1,\ldots,r_s} \prod_{q=1}^{s} \left(\frac{\beta-1}{q+1-\beta}\Gamma_q(\delta,\beta)\right)^{r_q}.$$

In order to compute f_{2s}, we must determine the set of integer sequences $\mathcal{F}_{2s}$. (This set is the outcome of step (1.d) of the algorithm presented in Appendix C.)

In Table 4.5, we compare evaluations of the symbolic expressions in Eqn. (4.45) with the spectral moments of one random realization of a power-law graph. In this illustration, we use the following set of parameters: $n = 512$ nodes, $\beta = 3.0$, $d = 10$, and $m = 20$. (It is important to notice that the numerical values in the table are obtained for one realization only, with no benefit from averaging.)

$2s$-th order	Analytical Expectation	Numerical Realization	Relative Error
$m_2(\widetilde{A}_n)$	7.7930	7.5899	2.60%
$m_4(\widetilde{A}_n)$	140.9294	140.0645	0.61%
$m_6(\widetilde{A}_n)$	3.4111e3	3.4563e3	1.32%
$m_8(\widetilde{A}_n)$	9.5799e4	9.8988e4	3.32%
$m_{10}(\widetilde{A}_n)$	2.9411e6	3.1152e6	5.91%

Table 4.5: Analytical expectations and numerical values for the even expected spectral moments of the random matrix defined in the example.

4.6.2 Spectral Moments of Random Exponential Graphs

Consider a Chung-Lu random graph with an exponential expected degree sequence: $w_i = m \exp(-\lambda i/n)$, $i = 1, 2, ..., n$, for $\lambda > 0$. In this case, the power sums W_k can be approximated by

$$W_k \approx \frac{n m^k}{\lambda k} \left[1 - \exp(-\lambda k)\right].$$

For simplicity, we assume the maximum expected degree m to be much larger than the average expected degree. Hence, we can approximate the power sums by: $W_k \approx n m^k / \lambda k$. Substituting W_k in the expressions of Theorem 4.4.1, and using the identities: $\sum_j r_j = s + 1$ and $\sum_j j r_j = 2s$, we derive the following expressions for the expected spectral moments of the centralized adjacency $\widetilde{A}_{\exp}$:

$$\mathbb{E}\left[m_{2s}\left(\widetilde{A}_{\exp}\right)\right] = (1 + o(1))\, g_{2s} \frac{\rho^s n^s m^{2s}}{\lambda^{s+1}}.$$

where

$$g_{2s} := \sum_{\mathbf{r} \in \mathcal{F}_{2s}} 2 \binom{s}{r_1, ..., r_s} \prod_{j=1}^{s} \frac{1}{j^{r_j}}.$$

In Table 4.6 we compare analytical expectations of the spectral moments with one random realization for the following values of parameters: $m = 10$, and $\lambda = 1$.

$2s$-th order	Analytical Expectation	Numerical Realization	Relative Error
$m_2(\widetilde{A}_n)$	6.3149	6.4448	2.01 %
$m_4(\widetilde{A}_n)$	86.2937	95.3967	9.54 %
$m_6(\widetilde{A}_n)$	1.5160e3	1.8410e3	17.65 %
$m_8(\widetilde{A}_n)$	2.2150e4	3.0576e4	26.33 %

Table 4.6: Analytical expectations and numerical values for the even expected spectral moments of a random graph with an exponential degree sequence with $m = 10$, and $\lambda = 1$.

4.7 Statistical Convergence of the Spectral Moments

In previous sections, we have studied spectral properties of the random adjacency matrix $A_n = [a_{ij}]$ associated with a random graph ensemble, $\mathcal{G}_n(\mathbf{w})$. As a result of our analysis, we have derived closed-form expressions for the expected spectral moments of this random graph ensemble. As yet, nothing has been formally stated concerning the concentration phenomenon illustrates in Section 4.2. In this section, we focus our attention on studying the concentration properties of the bulk of eigenvalues[1]. As we justified in Section 4.6, the bulk of eigenvalues concentrates around the spectrum of the centralized adjacency matrix $\widetilde{A}_n$. Consequently, in this section we derive concentration results regarding the spectral moments of the centralized adjacency matrix, $m_k(\widetilde{A}_n)$. Specifically, we prove quadratic convergence of the random spectral moments of $\widetilde{A}_n$ around their expectations.

For simplicity in our exposition, we limit our study to Chung-Lu random graphs with uniformly bounded expected degree sequences, i.e., $1 \leq w_i \leq D < \infty$. This case is specially relevant, since it corresponds to degree sequences measured from real-world networks presenting a physical limitation on the maximum number of connections per node.

Our main concentration result reads as follows:

Theorem 4.7.1 *Consider the centralized adjacency matrix $\widetilde{A}_n$ associated with a Chung-Lu random graph $\mathcal{G}_n(\mathbf{w})$ with a uniformly bounded expected degree sequence, $1 \leq w_i \leq D < \infty$. Then,*

$$Var[\bar{m}_k(\widetilde{A}_n)] = O\left(n^{-2}\right).$$

Proof (In Appendix F.)

[1] Concentration properties of the maximum isolated eigenvalue were already studied by Chung et al. in [58].

We illustrate the statement of the above theorem with a numerical example. Consider a random Chung-Lu graph with an expected degree sequence as follows: $w_i = 5 + 5(i/n)$, for $i = 1, ..., n$ (i.e., a degree sequence that grows linearly from 5 to 10 as i grows). In this numerical experiment, we take samples for the empirical spectral moments of the centralized adjacency for random graphs with different sizes. In particular, we choose a set of sizes growing from $n = 10$ to 500 in increments of 10 nodes. For each value of n, we compute the empirical mean and empirical standard deviation from 25 random realizations of the random network. In Fig. 4-5, we plot the evolution of the empirical mean for the first 3 odd and even spectral moments as a function of n, and compare them with their analytical expectations.

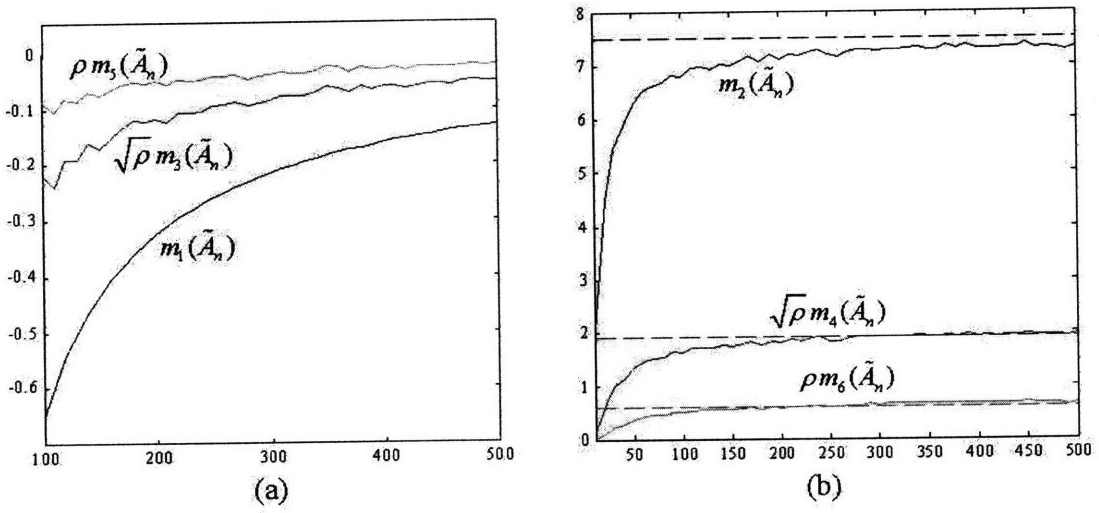

Figure 4-5: In (a) we represent the evolution of odd spectral moments from the above experiment. Observe how odd moments tend to zero for growing network size. This indicates that the limiting empirical spectral density is an even symmetric function. In (b), we represent the evolution of even spectral moments. We also include horizontal dashed lines corresponding to their limiting theoretical values.

More importantly, in Fig. 4-6, we plot the empirical standard deviation as a function of n. From this plot, we observe how the empirical standard deviations decays (though slowly) as the network grows.

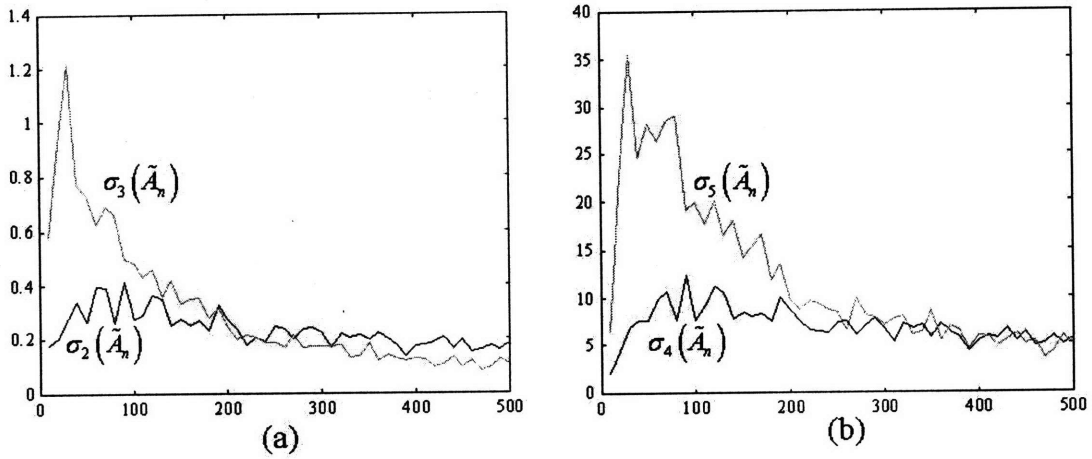

Figure 4-6: In (a), we represent the empirical standard deviation for the second (blue line) and third (green line) spectral moment of $\widetilde{A}_n$ as a function of n, and denoted by $\sigma_2(\widetilde{A}_n)$ and $\sigma_3(\widetilde{A}_n)$, respectively. In (b), we represent the same plot for the forth (blue line) and fifth (green line) moment, denoted by $\sigma_4(\widetilde{A}_n)$ and $\sigma_5(\widetilde{A}_n)$.

Chapter 5

Moment-Based Estimation of Spectral Properties

In the previous chapter we derived closed-form polynomial expressions for the expected spectral moments of static random graphs with a given expected degree sequence. In this chapter we introduce several techniques to extract features of the spectral distribution from a given sequence of spectral moments. In coming chapters, we shall derive expressions for the expected spectral moments of other random graph ensembles. The techniques introduced in this chapter are directly applicable to these other ensembles as well.

The following is an enumeration of techniques introduced in this chapter:

1. *Wigner's high-order method:* We can use this technique to bound the largest eigenvalue of the spectral distribution.

2. *Piecewise-linear reconstruction of the spectrum:* This methodology allows us to compute a piecewise-linear reconstruction of the spectral distribution given a sequence of moments.

3. *Optimal probabilistic bounds via semidefinite programming:* We also discuss a technique that uses semidefinite optimization to find optimal bounds of spectral properties, given a sequence of moments.

5.1 Wigner's High-Order Method

The following methodology, proposed by E.P. Wigner in [203], is useful to derive a probabilistic upper bound on the largest eigenvalue of a random symmetric matrix from the sequence of its spectral moments. Consider a real and symmetric $n \times n$ random matrix, M_n. Denote by $\lambda_1, ..., \lambda_n$ the set of real eigenvalues of M_n, and by $\lambda_{\max}(M_n) = \max_{1 \leq i \leq n} |\lambda_i|$. For even-order expected spectral moments we have the following:

$$\mathbb{E}[m_{2s}(M_n)] = \frac{1}{n} \sum_{i=1}^{n} \mathbb{E}[\lambda_i^{2s}] \geq \frac{1}{n} \mathbb{E}[\lambda_{\max}^{2s}(M_n)]. \tag{5.1}$$

Wigner's method exploits this to deduce an upper bounds on $\lambda_{\max}(M_n)$ from the sequence of high order expected spectral moments.

Consider a sequence of even expected spectral moments $\mathbb{E}[m_{2s}(M_n)]$. The first step in this method is to find positive constants σ, δ, c_1, and c_2, such that $2s = c_2 n^{\delta}$, and

$$\mathbb{E}[m_{2s}(M_n)] \leq c_1 \left(2\sigma\sqrt{n}\right)^{2s}.$$

If the upper-bounding sequence in the right-hand side of the above equation exists, one can derive the following probabilistic upper bound on $|\lambda_{\max}(M_n)|$, [198]:

$$\mathbb{P}\left(|\lambda_{\max}(M_n)| \geq 2\sigma\sqrt{n} + c\, n^{1/2-\delta} \ln n\right) \leq o(1), \tag{5.2}$$

for a sufficiently large c. This technique can be applied, for example, to estimate the spectral support of the Wigner's semicircle law [203].

Example Consider a random symmetric $n \times n$ matrix $\tilde{A}_n = [\tilde{a}_{ij}]$ with random i.i.d. upper-triangular and diagonal entries governed by the following discrete probability

distribution

$$\tilde{a}_{ij} = \begin{cases} -p, & \text{w.p. } 1-p, \\ 1-p, & \text{w.p. } p. \end{cases}$$

(The entries have zero mean $\mu = \mathbb{E}[\tilde{a}_{ij}] = 0$, and variance $\sigma^2 = Var[\tilde{a}_{i,j}] = p(1-p)$. From Theorem 4.4.1, we can compute the following sequence of expected moments:

$$\mathbb{E}\left[m_{2s}(\tilde{A}_n)\right] = (1+o(1))\, n^s \sigma^{2s} \frac{1}{s+1}\binom{2s}{s}.$$

Also, we can use the bound $\frac{1}{s+1}\binom{2s}{s} \leq 2^{2s}$ (found in [198]) to derive

$$\begin{aligned} \mathbb{E}\left[m_{2s}(\tilde{A}_n)\right] &\leq \left(2\sigma\sqrt{n}\right)^{2s} \\ &= \left(2\sqrt{np(1-p)}\right)^{2s}. \end{aligned}$$

Hence, from Eqn. (5.2), we find the following probabilistic bound on $\left|\lambda_{\max}\left(\tilde{A}_n\right)\right|$

$$\mathbb{P}\left(\left|\lambda_{\max}\left(\tilde{A}_n\right)\right| \geq 2\sqrt{np(1-p)} + c\, n^{1/2-\delta} \ln n\right) \leq o(1). \tag{5.3}$$

We now illustrate the above result with a numerical experiment. In Fig. 5-1, we plot the numerical values of $\lambda_{\max}(\tilde{A}_n)$ for one empirical realization of $\tilde{A}_n$ when $n = 500$ and p taking values in the set $\{i/500,\, i = 1, 2, ..., 50\}$. We also plot the values of the dominant term in the probabilistic bound in Eqn. (5.3), i.e., $2\sqrt{np(1-p)}$, for the same values of n and p. Observe that the numerical realization of $\lambda_{\max}(\tilde{A}_n)$ lies near the analytical upper bound $2\sqrt{p(1-p)\,n}$. This suggest that we can use $2\sqrt{p(1-p)\,n}$ as an estimation of $\lambda_{\max}(\tilde{A}_n)$.

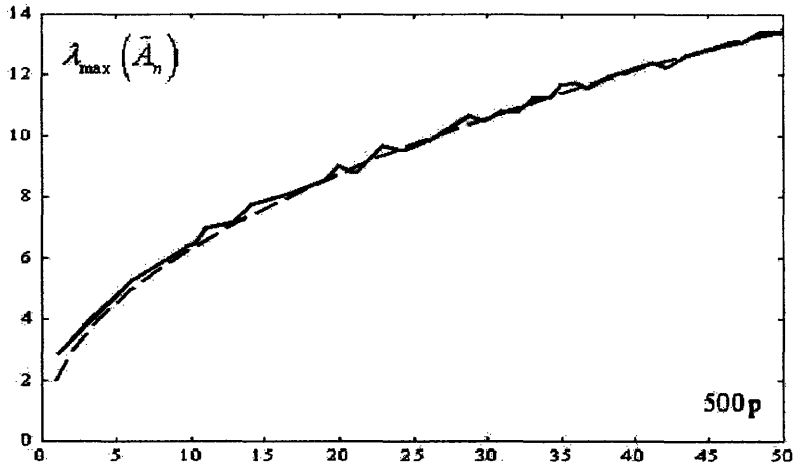

Figure 5-1: We plot the maximum eigenvalue $\lambda_{\max}(\tilde{A}_n)$ for one empirical realization of $\tilde{A}_n$ when $n = 500$ and $p \in \{i/500, i = 1, 2, ..., 50\}$ (blue line). We also plot $2\sqrt{np(1-p)}$ for the same values of n and p (dashed line).

5.2 Piecewise-Linear Reconstruction

In this section we introduce a technique that computes a piecewise-linear (PWL) reconstruction of an unknown spectral density given a sequence of its spectral moments. We present two versions of this methodology:

(i) In the first version, apart from a sequence of spectral moments, we are given an interval containing the spectral support.

(ii) In the second version, we are only given a sequence of three spectral moments (without any prior knowledge of the spectral support).

The methodology introduced in this section yields a PWL function that fits a given truncated sequence of spectral moments. We denote this PWL approximating function as $L_P(\lambda)$, and parameterize it using a set of P points on the plane, $\{(x_i, y_i), i = 1, 2, ..., P\}$, where we set the ordinates y_1 and y_P to be zero (see Fig. 5-2). In this parameterization, we have a total of $2P - 2$ unknown scalar parameters: P corresponding to the unknown abscissae $\{x_p\}_{1 \le p \le P}$, and $P - 2$ corresponding to the ordinates $\{y_p\}_{2 \le p \le P-1}$.

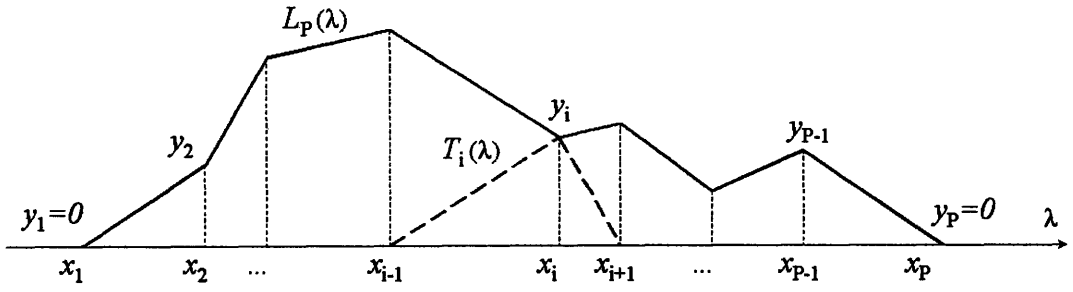

Figure 5-2: Plot of the parameterized version of the piecewise-linear function proposed in this section.

We decompose the PWL function $L_P(\lambda)$ into a linear combination of triangular functions. We denote each triangular function by $T_i(\lambda)$, for $i = 2, ..., P-1$, and parameterize it using three control points in the plane: $\{(x_{i-1}, 0), (x_i, y_i), (x_{i+1}, 0)\}$ (see dashed triangle in Fig. 5-2). Thus, we have the following linear decomposition:

$$L_P(\lambda) = \sum_{i=2}^{P-1} T_i(\lambda).$$

Since moments are linear functionals, the k-th spectral moment of the PWL function, denoted by $m_k(L_P)$, can be written as the sum of the moments of the individual triangles, denoted by $m_k(T_i)$, as follows:

$$m_k(L_P) = \sum_{i=2}^{P-1} m_k(T_i),$$

Furthermore, the k-th spectral moment of each triangular function can be written as

$$\begin{aligned} m_k(T_i) &= y_i \int_{x_{i-1}}^{x_i} x^h \frac{(x - x_{i-1})}{x_i - x_{i-1}} dx \\ &\quad - y_i \int_{x_i}^{x_{i+1}} x^h \frac{(x - x_{i+1})}{x_{i+1} - x_i} dx. \end{aligned}$$

Integrating the above expression, we obtain the following expressions for the moments of the triangular function (after considerable algebraic manipulation) :

$$m_k(T_i) = y_i \frac{2}{(k+1)(k+2)} \left[\frac{N_k(x_{i-1}, x_i, x_{i+1})}{D_k(x_{i-1}, x_i, x_{i+1})} \right], \tag{5.4}$$

where N_k and D_k are the following symmetric[1] polynomials:

$$\begin{aligned} N_k(x_{p-1}, x_p, x_{p+1}) &= x_{p-1}x_p^{k+2} + x_p x_{p+1}^{k+2} + x_{p+1}x_{p-1}^{k+2} \\ &\quad - x_{p-1}^{k+2}x_p - x_p^{k+2}x_{p+1} - x_{p+1}^{k+2}x_p, \end{aligned} \tag{5.5}$$

$$D_k(x_{p-1}, x_p, x_{p+1}) = (x_{p-1} - x_p)(x_p - x_{p+1})(x_{p+1} - x_{p-1}). \tag{5.6}$$

Therefore, the k-th spectral moment of $L_P(\lambda)$ is given by

$$m_k(L_P) = \frac{2}{(k+1)(k+2)} \sum_{i=2}^{P-1} y_i \frac{N_k(x_{i-1}, x_i, x_{i+1})}{D_k(x_{i-1}, x_i, x_{i+1})}. \tag{5.7}$$

Notice that the above expression for the k-th moment is linear in the set of ordinates $\{y_i\}_{i=2,\ldots,P-1}$, but nonlinear in the set of abscissae $\{x_i\}_{i=1,\ldots,P}$. Our final objective is to find a solution for both $\{y_i\}_{i=2,\ldots,P-1}$ and $\{x_i\}_{i=1,\ldots,P}$ given a truncated sequence of moment constrains, i.e.,

$$m_k(L_P) \equiv M_k, \text{ for } k = 0, 1, \ldots, K. \tag{5.8}$$

Despite the difficulties in solving this (nonlinear) system of equations, there are two cases in which we can find a closed-form solution:

(i) In the first case, the abscissae $\{x_i\}_{i=1,\ldots,P}$ are fixed a priori. Hence, the resulting system of equation is linear in the unknowns.

(ii) In the second case, we are given the first three moments of the distribution, but no prior knowledge on the spectral support. In this case, we exploit the

[1] A symmetric function is a multivariate function that takes the same value under any permutation of its arguments.

symmetry in Eqn. (5.7) to solve the nonlinear system of equations efficiently.

5.2.1 Piecewise-Linear Fitting with Fixed Abscissae

As mentioned above, when we fix the abscissae, the system of equations (5.8) becomes linear. Specifically, for a given set $\{x_i\}_{i=1,...,P}$, we define the coefficients

$$\mu_{k,i} = \frac{2}{(k+1)(k+2)} \frac{N_k(x_{i-1}, x_i, x_{i+1})}{D_k(x_{i-1}, x_i, x_{i+1})}, \tag{5.9}$$

for $k = 0, 1, ..., K$ and $i = 2, 3, ..., P-1$, where N_k and D_k are defined in Eqn. (5.5) and (5.6). From Eqn. (5.7) and (5.8), we have

$$\underbrace{\begin{bmatrix} 1 \\ M_1 \\ M_2 \\ \vdots \\ M_K \end{bmatrix}}_{\mathbf{m}} = \underbrace{\begin{bmatrix} \mu_{0,2} & \mu_{0,3} & \cdots & \mu_{0,P-1} \\ \mu_{1,2} & \mu_{1,3} & \cdots & \mu_{1,P-1} \\ \mu_{2,2} & \mu_{2,3} & \cdots & \mu_{2,P-1} \\ \vdots & \vdots & \ddots & \vdots \\ \mu_{K,2} & \mu_{K,3} & \cdots & \mu_{K,P-1} \end{bmatrix}}_{M} \underbrace{\begin{bmatrix} y_2 \\ y_3 \\ \vdots \\ y_{P-1} \end{bmatrix}}_{\mathbf{y}}, \tag{5.10}$$

If we choose the number of ordinates to match the number of given moments, i.e., $P-2 = K$, the matrix M becomes square, and the system of equation can be solved by a simple matrix inversion. We illustrate this technique with the following examples.

Example Without performing an explicit eigenvalue decomposition, we estimate the shape of the eigenvalue distribution of the Kirchhoff matrix K_{PL} associated to one random realization of a random power-law graph (see Subsection 4.6.1).

In this example, we use a piecewise-linear function to fit the shape of the eigenvalue distribution associated to a power-law random graph with paramaters: $n = 512$, $d = 15$, $m = 30$, and $\beta = 3.0$. Given one random realization, we can compute numerical values for the low-order Kirchhoff moments using matrix multiplication,

i.e.,

$$m_q(K_{PL}) = \frac{1}{n}\mathrm{tr}\, K_{PL}^q. \tag{5.11}$$

In our particular case, we compute the following values for the first 8 moments: 11.73, 160.20, 2.58e3, 4.84e4, 1.02e6, 2.34e7, 5.68e8, 1.43e10 (in increasing order of q).

In order to perform a PWL reconstruction, we first need an estimation of the spectral support. Since K_{PL} is positive semidefinite (see Chapter 2), the spectral support is in $[0, \infty)$. We can find several upper bounds on the largest eigenvalue of K_{PL} in the literature. In this example, we use the following simple bound proposed in [134]: let m_i denote the average of the degrees of the neighbors of vertex v_i, i.e.,

$$m_i = \frac{1}{d_i}\sum_{j=1}^{n} a_{ij} d_j.$$

Hence, a simple bound for the largest eigenvalue of K_{PL} is given by

$$\lambda_{\max}(K_{PL}) \leq \max_i d_i + m_i.$$

Using our random realization of the Chung-Lu graph, we compute this upper bound to be 52.65.

Once we have an estimation of the spectral support, we must choose a set of abscissae $\{x_i\}_{1\leq i\leq 10}$. In our case, we divide the region $(0, 52.65)$ into equispaced segments. Finally, applying Eqns. (5.9) and (5.10), we compute the set of unknown abscissae $\{y_i\}_{2\leq i\leq 9}$. We plot our PWL reconstruction in Fig. 5-3.

5.2.2 Triangular Fitting with Unknown Abscissae

In this subsection, we consider the case in which the abscissae are unknown and three spectral moments are given. In this case, we exploit the symmetries of the polynomials in Eqns. (5.5) and (5.6) to find an efficient solution to the problem.

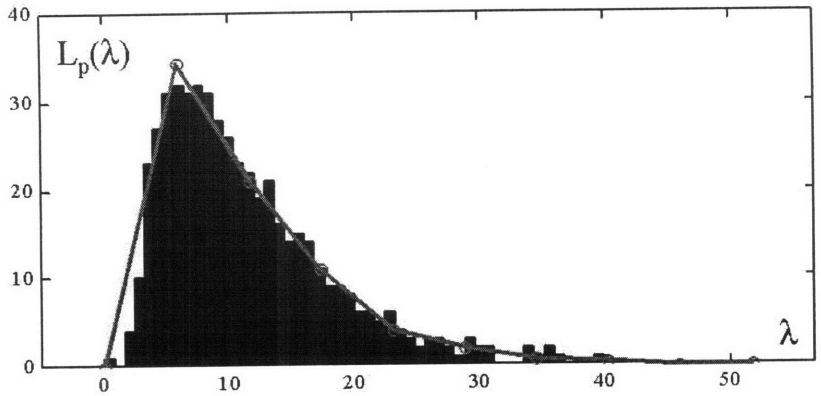

Figure 5-3: Plot of the piecewise-linear reconstruction of the spectrum of K_{PL}. We also include the histogram of eigenvalues in blue.

We present our approach for the case in which only three abscissae, $\{x_1, x_2, x_3\}$, are unknown. The PWL function $L_3(\lambda)$ in this case is a single triangular segment, and its moments are

$$\begin{aligned} M_1 &= \frac{1}{3}(x_1 + x_2 + x_3), \\ M_2 &= \frac{1}{6}\left(x_1^2 + x_2^2 + x_3^2 + x_1x_2 + x_1x_3 + x_2x_3\right), \\ M_3 &= \frac{1}{10}\left(x_1^3 + x_1^2x_2 + x_1^2x_3 + x_2^3 + x_2^2x_1 \right. \\ &\quad \left. + x_2^2x_3 + x_3^3 + x_3^2x_1 + x_3^2x_2 + x_1x_2x_3\right). \end{aligned} \tag{5.12}$$

(In order to compute these moments, we have fixed $y_2 = 2/(x_3 - x_1)$ to force the triangle to have unit area.). In the following, we show how to solve this system of nonlinear equations by exploiting the symmetries of the polynomials involved.

First, we introduce several basic results regarding symmetric polynomials

Definition A symmetric polynomial on q variables $x_1, ..., x_q$ is a polynomial that is unchanged under any permutation of its variables. In other words, the symmetric polynomials satisfy

$$p(y_1, y_2, ..., y_q) = p(x_1, x_2, ..., x_q),$$

where $y_i = x_{\pi(i)}$ and π is an arbitrary permutation of the indices $1, 2, ..., q$.

We now introduce two particular examples of symmetric polynomials. First, complete homogeneous symmetric polynomials (CHSPs) are defined as:

$$h_k(x_1, ..., x_q) := \sum_{i_1+...+i_q=k} x_1^{i_1} ... x_q^{i_q}. \tag{5.13}$$

In other words, $h_k(x_1, ..., x_q)$ is the sum of all monomials of degree k involving q variables. Second, elementary symmetric polynomials (ESPs) are defined as:

$$s_k(x_1, ..., x_q) = \sum_{1 \le i_1 < ... < i_k \le q} x_{i_1} ... x_{i_k}.$$

For example, in the case of three variables, $\{x_1, x_2, x_3\}$, we have

$$\begin{aligned} s_1(x_1, x_2, x_3) &= x_1 + x_2 + x_3, \\ s_2(x_1, x_2, x_3) &= x_1 x_2 + x_1 x_3 + x_2 x_3, \\ s_3(x_1, x_2, x_3) &= x_1 x_2 x_3, \end{aligned}$$

It is useful to express ESPs and CHSPs using the following generating functions [119]:

$$S(x) := \sum_{k=0}^{\infty} s_k(x_1, ..., x_q)\, x^k = \prod_{1 \le i \le q} (1 + x\, x_i), \tag{5.14}$$

$$H(x) := \sum_{k=0}^{\infty} h_k(x_1, ..., x_q)\, x^k = \prod_{1 \le i \le q} \frac{1}{1 - x\, x_i}. \tag{5.15}$$

Notice that the generating functions $S(x)$ and $H(x)$ are related by the equation:

$$S(x)\, H(-x) = 1.$$

Therefore, expanding the above expression, we obtain the following set of equalities:

$$\sum_{r=0}^{q} (-1)^r \, s_r \left(x_1, ..., x_q\right) \; h_{q-r} \left(x_1, ..., x_q\right) = 0. \tag{5.16}$$

We can make this relation more explicit by regarding $h_1, ..., h_q$ as fixed, and considering Eqn. (5.16) as a system of linear equations for $s_1, ..., s_q$. Solving the system of equations, we find that:

$$s_k = \det \begin{bmatrix} h_1 & 1 & 0 & ... & 0 \\ h_2 & h_1 & 1 & ... & 0 \\ ... & ... & ... & ... & ... \\ h_{k-1} & h_{k-2} & h_{k-3} & ... & 1 \\ h_k & h_{k-1} & h_{k-2} & ... & h_1 \end{bmatrix}. \tag{5.17}$$

Another result regarding ESPs is the following [119]:

Claim 5.2.1 *Given the values of the ESPs, $s_i \left(x_1, ..., x_q\right)$, for $i = 1, 2, ..., q$, one can determine the values of the variables $\{x_1, x_2, ..., x_q\}$ as roots of the polynomial*

$$x^q - s_1 x^{q-1} + s_2 x^{q-2} - ... + (-1)^q \, s_q = 0. \tag{5.18}$$

5.2.3 Exploiting Symmetric Polynomials

The first three moments of the triangular function in Eqn. (5.12) can be written in terms of CHSPs as follows:

$$\begin{aligned} M_1 &= \frac{1}{3} h_1 \left(x_1, x_2, x_3\right), \\ M_2 &= \frac{1}{6} h_2 \left(x_1, x_2, x_3\right), \\ M_3 &= \frac{1}{10} h_3 \left(x_1, x_2, x_3\right). \end{aligned} \tag{5.19}$$

From the above equations, we write the CHSPs in terms of the moments, $\{M_1, M_2, M_3\}$, and substitute them in Eqn. (5.17) to derive the following system of equations:

$$\begin{aligned} s_1(x_1, x_2, x_3) &= 3\,M_1, \\ s_2(x_1, x_2, x_3) &= 9\,M_1^2 - 6\,M_2, \\ s_3(x_1, x_2, x_3) &= 27\,M_1^3 - 36\,M_1 M_2 + 10\,M_3. \end{aligned} \tag{5.20}$$

For a set of given moments, we can use the above equations to compute the values of the ESP's, $\{s_1, s_2, s_3\}$. Then, we can use Claim 5.2.1 to compute the abscissae, $\{x_1, x_2, x_3\}$, associated with the triangular function $T_3(\lambda)$ as roots of the following polynomial:

$$x^3 - s_1 x^2 + s_2 x^1 - s_3 = 0. \tag{5.21}$$

As a final comment, the above procedure indicates what triads of moments $\{M_1, M_2, M_3\}$ can be fit using a triangular function. Those triads of moments producing imaginary roots in Eqn. (5.21) cannot be fitted by a triangular function.

Example Without performing an explicit eigenvalue decomposition, and without any prior knowledge of the spectral support, fit a triangular function to the Kirchhoff spectrum of one random realization of a Chung-Lu graph with the following expected degree sequence:

$$w_i = \frac{3}{100}\,(100 - i) + 10, \quad i = 1, 2, ..., 200.$$

We take one random realization of the above Chung-Lu graph, and compute the following values for the Kirchhoff moments using matrix multiplication (Eqn. (5.11)): $M_1 = 1997.542$, $M_2 = 4.793e6$, and $M_3 = 1.392e10$. We substitute these moments in (5.20), and compute the values for the ESP's s_1, s_2, and s_3. We then use the particular values of the ESP's in the polynomial (5.21), and compute the following values of the abscissae: $x_i = \{3594.3,\ 9463.4, 46534.3\}$. In Fig. 5-4, we compare the

histogram of the Kirchhoff eigenvalues with the triangular function preserving its first three moments.

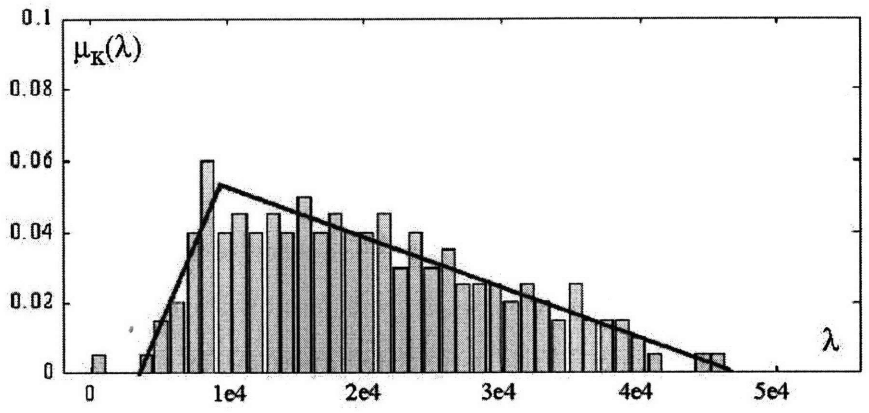

Figure 5-4: Plot of the triangular reconstruction and histogram of eigenvalues.

As a final comment in this section, we should mention that it is not always possible to fit a triangular function to any given three moments. We say that a sequence of three moments, $\{M_1, M_2, M_3\}$, is feasible if there exists a triangular function matching the sequence of moments. In general, a moment sequence $\{M_1, M_2, M_3\}$ is feasible if and only if the roots of the polynomial in (5.21) are all real. Hence, the discriminant of this polynomial provides us with an algebraic criterion to decide whether or not a sequence of moments is feasible.

Using the expressions in (5.20), we can write the discriminant of (5.21) as a function of the sequence of moments, $\{M_1, M_2, M_3\}$. After simple algebraic simplifications, we derive the following algebraic criterion for feasibility of a sequence of three moments:

$$8(M_1^2 - M_2)^3 + 25\,(2\,M_1^3 - 3\,M_1 M_2 + M_3)^2 < 0.$$

5.3 Optimal Spectral Bounds via Semidefinite Programming

In this section, we present a technique to find optimal bounds of spectral properties via semidefinite optimization, given a truncated sequence of moments [29], [120], [64]. A sequence of spectral moments, $\{1, M_1, M_2, ..., M_k\}$, is said to be feasible if there exists a spectral distribution matching the sequence of moments. The problem of deciding whether or not a moment sequence is feasible is called the classical moment problem [5]. Depending on the restrictions we impose on the support of the probability distribution, we find three classical cases:

1. The Hamburger moment problem, where the support is allowed to be the whole real line.

2. The Stieltjes moment problem, where the support is allowed to be within $[0, \infty)$.

3. The Hausdorff moment problem, where the support is in a bounded interval $[a, b]$.

A necessary and sufficient condition for a sequence of moments to be feasible for the Stieltjes moment problem is given by the following matrices being positive semidefinite:

$$R_{2l} = \begin{pmatrix} 1 & M_1 & \cdots & M_l \\ M_1 & M_2 & \cdots & M_{l+1} \\ \vdots & \vdots & \ddots & \vdots \\ M_l & M_{l+1} & \cdots & M_{2l} \end{pmatrix}, \; R_{2l+1} = \begin{pmatrix} M_1 & M_2 & \cdots & M_{l+1} \\ M_2 & M_3 & \cdots & M_{l+2} \\ \vdots & \vdots & \ddots & \vdots \\ M_{l+1} & M_{l+2} & \cdots & M_{2l+1} \end{pmatrix}.$$

for any integer $l \geq 0$. Similarly, a necessary and sufficient condition for a sequence of moments to be feasible for the Hamburger moment problem is that $R_{2\lfloor k/2 \rfloor}$ is positive semidefinite.

In the following subsection, we show how to use semidefinite programming to derive optimal probabilistic bounds on spectral properties from a given sequence of moments.

5.3.1 Notation and Problem Setup

Given a random variable λ, we describe a technique to find the best upper bound on $\mathbb{E}[\phi(\lambda)]$ for a given polynomial $\phi(\lambda)$, when λ satisfies certain moment constraints, $\mathbb{E}[\lambda^i] = M_i$. Given the first k moments $M_1, ..., M_k$ (we fix $M_0 = 1$) of a real random variable λ with domain $\Omega \subseteq \mathbb{R}$, we show how to find tight bounds on $\mathbb{P}(\lambda \in S)$ by solving a single semidefinite optimization problem. An upper bound on $\mathbb{P}(\lambda \in S)$ can be formulated as follows:

$$\begin{array}{rcll} Z_P & = & \text{maximize}_{\mu} & \int_S 1 \, d\mu \\ & & \text{such that} & \int_S \lambda^i \, d\mu = M_i, \quad \text{for } i = 0, 1, 2, ..., k, \end{array} \tag{5.22}$$

where μ is a probability measure that we restrict to be of a particular convex class P.

Using duality theory, one can associate a dual variable y_i to each equality constraint of the primal, and thereby, obtain [120]:

$$\begin{array}{rcll} Z_D & = & \text{minimize}_{y_i} & \sum_{i=1}^{k} y_i M_i \\ & & \text{such that} & g(\lambda) = \sum_{i=1}^{k} y_i \lambda^i \geq 1, \quad \text{for } \lambda \in S, \\ & & & g(\lambda) = \sum_{i=1}^{k} y_i \lambda^i \geq 0, \quad \text{for } \lambda \in \Omega. \end{array} \tag{5.23}$$

In general, the optimum in Problem (5.23) cannot be achieved. Whenever the primal optimum Z_P^* is achieved, we call the corresponding distribution μ^* an extremal distribution. It can be shown that if the truncated moment sequence $\{M_i | i = 0, 1, , ..., k\}$ is an interior point of the set of feasible moment vectors, then strong duality holds ($Z_P^* = Z_D^*$, where Z_P^* and Z_D^* are the optima for the primal and dual problems, respectively).

5.3.2 Tight Bounds as Semidefinite Optimization Problems

In [162], the author show how solve the dual Problem (5.23) using semidefinite programming. Notice that the constraints in this problem are given by the nonnegativity of univariate polynomials. This naturally leads us to investigate conditions for polynomials to be nonnegative. The feasibility region defined by semialgebraic constraints in problem (5.23) can be rewritten using semidefinite constraints, (see [162] for details).

Three interesting particular cases of the above optimization problem are where only *(i)* M_1, *(ii)* M_1, M_2, or *(iii)* M_1, M_2, M_3 are given (corresponding to the choices $k = 1, 2$, or 3 in the preceding development). For these three cases, one can deduce closed-form solutions for the optimization problem.

To present the result, it is helpful to define the squared coefficient of variation as

$$C_M^2 = \frac{M_2 - M_1^2}{M_1^2}.$$

and the third-order coefficient of variation as

$$D_M^2 = \frac{M_1 M_3 - M_2^2}{M_1^4},$$

Assume in the following that $\delta > 0$.

Theorem 5.3.1 *The following table presents tight bounds for $k = 1, 2, 3$ (the bounds marked with an asterisk assume that $\delta < 1$):*

(k, Ω)	$\mathbb{P}(\lambda > (1+\delta) M_1)$	$\mathbb{P}(\lambda > (1-\delta) M_1)$	$\mathbb{P}(\lvert\lambda - M_1\rvert > \delta M_1)$
$(1, \mathbb{R}_+)$	$\frac{1}{1+\delta}$	1^*	1^*
$(2, \mathbb{R})$	$\frac{C_M^2}{C_M^2+\delta^2}$	$\frac{C_M^2}{C_M^2+\delta^2}$	$\min\left(1, \frac{C_M^2}{\delta^2}\right)$
$(3, \mathbb{R}_+)$	$f_1(C_M^2, D_M^2, \delta)$	$f_2(C_M^2, D_M^2, \delta)^*$	$f_3(C_M^2, D_M^2, \delta)^*$

where

$$
\begin{aligned}
f_1\left(C_M^2, D_M^2, \delta\right) &= \begin{cases} \min\left(\frac{C_M^2}{C_M^2+\delta^2}, \frac{1}{1+\delta}\frac{D_M^2}{D_M^2+\left(C_M^2-\delta\right)^2}\right), & \text{if } \delta > C_M^2, \\ \frac{1}{1+\delta}\frac{D_M^2+(1+\delta)\left(C_M^2-\delta\right)}{D_M^2+\left(1+C_M^2\right)\left(C_M^2-\delta\right)}, & \text{if } \delta \leq C_M^2, \end{cases} \\
f_2\left(C_M^2, D_M^2, \delta\right) &= 1 - \frac{\left(C_M^2+\delta\right)^3}{\left(D_M^2+\left(C_M^2+1\right)\left(C_M^2+\delta\right)\right)\left(D_M^2+\left(C_M^2+\delta\right)^2\right)}, \\
f_3\left(C_M^2, D_M^2, \delta\right) &= \min\left(1, 1+3^3\frac{D_M^2+C_M^4-\delta^2}{4+3\left(1+3\delta^2\right)+2\left(1+3\delta^2\right)^{3/2}}\right).
\end{aligned}
$$

We now illustrate how to apply the above result to find bounds on the spectral distribution, given three spectral moments. We consider the Kirchhoff matrix K_{PL} of one random realization of a random power-law graph (see Subsection 4.6.1), with parameters $n = 512$, $m = 30$, $d = 15$, and $\beta = 3.0$. Using (5.11), we compute the first three spectral moments: M_1 =11.733, M_2 =160.200, and M_3 =2.582e3, without performing an explicit eigenvalue decomposition. We can use these moments in Theorem 5.3.1 to compute an upper bound on the complementary cumulative spectral distribution, i.e., $\mathbb{P}(\lambda > x)$, using the last row of the second column in the table in Theorem 5.3.1. We plot our result in Fig. 5-5, where we also include the empirical complementary cumulative spectral histogram (i.e., number of eigenvalues greater than x, in blue bars) for the Kirchhoff matrix under study. Better bounds can be found in [162], but these require further assumptions on the spectral density, such as convexity.

In coming chapters, we shall apply the arsenal of tools developed in this chapter to study spectral properties of random graph models.

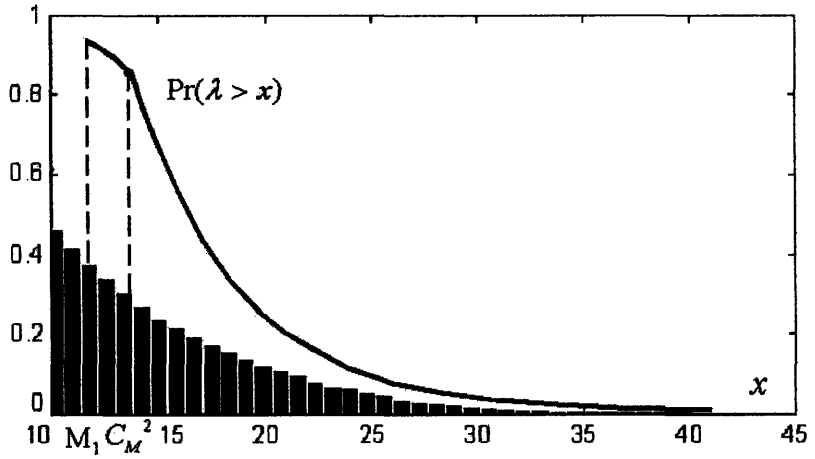

Figure 5-5: Plot of the empirical complementary cumulative spectral histogram (in blue bars), and the upper bound on the complementary cumulative spectral distribution given three spectral moments: M_1 =11.733, M_2 =160.200, and M_3 =2.582e3.

Chapter 6

Spectral Analysis of Dynamically Evolving Networks

Although static random graph ensembles are useful for fitting empirical measurements taken from a real-world network, they do not help us to understand how a real network develops those properties in the first place. As an alternative, dynamically evolving models try to represent the fundamental forces that produce global network characteristics. In a dynamically evolving model, a network grows in time according to a set of evolution rules aiming to replicate the growth processes taking place in a real network.

In recent years, dynamically evolving models (also called dynamic graphs) have been proposed to explain the origin of heavy-tailed degree distributions observed in many real-worlds networks. For example, in the context of the Web graph [113], the number of links per page follows a heavy-tailed distribution (which is usually approximated by a power law). Inspired by these measurements, Barabási and Albert proposed in [24] a network growth process aiming to explain the appearance of power-law degree distributions. The Barabási-Albert (BA) model has two fundamental ingredients:

(i) the sequential addition of nodes;

(ii) the so-called preferential attachment process.

The first ingredient causes the number of nodes in the BA network to grow in time. The second ingredient causes new edges to attach to existing nodes of high degree with a higher probability than to nodes of low degree (in other words, "popularity is attractive").

While many structural characteristics of the BA model are well known, analytical results concerning spectral properties of this model are still an open question. In this chapter, we present new results regarding the moments of the adjacency matrix for the BA model, which can be used to obtain information about the eigenvalue spectrum, using the ideas and tools presented in the previous chapters. Our approach is based on the method of moments [103]. This method allows us to translate the algebraic problem of computing the spectral moments of a graph into the combinatorial problem of counting the number of closed walks of a particular length in the graph.

6.1 Preferential Attachment Model

In this first subsection, we describe the random graph process proposed by Barabási and Albert [24]. Loosely speaking, we start with a particular initial graph, and make it evolve in discrete-time steps. At each time step, we add one new node that has m new edges attached to it. The other end of each new edge attaches to an existing node according to a probabilistic rule. In the particular case of a BA graph, each new edge attaches to an existing node with a probability proportional to the degree of that existing node.

Before we provide a formal description of this model, we introduce our nomenclature. First, for clarity of notation, we match the time slot with the size of the network, i.e., at the n-th discrete time slot, there are n nodes in the network. Hence, the initial time slot, denoted by n_0, is equal to the size of the initial graph configuration. For simplicity, we choose this initial graph to be the complete graph with $2m+1$ nodes. The average degree of our initial graph is obviously equal to $2m$, and one can easily prove that the addition of m edges at each time slot maintains this

average unchanged over time. We denote by v_i the node added at the i-th time slot, and by $d_i[n]$ the degree of v_i at the n-th time slot. We also denote by $N_k[n]$ the number of nodes with degree k at time slot n. For a given i and k, both $d_i[n]$ and $N_k[n]$ are discrete-time stochastic processes that evolve with n.

6.1.1 Algorithmic Description

In this section we provide an algorithmic description of the BA model. The model herein presented is not exactly the one given in [24]; instead, we introduce slight modifications in order to avoid certain mathematical issues that appeared in the original model [38]. The BA model is a random graph process, denoted by $(G_m[n])_{n\geq 2m+1}$, where $G_m[n]$ is a graph with n nodes and m new links per time slot. To each graph $G_m[n]$, we associate an adjacency matrix $A_m[n] = A_n(G_m[n])$.

We describe the random graph process $(G_m[n])_{n\geq 2m+1}$ in algorithmic terms as follows:

1. We choose the complete graph with $n_0 = 2m+1$ nodes, K_{2m+1}, to be our initial graph $G_m[n_0]$. Set $n = n_0 + 1$.

2. Generate $G_m[n]$ by adding to $G_m[n-1]$ a new node, v_n, together with m new edges connected to v_n. The m new edges also connect to a set of m randomly selected nodes in $G_m[n-1]$. We denote the set of m randomly selected nodes at time n by $S_m[n] = \{u_p[n]\}_{1\leq p\leq m}$. The nodes in $S_m[n]$ are iteratively chosen according to the following algorithm:

   (a) *Initialization:* We first define the intermediate variables $d_i^{(p)}[n]$, for $1 \leq i \leq n$ and $1 \leq p \leq m$. We call these variables intermediate degrees. We initialize those variables at $p = 1$ to be: $d_i^{(1)}[n] \equiv d_i[n-1]$, for $1 \leq i \leq n-1$, and $d_n^{(1)}[n] = m$.

(b) *Iterative random growth:* Choose one node from the set $\{v_j\}_{1\leq j\leq n-1}$ to be $u_p[n] \in S_m[n]$ with probability proportional to its intermediate degree, i.e.,

$$\mathbb{P}\left(u_p[n] = v_j\right) = \frac{d_j^{(p)}[n]}{\sum_{k=1}^{n-1} d_k^{(p)}[n]}, \text{ for } 1 \leq j \leq n-1. \tag{6.1}$$

Consider v_i to be the outcome of this random choice, i.e., $u_p[n] = v_i$. Now, upgrade the intermediate degree sequence as follows:

$$\begin{aligned} d_i^{(p+1)}[n] &= d_i^{(p)}[n] + 1, \\ d_r^{(p+1)}[n] &= d_r^{(p)}[n] \text{ for } r \neq i. \end{aligned}$$

Finally, increment p by one.

(c) *Stopping condition:* If $p \leq m$, return to (b) and repeat. If $p = m+1$, we assign $S_m[n]$ to be $\{v_p[n]\}_{1\leq p\leq m}$, increment n by 1 and return to (2).

Several comments are in order. First, since the probability of connection in Eqn. (6.1) is linearly proportional to the degree of v_j, this growth process is usually called linear preferential attachment (LPA). Notice that this process allows the existence of multiple edges between two given nodes, although this event is very rare for large n. Also, it can be proved that different initial graphs give rise to the same asymptotic behavior from a spectral point of view.

6.2 Evolution of Structural Properties

In this section, we review several results regarding dynamically evolving networks. In particular, we discuss about both the evolution of the expected values of the degree distribution $N_k[n]$, and of the degree $d_j[n]$ of the node added at time j. The main technique used in this section, as in the BA paper [24], is the rate equation approach from statistical physics [114], [72].

6.2.1 Degree Distribution

The evolution of the expected number of nodes with degree k, $\mathbb{E}[N_k[n]]$, can be described using the model of bins and balls represented in Fig. 6-1. Each ball in the model represents a node, and the k-th bin represents the collection of nodes with degree k. In other words, the number of balls in the k-th bin at time n is equal to $N_k[n]$.

There are three mechanisms that can modify the number of balls in the k-th bin at a given time n, as illustrated in Fig. 6-1:

(1) If the new node v_n attaches to an existing node of degree $k-1$, then a ball jumps from the $(k-1)$-th bin into the k-th bin.

(2) If the new node v_n attaches to a node of degree k, then a ball jumps out of the k-th bin into the $(k+1)$-th bin.

(3) Every new node v_n is initially attached to m edges; thus, a new ball is placed in the m-th bin at every time slot.

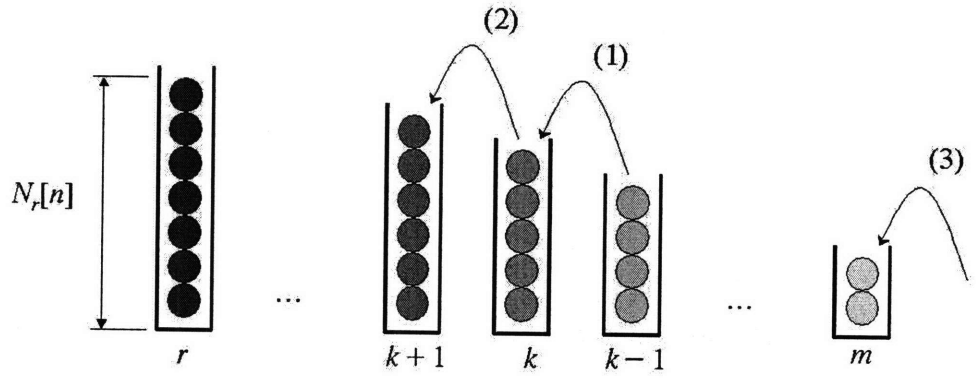

Figure 6-1: Bins-and-balls model for the evolution of the degree distribution.

With these mechanisms in mind, one can write down the following difference equation describing the evolution of the expected number of nodes in the k-th bin

[114]:

$$\mathbb{E}[N_k[n+1]] = \mathbb{E}[N_k[n]] + \frac{k-1}{2n}\mathbb{E}[N_{k-1}[n]] - \frac{k}{2n}\mathbb{E}[N_k[n]] + \delta[k-m], \qquad (6.2)$$

for $k \geq m$. (Notice that for $k < m$, $N_k[n] = 0$ at all times.) The terms in the above difference equation account for the following:

(i) The first term, $\mathbb{E}[N_k[n]]$, accounts for the number of nodes of degree k in the previous time slot.

(ii) The second term, $\frac{k-1}{2n}\mathbb{E}[N_{k-1}[n]]$, accounts for the creation of a node of degree k (if the new node v_n attaches to a node of degree $k-1$).

(iii) The third (negative) term, $\frac{k}{2n}\mathbb{E}[N_k[n]]$, represents the loss of a node of degree k (if v_n attaches to a node of degree k).

(iv) The last term is a discrete Dirac delta (i.e., $\delta[k-m] = 1$ for $k = m$; 0 for $k \neq m$) representing the creation of a new node of degree m at every time slot.

Since we start with the complete graph K_{2m+1} at the $(2m+1)$-th time slot, the initial conditions in Eqn. (6.2) are: $N_{2m}[2m+1] = 2m+1$, and $N_k[2m+1] = 0$, for $k \neq 2m$. The evolution of (6.2) has been studied in several papers [38], [114]. We limit our discussion to the stationary behavior of (6.2) in the limit $n \to \infty$ (as proved in [72], this stationary limit exists). Let us define $\mathcal{N}_k = \lim_{n\to\infty} \mathbb{E}[N_k[n]]/n$. Thus, in the stationary limit, Eqn. (6.2) becomes

$$\mathcal{N}_k = \frac{k-1}{k+m}\mathcal{N}_{k-1}, \text{ for } k > m, \qquad (6.3)$$

with boundary condition $\mathcal{N}_m = m/m+k$ (which is derived from Eqn. (6.2) for $k = m$). Eqn. (6.3) presents the following stationary solution:

$$\mathcal{N}_k = \frac{m}{m+k}\prod_{j=m}^{k-1}\frac{j}{j+m+1} = \frac{m}{m+k}\frac{(k-1)!}{(m-1)!}\frac{(2m+1)!}{(k+m-1)!}. \qquad (6.4)$$

For large degrees k, the stationary distribution in (6.4) can be approximated as $\mathcal{N}_k \propto k^{-m-1}$. In [24], the authors studied the specific case $m = 2$ and derived a degree distribution $\mathcal{N}_k \propto k^{-3}$, which is in accordance with the result in Eqn. (6.4).

6.2.2 Degree Evolution

In this subsection, we review results regarding the evolution of the expected degree of a given node j, i.e., $\mathbb{E}[d_j[n]]$ as n grows [114]. We represent the evolution of $d_j[n]$ using the bins-and-balls model in Fig. 6-2. In this case, bins correspond to individual nodes, and each ball represents an edge connected to that node. The probability of a new ball falling in the j-th bin at time n is equal to: $d_j[n-1]/(2n)$. Accordingly, we can describe the evolution of the expected degree using the following discrete-time equation [114]:

$$\mathbb{E}[d_j[n]] = \mathbb{E}[d_j[n-1]] + \frac{d_j[n-1]}{2n}. \tag{6.5}$$

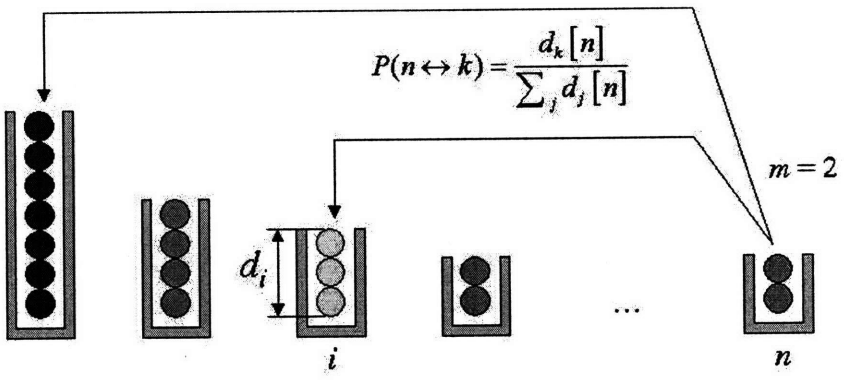

Figure 6-2: Bins-and-balls model for the evolution of the degrees, $d_j[n]$.

We continue our analysis by performing a mean-field approximation of (6.5). In particular, we substitute $d_j[n-1]$ in (6.5) by its expectation to find:

$$\mathbb{E}[d_j[n]] = \mathbb{E}[d_j[n-1]]\left(1 + \frac{1}{2n}\right). \tag{6.6}$$

The solution to the recursion in (6.6) is

$$\mathbb{E}[d_j[n]] = \mathbb{E}[d_j[j]] \prod_{k=j+1}^{n} \left(1 + \frac{1}{2k}\right), \tag{6.7}$$

where $\mathbb{E}[d_j[j]] = m$. Furthermore, for $j \gg 1$, the product in (6.7) can be approximated as follows:

$$\begin{aligned} \prod_{k=j+1}^{n} \left(1 + \frac{1}{2k}\right) &\approx \exp\left(\sum_{k=j+1}^{n} -\frac{1}{2k}\right) \\ &\approx \exp\left(\frac{1}{2}(\log n - \log j)\right) \\ &= \left(\frac{j}{n}\right)^{1/2}. \end{aligned} \tag{6.8}$$

In conclusion, using (6.8) in (6.7), we can approximate the evolution of the expected degree of the j-th node as

$$\mathbb{E}[d_j[n]] \approx m\left(\frac{j}{n}\right)^{1/2}. \tag{6.9}$$

6.3 Expected Spectral Moments for Asymptotically Large Networks

Analytical results regarding spectral properties of dynamically evolving BA graphs are, to our knowledge, an open question. In this section, we deduce approximate closed-form expressions for the spectral moments of $G_m[n]$ for $n \to \infty$. The adjacency matrix $A_m[n]$ associated with a BA graph is a random matrix that evolves in time, i.e., $(A_m[n])_{n>n_0}$ is a random matrix process. Consequently, the k-th spectral moment of this matrix, $m_k(A_m[n])$, is a discrete-time random processes that evolves with n.

In this section we apply the method of moments, introduced in Chapter 4, to study the spectral moments of a BA graph. Consider the adjacency matrix of a BA graph, $A_m[n] = [a_{ij}^{(n)}]$. According to this method, the expected spectral moments of

$A_m[n]$ can be written as

$$\mathbb{E}[m_k(A_m[n])] = \frac{1}{n} \sum_{1 \le i_1, i_2, \ldots, i_k \le n} \mathbb{E}[a_{i_1 i_2}^{(n)} a_{i_2 i_3}^{(n)} \ldots a_{i_{k-1} i_k}^{(n)} a_{i_k i_1}^{(n)}]. \tag{6.10}$$

We now rewrite Eqn. (6.10) using graph-theoretical elements introduced in Subsection 4.3.2. In particular, we use Eqn. (4.7) from Chapter 4, to rewrite (6.10) as follows:

$$\mathbb{E}[m_k(A_m[n])] = \frac{1}{n} \sum_{\mathbf{c}_k \in C_k^{(n)}} \mathbb{E}\left[\omega_{G_m[n]}(\mathbf{c}_k)\right], \tag{6.11}$$

where $\mathbf{c}_k$ is a closed walk of length k, $C_k^{(n)}$ is the set of all closed walks of length k in the complete graph K_n, and $\omega_{G_m[n]}(\mathbf{c}_k)$ is defined as

$$\omega_{G_m[n]}(\mathbf{c}_k) = \prod_{(i,j) \in \mathcal{E}(\mathbf{c}_k)} (a_{ij}^{(n)})^{m_{i,j}}, \tag{6.12}$$

where $\mathcal{E}(\mathbf{c}_k)$ is the set of edges visited by the closed walk $\mathbf{c}_k$, and $m_{i,j}$ is the number of times $\mathbf{c}_k$ visits edge (i,j) (see Chapter 4 for more details). From Eqns. (4.7) and (6.12), we have the following expression for the expected spectral moments of the adjacency matrix:

$$\mathbb{E}[m_k(A_m[n])] = \frac{1}{n} \sum_{\mathbf{c}_k \in C_k^{(n)}} \mathbb{E}[\prod_{(ij) \in \mathcal{E}(\mathbf{c}_k)} (a_{ij}^{(n)})^{m_{ij}}]. \tag{6.13}$$

The above expression is difficult to analyze due to the dependencies among the adjacency entries $a_{ij}^{(n)}$. In the following paragraph we introduce and justify a conjecture that simplifies this analysis.

Recent studies on the correlation properties of several power-law graph models, including the BA model, indicate that correlation among adjacency entries vanishes as the network size grows to infinity. In particular, in [199] the authors studied the asymptotic behavior of the degree correlation coefficient for several scale-free graphs (including the BA model), and concluded that these graphs behave like if uncorrelated

for $n \to \infty$. Based on these results, we propose the following conjecture:

Conjecture 6.3.1 *Consider a BA random graph process, $(G_m[n])_{n \geq n_0}$. Then,*

$$\sum_{\mathbf{c}_k \in C_k^{(n)}} \mathbb{E}[\prod_{(i,j) \in \mathcal{E}(\mathbf{c}_k)} (a_{ij}^{(n)})^{m_{ij}}] \to \sum_{\mathbf{c}_k \in C_k^{(n)}} \prod_{(i,j) \in \mathcal{E}(\mathbf{c}_k)} \mathbb{E}\left[(a_{ij}^{(n)})^{m_{ij}}\right], \tag{6.14}$$

for $n \to \infty$.

Although we have not found a rigorous proof of the above conjecture, subsequent analytical results based on (6.14) are in excellent agreement with numerical simulations. In particular, using the above conjecture in Eqn. (6.13), we have that

$$\mathbb{E}[m_k(A_m[n])] \to \frac{1}{n} \sum_{\mathbf{c}_k \in C_k^{(n)}} \prod_{(i,j) \in \mathcal{E}(\mathbf{c}_k)} \mathbb{E}\left[a_{ij}^{(n)}\right], \tag{6.15}$$

for $n \to \infty$ (where, since $a_{ij}^{(n)}$ is a 0-1 variable, we can remove the power inside the expectation, i.e., $\mathbb{E}[\left(a_{ij}^{(n)}\right)^{m_{ij}}] = \mathbb{E}[a_{ij}^{(n)}]$).

In the following, we study the expectation of the binary random variable $a_{ij}^{(n)}$. Assume $i < j$ (i.e., the i-th node is 'older' than the j-th node). Obviously, there cannot be a connection between v_i and v_j before v_j is created; thus, $a_{ij}^{(q)} = 0$ for $q < j$. At the j-th time slot, the new node v_j might connect to the existing node v_i. According to the linear preferential attachment rule, the probability of this connection is given by

$$\mathbb{P}(a_{ij}^{(j)} = 1) = \frac{d_i[j]}{2j}. \tag{6.16}$$

Note that if v_j does not connect to v_i at the j-th time slot, they will never connect. Furthermore, since in the BA model existing edges are not deleted, we conclude that $a_{ij}^{(j)} = a_{ij}^{(n)}$. Hence, from (6.16), we have

$$\mathbb{E}[a_{ij}^{(n)}] = \mathbb{E}[a_{ij}^{(j)}] = \frac{d_i[j]}{2j}. \tag{6.17}$$

Performing a mean-field approximation of (6.17), i.e., replacing $d_i[j]$ by its expected value, we obtain

$$\mathbb{E}[a_{ij}^{(n)}] \approx \frac{\mathbb{E}[d_i[j]]}{2j}. \tag{6.18}$$

According to (6.9), we have that $\mathbb{E}[d_i[j]] \approx m\sqrt{j/i}$. Hence, (6.18) becomes

$$\mathbb{E}[a_{ij}^{(n)}] \approx \frac{m/2}{\sqrt{ij}}, \ i < j \leq n. \tag{6.19}$$

(Notice that the same exact argument, with the same exact result, holds for $j < i \leq n$.)

In the following, we use the above results to derive a closed-form expression for the asymptotic value of $\mathbb{E}[m_k(A_m[n])]$. Our approach is based on constructing a Chung-Lu static random graph, $\mathcal{G}_n(\mathbf{w})$, with expected spectral moments matching those of $A_m[n]$ for $n \to \infty$. In particular, we define a random graph ensemble $\mathcal{G}_n(\mathbf{w})$ with the following prescribed expected degree sequence:

$$\mathbf{w} = (w_i)_{1 \leq i \leq n} \text{ with } w_i = m\sqrt{\frac{n}{i}}. \tag{6.20}$$

The adjacency matrix, $A_n = A_n(\mathbf{w}) = [a_{ij}]$, is a symmetric matrix with upper-triangular independent random entries satisfying

$$\mathbb{P}(a_{ij} = 1) = \mathbb{E}[a_{ij}] = \rho w_i w_j. \tag{6.21}$$

For the degree sequence in (6.20), we can approximate ρ as follows:

$$\rho = \left(\sum_i w_i\right)^{-1} \approx \left(\int_1^n m\sqrt{\frac{n}{x}}dx\right)^{-1} \approx \frac{1}{2mn},$$

for $n \to \infty$. Thus, from (6.20) and (6.21) we have

$$\begin{aligned} \mathbb{E}[a_{ij}] &\approx \frac{1}{2mn} w_i w_j \\ &= \frac{m/2}{\sqrt{ij}}. \end{aligned} \tag{6.22}$$

Notice that, although formally equivalent, the expressions in (6.22) and (6.19) correspond to a static and a dynamic random graph, respectively. This observation will be key in subsequent derivations.

We now argue that the expected spectral moments of $A_m[n]$ (the adjacency matrix of a dynamic random graph) tend to the moments of A_n (the adjacency matrix of a static random graph) for $n \to \infty$ (under Conjecture 6.3.1). Applying the method of moments to the random adjacency matrix A_n, we find

$$\mathbb{E}[m_k(A_n)] = \frac{1}{n} \sum_{\mathbf{c}_k \in C_k^{(n)}} \prod_{(i,j) \in \mathcal{E}(\mathbf{c}_k)} \mathbb{E}[a_{ij}], \tag{6.23}$$

Since $\mathbb{E}[a_{ij}]$ in Eqn. (6.22) is (asymptotically) the same as $\mathbb{E}[a_{ij}^{(n)}]$ in Eqn. (6.19), we have that $\mathbb{E}[m_k(A_n)]$ in (6.23) is asymptotically equal to the right-hand side of (6.15); therefore,

$$\mathbb{E}[m_k(A_m[n])] \to \mathbb{E}[m_k(A_n)], \tag{6.24}$$

for $n \to \infty$. In other words, we can approximate the asymptotic expected spectral moments of the BA model using the expected spectral moments of a Chung-Lu random graph $\mathcal{G}_n(\mathbf{w})$ with $\mathbf{w}$ defined in (6.20).

We illustrate (6.24) with the following numerical example. In Fig. 6-3, we plot the eigenvalue histograms for the following two random graphs:

(R1) A Barabási-Albert dynamic graph with $m = 6$ and $n = 3000$.

(R2) A Chung-Lu static graph with $w_i = 6\sqrt{3000/i}$ for $i = 1, ..., 3000$.

In agreement with the result in (6.24), we observe a remarkable similarity between

both eigenvalue histograms.

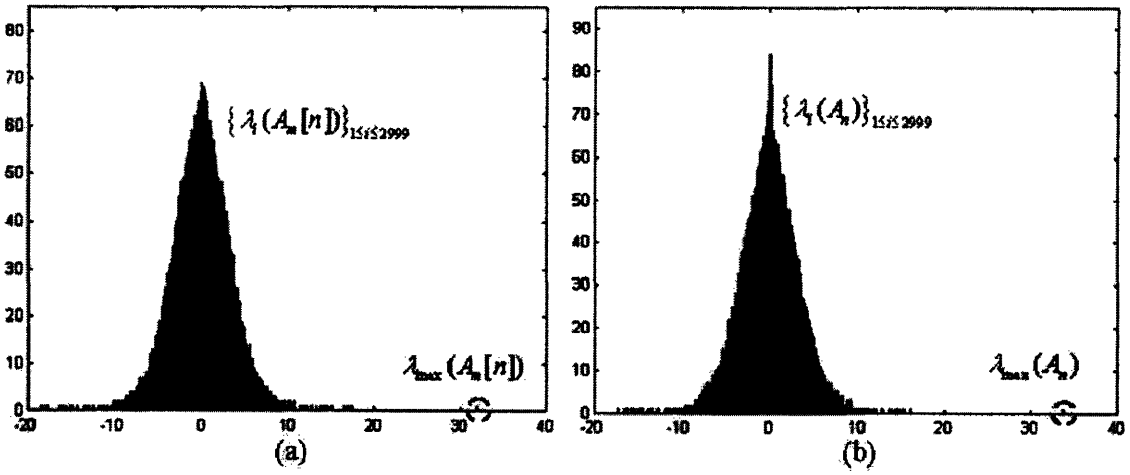

Figure 6-3: In the figure we compare the eigenvalue histograms of a BA random graph with $m = 6$ and $n = 3000$ (plot in (a)) to a Chung-Lu random graph (in (b)) with an expected degree sequence equal to the degree sequence of (R1). We observe a remarkable similarity between the largest eigenvalues, as well as the bulk of eigenvalues, of both models. The higher center peak in the bulk of the Chung-Lu random graph is due to the presence of isolated nodes in the random realization.

Table 6.1 contains numerical values of the empirical spectral moments of both random graphs, *(R1)* and *(R2)*. Although the relative error is small for low-order moments, the errors become unacceptable for higher-order moments. This mismatch is mainly due to the extreme sensitivity presented by high-order moments to the location of the largest eigenvalue, $\lambda_{\max}$.

k-th Moment	$m_k(A_m[n])$	$m_k(A_n)$	Relative Error
1	-2.793e-15	-2.1672e-016	–
2	12.1920	11.9653	1.85%
3	6.8700	5.6600	17.61%
4	1.0040e3	793.8893	20.92%
5	8.6724e3	6.0107e3	30.69%
6	3.9873e5	2.5511e5	36.02%

Table 6.1: Comparison of the spectral moments of one random realization of a BA network to the Chung-Lu model *(R2)*. The values for the parameters are $m = 6$ and $n = 3000$.

In Fig. 6-4, we plot the largest eigenvalue of both random graphs, *(R1)* and *(R2)*, as a function of the network size n. We observe that $\lambda_{\max}(A_n)$ provides us with a very

good estimation of $\lambda_{\max}(A_m[n])$. In the following paragraphs, we apply the results introduced in Chapter 4 to study the spectral moments of the bulk of eigenvalues of $A_m[n]$.

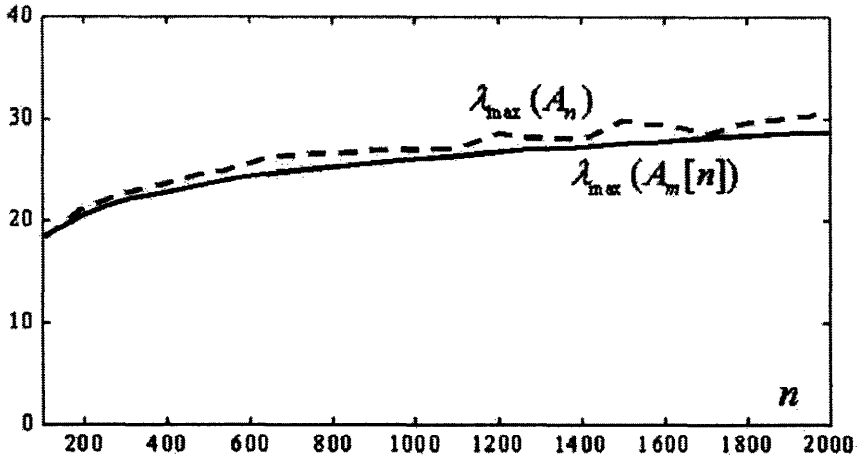

Figure 6-4: The figure plots the evolution of the spectral radii, $\lambda_{\max}(A_m[n])$ and $\lambda_{\max}(A_n)$, as a function of network size n.

As we discussed in Chapter 4, the effect of centralization on the spectrum of the adjacency matrix (under certain conditions) is to remove the isolated largest eigenvalue for the eigenvalue spectrum. In this section, we have the following centralized adjacency matrices

$$\begin{aligned} \widetilde{A}_n &= A_n - \mathbb{E}[A_n], \\ \widetilde{A}_m[n] &= A_m[n] - \mathbb{E}[A_m[n]], \end{aligned}$$

where, from (6.19) and (6.22), we have

$$\mathbb{E}[A_m[n]] \approx \mathbb{E}[A_n] = \rho \mathbf{w}\mathbf{w}^T.$$

In Fig. 6-5, we plot the eigenvalue histograms of the centralized adjacency matrices for both the Barabási-Albert and the Chung-Lu random graphs. As expected, we observe in Fig. 6-5 how the bulk spectrum is only slightly perturbed in each case when the isolated largest eigenvalue is removed from the histogram.

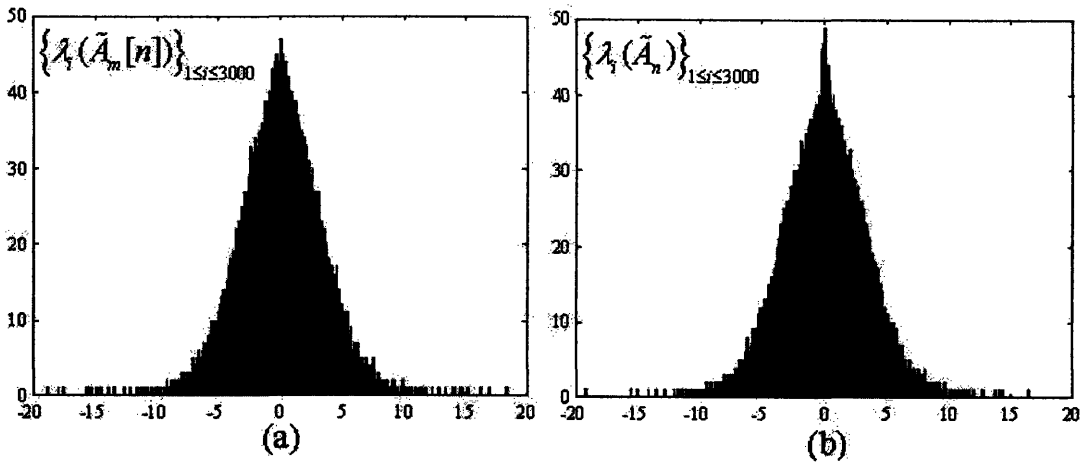

Figure 6-5: Fig. (a) represents the centralized eigenvalue histogram of the centralized adjacency for the dynamic random graph (R1), and Fig. (b) represents the centralized histogram for the corresponding to the centralized adjacency of the static random graph (R2).

Hence, we can use the expected spectral moments of $\widetilde{A}_n$ to describe the shape of the bulk of eigenvalues of $\widetilde{A}_m[n]$. Theorem 4.4.1 in Chapter 4 provides us with closed-form expressions for the asymptotic values of $\mathbb{E}[m_k(\widetilde{A}_n)]$. In order to apply this theorem, we first define the sequence $\sigma = \{\sigma_i\}_{1\le i\le n}$ such that $\sigma_i = \sqrt{\rho} w_i$, where w_i is defined in (6.20). Thus, the power-sums $S_k = \sum_{i=1}^{n} \sigma_i$ are equal to

$$\begin{aligned} S_k &= \sum_{i=1}^{n} (\sqrt{\rho} w_i)^k = \rho^{k/2} \sum_{i=1}^{n} w_i^k \\ &= \rho^{k/2} m^k n^{k/2} \sum_{i=1}^{n} \frac{1}{i^{k/2}} = \rho^{k/2} m^k n^{k/2} H_{n,k/2}, \end{aligned}$$

where $H_{n,k/2}$ is the generalized harmonic number of $k/2$ of order n. For large n, $H_{n,k/2}$ converges to the Riemann zeta function, $\zeta(k/2)$, and ρ converges to $(2mn)^{-1}$. Hence, for large n, we have

$$S_k = \begin{cases} \sqrt{2\,m\,n}, & \text{for } k = 1, \\ \frac{m}{2}(\ln n + \gamma), & \text{for } k = 2, \\ \left(\frac{m}{2}\right)^{k/2} \zeta(k/2), & \text{for } k \ge 3, \end{cases} \tag{6.25}$$

where γ is the Euler-Mascheroni constant ($\gamma \approx 0.5772...$). For convenience, we rewrite

(6.25) as

$$S_k = \left(\frac{m}{2}\right)^{k/2} s_k, \tag{6.26}$$

where

$$s_k = \begin{cases} 2\sqrt{n}, & \text{for } k = 1, \\ \ln n + \gamma, & \text{for } k = 2, \\ \zeta\left(k/2\right), & \text{for } k \geq 3. \end{cases} \tag{6.27}$$

We now substitute (6.26) in the expression (4.10) from Chapter 4 to derive the following expression for the even expected spectral moments of the centralized adjacency $\widetilde{A}_n$:

$$\mathbb{E}[m_{2s}(\widetilde{A}_n)] = (1 + o(1)) \frac{1}{n} \left(\frac{m}{2}\right)^s \sum_{\mathbf{r} \in \mathcal{F}_s} 2 \binom{s}{r_1, \ldots, r_s} \prod_{j=1}^{s} s_j^{r_j}, \tag{6.28}$$

where the set of integer sequences, $\mathcal{F}_s$, is defined in Theorem 4.4.1, Chapter 4. Substituting (6.27) in the above expression, we find the following explicit expressions for the first few even expected spectral moments of $\widetilde{A}_n$:

$$\begin{aligned} \mathbb{E}[m_2(\widetilde{A}_n)] &= (1 + o(1))\, 2m, \\ \mathbb{E}[m_4(\widetilde{A}_n)] &= (1 + o(1))\, 2m^2 (\ln n + \gamma), \\ \mathbb{E}[m_6(\widetilde{A}_n)] &= (1 + o(1)) \frac{1}{n} \left(\frac{m}{2}\right)^3 (16n^{3/2}\zeta(3/2) + 12n(\ln n + \gamma)^2), \\ \mathbb{E}[m_8(\widetilde{A}_n)] &= (1 + o(1)) \frac{1}{n} \left(\frac{m}{2}\right)^4 (32n^2\zeta(2) + 64n^{3/2}(\ln n + \gamma)\zeta(3/2) \\ &\quad + 16n(\ln n + \gamma)^2), \end{aligned} \tag{6.29}$$

In agreement with the even symmetry observed in the bulk spectra, the odd expected spectral moments of $\widetilde{A}_n$ are of smaller order.

In Table 6.2 we compare the predictions of analytical expressions in (6.29) with empirical spectral moments of one random realization of the BA graph using param-

eters $m = 6$ and $n = 3000$.

$2s$-th order	$\mathbb{E}[m_{2s}(\widetilde{A}_n)]$	$m_{2s}(\widetilde{A}_m[n])$	Error (%)
2	11.8410	11.9610	1.01%
4	618.030	727.6319	15.06 %
6	8.514e4	1.1146e5	23.60 %
8	1.915e7	2.5051e7	23.55 %

Table 6.2: In the second and third columns, we present numerical values for the analytical prediction, $\mathbb{E}[m_{2s}(\widetilde{A}_n)]$, and one numerical realization of the even spectral moments of $\widetilde{A}_m[n]$, respectively.

In this section, we derive asymptotic spectral properties of the BA model for $n \to \infty$. We now illustrate, via numerical simulations, how empirical spectral moments of the BA model converge to the analytical estimation, $\mathbb{E}[m_{2s}(\widetilde{A}_n)]$, as n grows. In Fig. 6-6, we plot the values of the first three even moments for both the analytical estimation in Eqn. (6.28) and one random realization of the empirical spectral moments as a function of n.

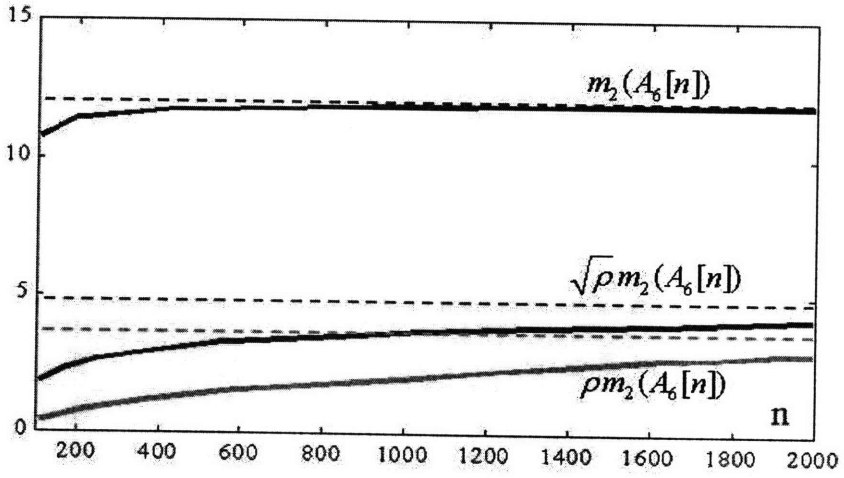

Figure 6-6: Evolution of the second, fourth and sixth spectral moments of $A_m[n]$, for $m = 6$, as a function of n. We include the factors $\sqrt{\rho}$ and ρ to bring the numerical values into a similar range.

In the final part of this section, we study the behavior of large-order expected spectral moments in Eqn. (6.28). The expression for the $2s$-th order expected spectral moments in (6.28) is a multivariate polynomial with variables $S_1, ..., S_s$. From (6.25), we have that the asymptotic behavior of the variables involved in (6.28) are: $S_1 =$

$\Theta(\sqrt{n})$, $S_2 = \Theta(\log n)$, and $S_k = \Theta(1)$ for $k \geq 3$. Hence, the dominant term in (6.28), for $n \to \infty$, corresponds to the monomial with the highest power in S_1. By inspection of (6.29), we deduce that the dominant monomial in (6.28) is equal to $2S_1^s S_s$. Therefore, we have the following asymptotic expression for the even expected spectral moments:

$$\begin{aligned} \mathbb{E}[m_{2s}(\widetilde{A}_n)] &= (1+o(1))\frac{2}{n}S_1^s S_s \\ &= (1+o(1))\frac{2}{n}\left(\frac{m}{2}\right)^s s_1^s s_s. \end{aligned}$$

For $s \geq 3$, we have:

$$\mathbb{E}[m_{2s}(\widetilde{A}_n)] = (1+o(1))\frac{2}{n}m^s n^{s/2}\zeta(s/2).$$

Furthermore, the Riemann Zeta function, $\zeta(s/2)$, converges very fast to 1 as s increases; thus, expected spectral moments of the centralized adjacency grow as

$$\mathbb{E}[m_{2s}(\widetilde{A}_n)] = (1+o(1))\frac{2}{n}m^s n^{s/2}, \tag{6.30}$$

for $n \to \infty$, and $s \geq 3$.

We can extract interesting information from Eqn. (6.30). For example, we can apply Wigner's high-moment method (introduced in Chapter 5) to study the asymptotic behavior of the largest eigenvalue of $\widetilde{A}_m[n]$ (in other words, the largest eigenvalue in the spectral bulk of $A_m[n]$). We denote this eigenvalue by $\widetilde{\lambda}_{\max}[n]$. Applying Wigner's method, one can derive that:

$$\mathbb{P}(\widetilde{\lambda}_{\max}[n] \in \Theta(n^{1/4})) = 1 - o(1).$$

In Fig. 6-7, we plot empirical values for $\widetilde{\lambda}_{\max}[n]$ and observe that in fact $\widetilde{\lambda}_{\max}[n]$ does depends on the network size n as $\widetilde{\lambda}_{\max}[n] \propto n^{1/4}$, for large n.

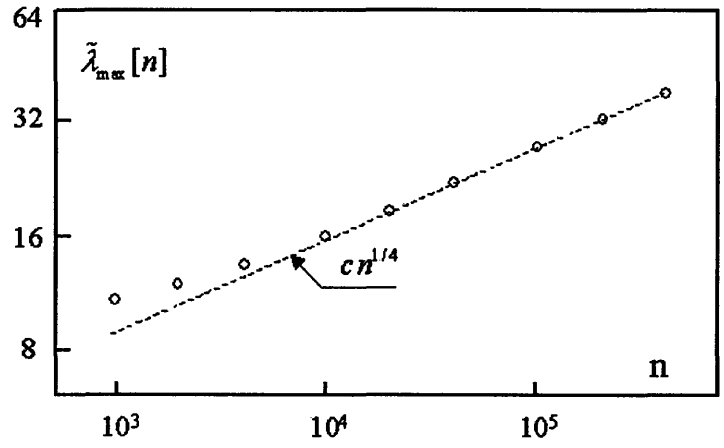

Figure 6-7: Plot, in double logarithmic scale, of the largest eigenvalue of $\widetilde{A}_6[n]$ as a function of n (circular dots). We also include a dashed line with rate of growth $\propto n^{1/4}$ for visual reference.

6.4 Evolution of the Number of Self-Avoiding Walks

A self-avoiding walk (SAW) in a graph is a path between two nodes that never visits any intermediate node more than once. The study of SAW's in lattice grids is a well developed field with many implications in statistical physics [128]. In this section, we study SAW's in the context of large-scale random graphs. In particular, we study the number of *closed* SAW's of length l in the BA dynamic model, $(G_m[n])_{n>n_0}$. We denote the number of closed SAW's of length l by $q_l[n]$. Since $(G_m[n])_{n>n_0}$ is a random graph process, $q_l[n]$ is a discrete-time random process that evolves in n. In this section, we study the evolution of the expected number of closed SAW's, $\mathbb{E}[q_l[n]]$, for asymptotically large graphs.

In the BA evolving graph, nodes and edges are added to the graph in each time slot (and never removed). Thus, as n grows, new closed SAW's are added to the graph (and never removed). In other words, $q_l[n]$ is a monotonically non-decreasing function in n. Obviously, all closed SAW's generated at the n-th time slot must include edges added at the same time slot n. Since all m new edges are attached to the new node v_n, new closed SAW's must pass through v_n. Based on this concept, we propose the following criterion to detect new closed SAW's:

Criterion 6.4.1 *New closed SAW's of length l are generated at the n-th time slot when the new node v_n connects to a pair of existing nodes, v_i and v_j, that are already connected by an open SAW of length $l-2$ (see Fig. 6-8).*

Note that this criterion is applicable for $m \geq 2$, since for $m = 1$ the new node v_n cannot connect to a pair of existing nodes (only to one node).

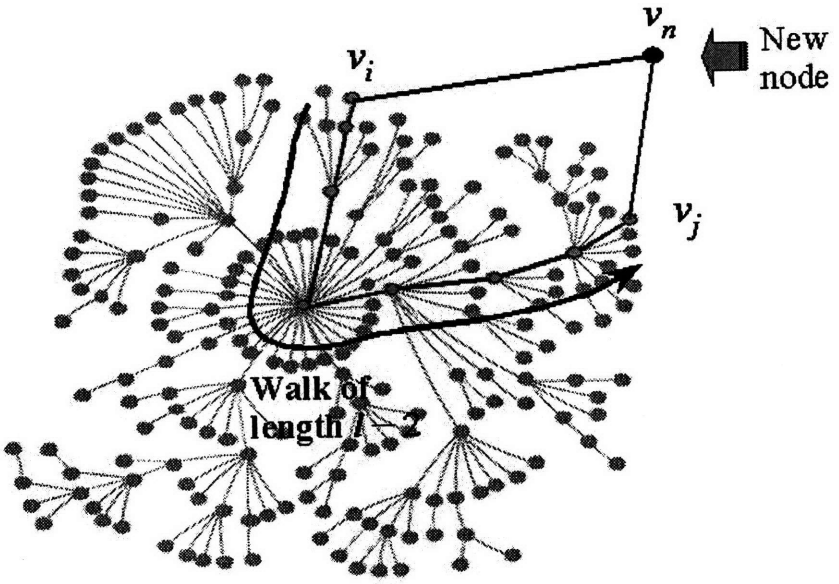

Figure 6-8: A new node v_n connects to a pair of existing nodes, v_i and v_j, which are already connected by an open SAW of length $k-2$. This event generates a new closed SAW of length k.

In the following, we apply the above criterion to compute the number of closed SAW's generated at a given time slot. Denote by $q_h^{(i,j)}[n]$ the number of open SAW's of length h from node v_i to node v_j in $G_m[n]$. We then define the following variable:

$$\Delta q_l^{(i,j)}[n] := 2l\, a_{in}^{(n)} a_{jn}^{(n)}\, q_{l-2}^{(i,j)}[n]. \tag{6.31}$$

Notice that the factor $a_{in}^{(n)} a_{jn}^{(n)}$ in (6.31) is equal to 1 if the v_n connects to a pair of existing nodes, v_i and v_j; and this factor is 0 otherwise. Also, $q_{l-2}^{(i,j)}[n]$ is greater than 0 if there exists at least one (open) SAW of length $l-2$ connecting nodes v_i and v_j. Therefore, according to Criterion 6.4.1, new closed SAW's of length l are generated at

the n-th time slot when $\Delta q_l^{(i,j)}[n]$ is greater than 0. Furthermore, $\Delta q_l^{(i,j)}[n]$ provides us with the exact number of new closed SAW's of length l passing through nodes v_i and v_j generated at the n-th time slot. The factor $2l$ in (6.31) takes into account that:

(i) There are 2 possible directions for each new closed SAW (i.e., $v_n \to v_i \to ... \to v_j \to v_n$, or $v_n \to v_j \to ... \to v_i \to v_n$), and

(ii) There are l possible nodes on which each new closed SAW can start.

Therefore, summing over all possible pairs of vertices, the total number of closed SAW's of length l generated at the n-th time slot is:

$$\begin{aligned} \Delta q_l[n] &= \sum_{1 \le i < j \le n-1} \Delta q_l^{(i,j)}[n] \\ &= 2l \sum_{1 \le i < j \le n-1} a_{in}^{(n)} a_{jn}^{(n)} q_{l-2}^{(i,j)}[n], \end{aligned} \tag{6.32}$$

Consequently, the evolution of $q_l[n]$ can be described using the following stochastic discrete-time equation:

$$q_l[n] = q_l[n-1] + 2l \sum_{1 \le i < j \le n-1} a_{in}^{(n)} a_{jn}^{(n)} q_{l-2}^{(i,j)}[n]. \tag{6.33}$$

In this section, we study the evolution of the expected number of closed SAW's, $\mathbb{E}[q_l[n]]$. From (6.33), we have that $\mathbb{E}[q_l[n]]$ satisfies the following differential equation:

$$\mathbb{E}[q_l[n]] = \mathbb{E}[q_l[n-1]] + 2l \sum_{1 \le i < j \le n-1} \mathbb{E}[a_{in}^{(n)} a_{jn}^{(n)} q_{l-2}^{(i,j)}[n]]. \tag{6.34}$$

The above expression is difficult to analyze due to the dependencies among the terms inside the righmost expectation. In the following paragraph, we introduce a conjecture that allows us to derive analytical results. As Conjecture 6.3.1, this second conjecture is also motivated by the results in [199]. As mentioned before, the BA model behaves like if uncorrelated for $n \to \infty$. Accordingly, we draw the following

conjecture:

Conjecture 6.4.2 *Consider a BA random graph process, $(G_m[n])_{n\geq n_0}$. Then,*

$$\sum_{1\leq i<j\leq n-1} \mathbb{E}[a_{in}^{(n)} a_{jn}^{(n)} q_{l-2}^{(i,j)}[n]] \to \sum_{1\leq i<j\leq n-1} \mathbb{E}[a_{in}^{(n)}]\,\mathbb{E}[a_{jn}^{(n)}]\,\mathbb{E}[q_{l-2}^{(i,j)}[n]], \tag{6.35}$$

for $n \to \infty$.

Eqn. (6.35) becomes an equality for all n in the case of uncorrelated random graphs. Based on the above conjecture, we now derive analytical results concerning the evolution of $\mathbb{E}[q_l[n]]$ that are in excellent agreement with numerical simulations. In particular, using Conjecture 6.4.2, we have that

$$\mathbb{E}[q_l[n]] = \mathbb{E}[q_l[n-1]] + 2l \sum_{1\leq i<j\leq n-1} \mathbb{E}[a_{in}^{(n)}]\,\mathbb{E}[a_{jn}^{(n)}]\,\mathbb{E}[q_{l-2}^{(i,j)}[n]]. \tag{6.36}$$

In Section 6.3, we studied the expectation of the binary random variable, $a_{ij}^{(n)}$, via a mean-field analysis, and found:

$$\mathbb{E}[a_{ij}^{(n)}] \approx \frac{m/2}{\sqrt{i\,j}}. \tag{6.37}$$

Hence, applying the above expression to $\mathbb{E}[a_{in}^{(n)}]$ and $\mathbb{E}[a_{jn}^{(n)}]$, we find that:

$$\mathbb{E}[a_{in}^{(n)}]\,\mathbb{E}[a_{jn}^{(n)}] \approx \frac{(m/2)^2}{n\sqrt{i\,j}} = \frac{m}{2n}\frac{m/2}{\sqrt{i\,j}} \approx \frac{m}{2n}\mathbb{E}[a_{ij}^{(n)}], \tag{6.38}$$

where we have used (6.37) to derive the last equality in (6.38). Substituting (6.38) in (6.36), we find that:

$$\mathbb{E}[q_l[n]] \approx \mathbb{E}[q_l[n-1]] + \frac{ml}{n} \sum_{1\leq i<j\leq n-1} \mathbb{E}[a_{ij}^{(n)}]\,\mathbb{E}[q_{l-2}^{(i,j)}[n]]. \tag{6.39}$$

In our previous conjectures, we assume that the BA model behaves like an uncorrelated random graph for $n \to \infty$. In the following, we use the same justification to

draw a final conjecture:

Conjecture 6.4.3 *Consider a BA random graph process, $(G_m[n])_{n\geq n_0}$. Then,*

$$\sum_{1\leq i<j\leq n-1} \mathbb{E}[a_{ij}^{(n)}]\,\mathbb{E}[\,q_{l-2}^{(i,j)}[n]] \to \sum_{1\leq i<j\leq n-1} \mathbb{E}[a_{ij}^{(n)} q_{l-2}^{(i,j)}[n]],$$

for $n \to \infty$.

This conjecture is exactly true for all n in the case of uncorrelated random graphs. Based on Conjecture 6.4.3, we can rewrite (6.39) as:

$$\mathbb{E}[q_l[n]] = \mathbb{E}[q_l[n-1]] + \frac{ml}{n}\mathbb{E}[\sum_{1\leq i<j\leq n-1} a_{ij}^{(n)} q_{l-2}^{(i,j)}[n]].$$

In the following, we show that the summation in the above equation is proportional to the number of closed SAW's of length $l-1$, i.e.,$q_{l-1}[n]$. Note that, if $a_{ij}^{(n)} = 1$ and $q_{l-2}^{(i,j)}[n] \geq 1$, then v_i and v_j belong to a closed SAW of length $l-1$. Furthermore, we obtain the number of closed SAW's of length $l-1$ by summing $a_{ij}^{(n)} q_{l-2}^{(i,j)}[n]$ over all pairs of nodes, $1 \leq i, j \leq n-1$, in the network. Hence, we have:

$$q_{l-1}[n] = 2 \sum_{1\leq i<j\leq n-1} a_{ij}^{(n)} q_{l-2}^{(i,j)}[n], \tag{6.40}$$

(where the factor 2 is a consequence of summing over half the pairs of nodes, $1 \leq i < j \leq n-1$.)

Using (6.40), we can write Eqn. (6.39) as follows

$$\mathbb{E}[q_l[n]] = \mathbb{E}[q_l[n-1]] + \frac{ml}{2n}\mathbb{E}[q_{l-1}[n]].$$

The solution to the above recursion is given by

$$\mathbb{E}[q_l[n]] = q_l[n_0] + \frac{m}{2}\sum_{k=n_0+1}^{n} \frac{l}{k}\mathbb{E}[q_{l-1}[k]], \tag{6.41}$$

where $q_l[n_0]$ is the number of closed SAW's of length l at the initial time slot n_0. As we mentioned in the description of the BA model, the asymptotic behavior of this model is independent of the initial configuration graph, $G_m[n_0]$. For simplicity, we assume the initial configuration to be a tree. Since a tree does not contain closed SAW's of any length, the initial condition simplifies to $q_l[n_0] = 0$ for all $l \geq 1$. (One can verify that the following derivations also hold for other initial configurations, although the intermediate expressions are more intricate.)

We can exploit the recursive structure provided by Eqn. (6.41) (with $q_l[n_0] = 0$ for all $l \geq 1$) to find the following expression:

$$\mathbb{E}[q_l[n]] = \left(\frac{m}{2}\right)^{l-3} \left(\sum_{k_1=n_0+1}^{n} \frac{l}{k_1} \left(\sum_{k_2=n_0+1}^{k_1} \frac{l-1}{k_2} \cdots \left(\sum_{k_{l-3}=n_0+1}^{k_{l-4}} \frac{4}{k_{l-3}} \mathbb{E}[q_3[k_{l-3}]] \right) \right) \right). \tag{6.42}$$

Furthermore, in [89] we find the following expression for the number of triangular SAW's, i.e., $\mathbb{E}[q_3[n]]$:

$$\mathbb{E}[q_3[n]] = \left(1 + O\left(\log^{-1} n\right)\right) \left(\frac{m}{2}\right)^3 \log^3 n. \tag{6.43}$$

Hence, substituting the above equation in (6.42), we have:

$$\mathbb{E}[q_l[n]] = \left(1 + O\left(\log^{-1} n\right)\right) \left(\frac{m}{2}\right)^l \left(\sum_{k_1=n_0+1}^{n} \frac{l}{k_1} \left(\cdots \left(\sum_{k_{l-3}=n_0+1}^{k_{l-4}} \frac{4}{k_{l-3}} \ln^3 k_{l-3} \right) \right) \right) \tag{6.44}$$

The cascade of summations in (6.44) can be solved by using the following approximation:

$$\begin{aligned} \sum_{k=y_0}^{y} \frac{1}{k} \log^p k &\approx \int_{y_0}^{y} \frac{\log^p x}{x} dx \\ &= \frac{1}{p+1} \left(\ln^{p+1} y - \ln^{p+1} y_0 \right). \end{aligned}$$

We finally apply this approximation in (6.44) recursively, and isolate the dominant term in the resulting expression to find our main result:

$$\mathbb{E}[q_l[n]] = \left(1 + O\left(\log^{-1} n\right)\right) \left(\frac{m}{2}\right)^l \log^l n, \text{ for } m \geq 2. \tag{6.45}$$

(We can check that, for $l = 3$, we recover Eqn. (6.43).) Eqn. 6.45 provides us with the asymptotic rate of growth of the number of closed SAW's of length l in a BA random graph process $(G_m[n])_{n \geq n_0}$ as n grows.

We now illustrate our main result with several numerical simulations. In our illustrations, we use a BA random graph model with $m = 2$, and a complete graph, K_{2m+1} as the initial configuration. In Fig. 6-9, we plot the numerical evolution of the empirical average for 25 random realizations of $q_l[n]$ for $l = 3, 4$, and 5 in a log-log scale. As predicted by (6.45), our numerical values lie around straight lines. The slopes of these lines depend on the particular value of l.

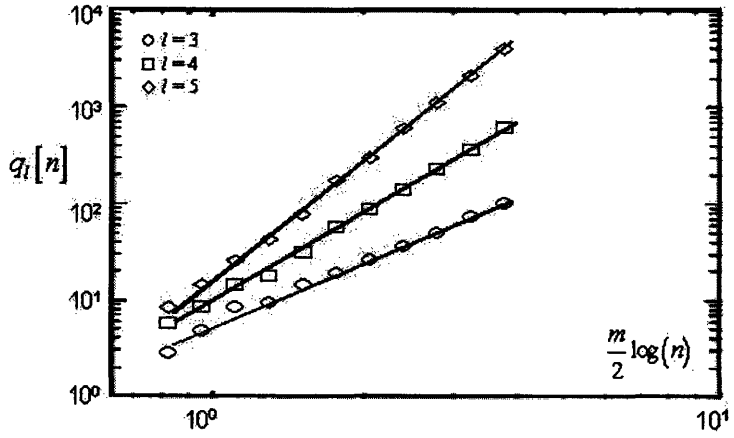

Figure 6-9: Evolution of the number of SAW's of length 2, 3, and 4 as a function of the network size, n. In the figure we observe an excellent agreement of our numerical simulations with the rate of growth predicted in Eqn. (6.45).

In Chapter 4 and 6, we have studied the eigenvalue spectrum of the adjacency matrix for both static and dynamic random graph models. In the following Chapter, we study spectral moments for both the Laplacian and Kirchhoff matrices.

Chapter 7

Moment-Based Analysis of Laplacian and Kirchhoff Matrices

In previous chapters, we have studied the eigenvalue spectrum of the adjacency matrices corresponding to both static and dynamic random graph models. In this section, we study the eigenvalue spectrum of two other matrices representing the graph structure: the Laplacian and Kirchhoff matrices. In particular, we derive expressions for the first three spectral moments, for both the Laplacian and Kirchhoff matrices, based on algebraic graph theory.

To measure topological properties of many real-world networks, researchers usually design automatic agents that scan the network topology node by node. In the design of these agents, one must take into account what topological information is accessible to the agent while sampling a particular node. Usually, the agent can only extract information about the particular node and its neighboring nodes. For example, in on-line cyber-communities (such as Facebook), each person (or node) can only access information about his/her friends (neighboring nodes). Motivated by potential applications, we study spectral properties of Laplacian and Kirchhoff matrices based on properties that are locally measurable. We say that a node property is locally measurable if its value at a particular node can be computed based on the topology of the neighborhood around the node. For example, the degree of a node and the

number of triangles touching a node are easily measurable locally, while the number of self-avoiding walks of length greater than three is not.

7.1 Moment-Based Analysis of Kirchhoff Matrices

In this section, we study spectral properties of the Kirchhoff matrix K_G of a given graph G. In the first subsection we derive expressions for the first three moments of K_G (also called Kirchhoff moments) for any given graph. These expressions are functions of locally-measurable properties, in particular, the degree sequence and the number of triangles in the graph. We illustrate our results with real data and analyze implications. In the second subsection, we apply these expressions to compute the expected Kirchhoff moments for the Chung-Lu random graph. We apply our results to study the dynamic problem of synchronization of a network of oscillators.

7.1.1 Algebraic Analysis of Low-Order Kirchhoff Moments

In this subsection, we derive closed-form expressions for the first three Kirchhoff moments based on algebraic graph theory. Using the method of moments (Eqn. (4.6)), we write down the s-th order Kirchhoff moments as

$$m_s(K_G) = \frac{1}{n}\sum_{i=1}^{n} \lambda_i^s(K_G) = \frac{1}{n}\,\mathrm{tr}\,(D_G - A_G)^s\,. \tag{7.1}$$

where D_G and A_G are the diagonal matrix of degrees and the adjacency matrix of G, respectively. For example, the first spectral moment is given by

$$m_1(K_G) = \frac{1}{n}\mathrm{tr}\,(D_G - A_G) = \frac{1}{n}\sum_{i=1}^{n} d_i = \overline{d},$$

where $\overline{d}$ is the average degree of the graph G. We now study the trace of $(D_G - A_G)^s$ for higher values of s. Since the multiplication of matrices D_G and A_G is not commutative, we cannot use Newton's binomial expansion on $(D_G - A_G)^s$. However,

the trace operator allows us to cyclically permute any multiplicative chain of square matrices (for example, $\mathrm{tr}\,(A_G A_G D_G) = \mathrm{tr}\,(A_G D_G A_G) = \mathrm{tr}\,(D_G A_G A_G)$).

For multiplicative chains of matrices of length $s \leq 3$ involving matrices A_G and D_G, one can cyclically arrange all the terms in the expansion of Eqn. (7.1) into the standard binomial expression:

$$m_s\,(K_G) = \frac{1}{n}\sum_{p=0}^{s}\binom{s}{p}(-1)^p \mathrm{tr}(A_G^p D_G^{s-p}), \quad \text{for } s \leq 3. \tag{7.2}$$

We also have that $\mathrm{tr}\big(A_G^p D_G^{s-p}\big) = \sum_{i=1}^{n}\left(A_G^p\right)_{ii} d_i^{s-p}$. Thus, we can write Eqn. (7.2) as

$$m_s\,(K_G) = \frac{1}{n}\sum_{i=1}^{n}\sum_{p=0}^{s}\binom{s}{p}(-1)^p d_i^{s-p}\left(A_G^p\right)_{ii}, \quad \text{for } k \leq 3. \tag{7.3}$$

Notice that this expression is not valid for $s \geq 4$ (for example, for $k = 4$, we have that $\mathrm{tr}(A_G A_G D_G D_G) \neq \mathrm{tr}(D_G A_G D_G A_G)$).

We now rewrite Eqn. (7.3) in terms of the degree sequence and the number of triangles in the network. We make use of the following result from algebraic graph theory [32]:

Lemma 7.1.1 *Let G be a simple graph (without self-loops or multiedges). Denote by d_i the degree of node i, and by t_i the number of triangles incident on node i. Then*

$$(A_G)_{ii} = 0, \;\; \left(A_G^2\right)_{ii} = d_i, \;\; \textit{and} \;\; \left(A_G^3\right)_{ii} = 2\,t_i. \tag{7.4}$$

We apply this lemma in Eqn. (7.3), and perform simple algebraic simplifications to derive the following expressions for the low-order Kirchhoff moments of G:

$$m_s\,(K_G) = \begin{cases} \frac{1}{n}\sum_{i=1}^{n} d_i, & \text{for } s = 1, \\ \frac{1}{n}\left(\sum_{i=1}^{n} d_i^2 + d_i\right), & \text{for } s = 2, \\ \frac{1}{n}\left[\left(\sum_{i=1}^{n} d_i^3 + 3d_i^2\right) - 6\,T_G\right], & \text{for } s = 3, \end{cases} \tag{7.5}$$

where T_G is the total number of triangles in the network. Notice that these expressions are valid for any simple graph. In the following examples, we illustrate the utility of the above results and use them to study implications for further spectral properties.

Example Compute the low-order Kirchhoff moments of a complete (all-to-all) graph of n nodes. This graph has $n-1$ Kirchhoff eigenvalues located at n, and one trivial eigenvalue at 0. Thus, the first-, second-, and third-order moments are $n-1$, $(n-1)\,n$, $(n-1)\,n^2$, respectively. Eqn. (7.5) allows us to compute these moments without an explicit eigenvalue decomposition. In a complete graph, the degree sequence presents a uniform value $d_i = n-1$. Also, the total number of triangles T_G is $\binom{N}{3}$. Therefore, after substituting these values of d_i and T_G in Eqn. (7.5), and simple algebraic simplifications, we reach $m_1(K_G) = (n-1)$, $m_2(K_G) = n^2-n$, and $m_3(K_G) = n^3-n^2$, in agreement with the above results from the eigenvalue decomposition.

Both the degree sequence and the number of triangles are publicly available data for many real-world networks (see [34] or [150], for examples). Hence, we can estimate the low-order spectral moments of these networks based on partial knowledge of the topology. In the following example, we illustrate how to compute the low-order Kirchhoff moments in a real-world network: the Western States power grid. Although we only use the degree sequence and the number of triangles in the network in our computations, the complete topology is available at [66] to compare our results with a complete eigenvalue decomposition. (Of course, our approach is more valuable in cases where we do not have access to the complete topology.)

Example Compute the first three Kirchhoff moments of the Western States power grid based on local measurements, namely, the sequence of degrees and the number of triangles touching each node. In Figs. 7-1.(a) and (b), we plot both the degree and triangle sequences, in non-increasing order.

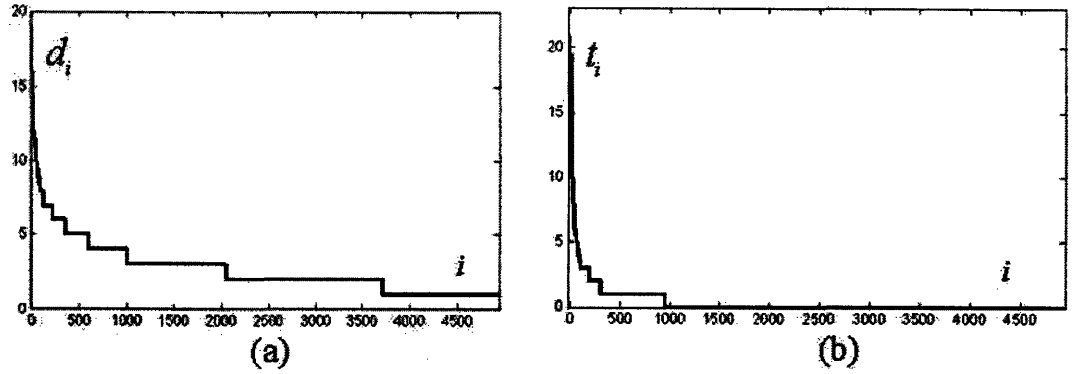

Figure 7-1: The sequences of (a) degrees and (b) triangles per node in the power grid. We consider the undirected graph with 4941 nodes and 6594 edges.

From the given data, we compute: $\sum_i d_i = 13188$, $\sum_i d_i^2 = 51054$, $\sum_i d_i^3 = 283086$, and $T = 651$. Hence, the Kirchhoff moments from Eqn. (7.5) are:

$$m_1(K_G) = 2.6691, \; m_2(K_G) = 13.0018, \text{ and } m_3(K_G) = 87.5009.$$

(Since we have access to the complete topology in [66], we have verified, via complete eigenvalue decomposition, that these moments are exact.)

7.1.2 Probabilistic Analysis of Low-Order Kirchhoff Moments

In this section, we apply the results of the previous section to compute the expected low-order Kirchhoff moments, $\mathbb{E}[m_s(K_G)]$, of the random Chung-Lu graph as a function of the given expected degree sequence, $(w_i)_{1 \le i \le n}$. We derive closed-form expressions for the expected moments for asymptotically large graphs, $n \to \infty$, and bounded expected degree sequences, i.e., $1 \le w_i \le D < \infty$ for $i = 1, ..., n$.

We now introduce several results needed in our derivations. First, we introduce a lemma that describes the behavior of the sum of non-identical, but independent, random variables satisfying certain conditions [121]:

Lemma 7.1.2 *Consider n non-identical binomial trials, with probability of success of the i-th trial equal to p_i. Denote by X the number of successes out of all the n trials.*

If, for $n \to \infty$, *have that* $\sum_{i=1}^{n} p_i \to w$ *and* $p_i \to 0$, *then* X *behaves asymptotically as a Poisson variable with rate* w, *i.e.,* $X \sim Poi(w)$ *for* $n \to \infty$.

One can verify that in a Chung-Lu random graph with a bounded expected degree sequence, the (i,j)-th entry of the adjacency matrix, a_{ij}, is a binomial trial with probability of success equal to $p_{ij} = \rho w_i w_j = o(1)$. Hence, the degree of node i, $d_i = \sum_j a_{ij}$, satisfies the conditions of Lemma 7.1.2. Thus, d_i behaves asyptotically like a Poisson variable with rate w_i for $n \to \infty$. It is useful to have expressions for the asymptotic expected moments of the random degree, $\mathbb{E}\left[d_i^k\right]$:

$$\begin{aligned} \mathbb{E}[d_i] &\to w_i, \\ \mathbb{E}\left[d_i^2\right] &\to w_i^2 + w_i, \\ \mathbb{E}\left[d_i^3\right] &\to w_i^3 + 3\,w_i^2 + w_i, \end{aligned} \tag{7.6}$$

for $n \to \infty$.

We now introduce another important result to compute the expected Kirchhoff moments in Eqn. (7.5):

Lemma 7.1.3 *Consider the Chung-Lu random graph model,* $\mathcal{G}(\mathbf{w}_n)$, *with* $w_i \leq D < \infty$, *for* $i = 1, ..., n$. *Denote by* T_G *the number of triangles in a graph* G. *Then, the expected number of triangles satisfies*

$$\mathbb{E}[T_G] = O(1).$$

Proof The number of triangles can be written in terms of the adjacency matrix entries as:

$$T_G = \sum_{1 \leq i < j < k \leq n} a_{ij} a_{jk} a_{ki}.$$

Since $\rho = 1/n\bar{w}$, we have that $\mathbb{E}[a_{ij}] = \frac{1}{n\bar{w}} w_i w_j$. Hence,

$$\begin{aligned} \mathbb{E}[T] &= \frac{1}{\overline{w}^3 n^3} \sum_{1 \le i < j < k \le n} w_i^2 w_j^2 w_k^2 \\ &\le \frac{w_1^6}{\overline{w}^3 n^3} \binom{n}{3} = O(1). \end{aligned}$$

We now apply the above results to compute the expectation of the asymptotic low-order Kirchhoff moments in Eqn. (7.5):

Theorem 7.1.4 *Consider the Chung-Lu random graph ensemble $\mathcal{G}(\mathbf{w}_n)$, with $w_i \le D < \infty$ for $i = 1, ..., n$. Denote $W_k = \sum_i w_i^k$. The expected Kirchhoff moments of the ensemble, for $n \to \infty$, are:*

$$\mathbb{E}_{G \in \mathcal{G}(\mathbf{w}_n)}[m_s(K_G)] = (1 + o(1)) \begin{cases} \frac{1}{n} W_1, & \text{for } s = 1, \\ \frac{1}{n}(W_2 + 2W_1), & \text{for } s = 2, \\ \frac{1}{n}(W_3 + 6W_2 + 4W_1), & \text{for } s = 3. \end{cases} \tag{7.7}$$

Proof Eqn. (7.7) is a direct consequence of applying Lemmas 7.1.2 and 7.1.3 to Eqn. (7.5).

We illustrate the above result with the following example:

Example Compute the expected Kirchhoff moments of a random power-law graph with degree sequence defined in [58] as:

$$w_i = c i^{-1/\beta - 1} \text{ for } i_0 \le i \le i_0 + n, \tag{7.8}$$

where

$$\begin{aligned} c &= \frac{\beta - 2}{\beta - 1} \overline{w} n^{\frac{1}{\beta - 1}}, \\ i_0 &= n \left(\frac{\overline{w}(\beta - 2)}{m(\beta - 1)} \right)^{\beta - 1}. \end{aligned}$$

The parameters $\overline{w}$ and m are prescribed average and maximum expected degrees, respectively. In this example, we use the following values for the parameters: $\overline{w} = 50$, $m = 100$, $\beta = 3.0$, and $n = 500$.

First, we approximate the power-sums, W_k, in Theorem 7.1.4 as

$$W_k = \sum_{j=i_0}^{i_0+n} w_j^k \approx c^k \frac{(\beta-1)}{(\beta-1-k)} \left((i_0+n)^{\frac{\beta-1-k}{\beta-1}} \right).$$

In the second column of Table 7.1, we include the values of the analytical estimations from Eqn. (7.7). We compare these estimations with the empirical values of the moments for one random realization of this random graph with no benefit from averaging. We include the empirical moments in the third column of Table 7.1. The match is very good.

s-th order	$\mathbb{E}[m_s(K_G)]$	$m_s(K_G)$	Error (%)
1^{st}	25e3	25.062e3	0.25%
2^{nd}	30.307e3	30.447e3	0.55%
3^{rd}	44.175e3	44.615e3	1.75%

Table 7.1: Analytical expectations and empirical realization of the first three Kirchhoff moments of a random power-law graph.

In the following section, we apply the above results to study the dynamical problem of synchronization in a random network of identical oscillators.

7.1.3 Application in Synchronization of Oscillators

In this subsection, we use our results regarding Kirchhoff moments to predict synchronization in a random network of identical oscillators. In Chapter 3, we introduced the master stability function (MSF) approach to study synchronization of a network of identical oscillators. We showed how the network synchronized whenever the spectrum of Kirchhoff eigenvalues was contained in a certain region on the real line. We also illustrated this approach with an examination of how a network of identical Rössler oscillators synchronizes.

Based on the MSF approach, we can follow the steps below to predict if a random network of oscillators with a given expected degree sequence synchronizes:

1. Given the expected degree sequence of a random Chung-Lu network, $(w_i)_{1\leq i\leq n}$, we compute the first three expected Kirchhoff moments of the random graph ensemble using Eqn. (7.7).

2. Using the piecewise-linear approximation introduced in Chapter 5, we use the first three Kirchhoff moments to fit a triangular function to the unknown spectrum of Kirchhoff eigenvalues. For many expected degree sequences, this approximation provides us with a reasonable estimation of the support of the Kirchhoff eigenvalue spectrum.

3. From the estimation of the spectral support, we can decide whether or not the (estimated) Kirchhoff eigenvalue spectrum lies in the region of stability for the network to synchronize.

We illustrate the above steps in the following example:

Example Predict synchronization in a random Chung-Lu network with 200 identical Rössler oscillators. The dynamics of the network is described by:

$$\begin{bmatrix} \dot{x}_i \\ \dot{y}_i \\ \dot{z}_i \end{bmatrix} = \begin{bmatrix} -(y_i + z_i) \\ x_i + a\, y_i \\ b + z_i\,(x_i - c) \end{bmatrix} + \gamma \sum_{j=1}^{n} [K_G]_{ij} \begin{bmatrix} 1 & 0 & 0 \\ 0 & 0 & 0 \\ 0 & 0 & 0 \end{bmatrix} \begin{bmatrix} x_j \\ y_j \\ z_j \end{bmatrix},$$

where $i = 1, ..., 200$ and K_G is the Kirchhoff matrix corresponding to a random graph with the following affine expected degree sequence:

$$w_i := 0.03\ (100 - i) + 10,\ i = 1, 2, ..., 200$$

First, using Theorem 7.1.4, we compute the first three expected Kirchhoff moments: $m_1 = 10$, $m_2 = 122.67$, and $m_3 = 1742.5$. Second, following the methodology

in Chapter 5, we use these moments to approximate a triangular function to the Kirchhoff eigenvalue distribution. We obtain the following knot points for this triangular function: $x_1 = 1.798$, $x_2 = 4.732$, and $x_3 = 23.470$. In Fig. 7-2 we plot this triangular function, as well as one random realization of the Kirchhoff spectrum. Third, we use the extreme knot points, x_1 and x_3, to provide a reasonable estimate of the spectral support. We then use this estimate to study the stability of synchronization in a random network with the given affine expected degree sequence. As a result of this analysis, we conclude that a random network of Rössler oscillators with the given affine expected degree sequence synchronizes if the global coupling strength, γ, is in the interval $(0.0444, 0.2113)$.

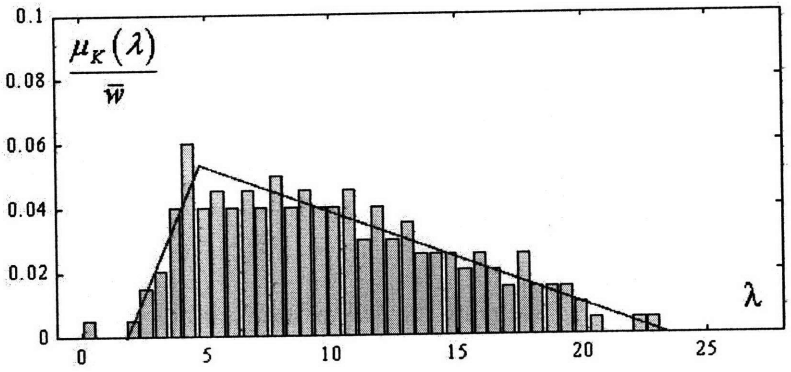

Figure 7-2: Eigenvalue histogram and triangular estimation of a 200 nodes network with an affine expected degree sequence.

In Fig. 7-3, we plot the dynamical evolution of the network of oscillators for several values of γ. For each coupling strength, we plot a superposition of 200 plots representing the time evolution of all the x states. Also, we plot 199 plots representing the errors between the x state of each oscillator and the one with the highest degree, i.e., $x_i(t) - x_1(t), i = 2, 3, ..., 200$ (these errors are scaled in the plot for better discernment).

In Fig. 7-3 (a), we use a coupling strength $\gamma_a = 0.01$. Since this coupling strength is below 0.0444, the eigenvalue spectrum invades the unstable regions. Fig. 7-3 (a) shows how synchronization is clearly not achieved. In fact, we observe an exponential divergence in the scaled error plots. In Fig. 7-3 (b) we plot the temporal evolution for

a coupling strength $\gamma_b = 0.1$ (which lies within the region of stable coupling strength). In this case, we observe an exponential convergence of the errors. In Fig. 7-3 (c), we use a strength $\gamma_c = 0.35$ (which is outside the region of stable coupling strength). Although we observe an initial period of convergence in the time evolution, this is followed by a region of clear divergence.

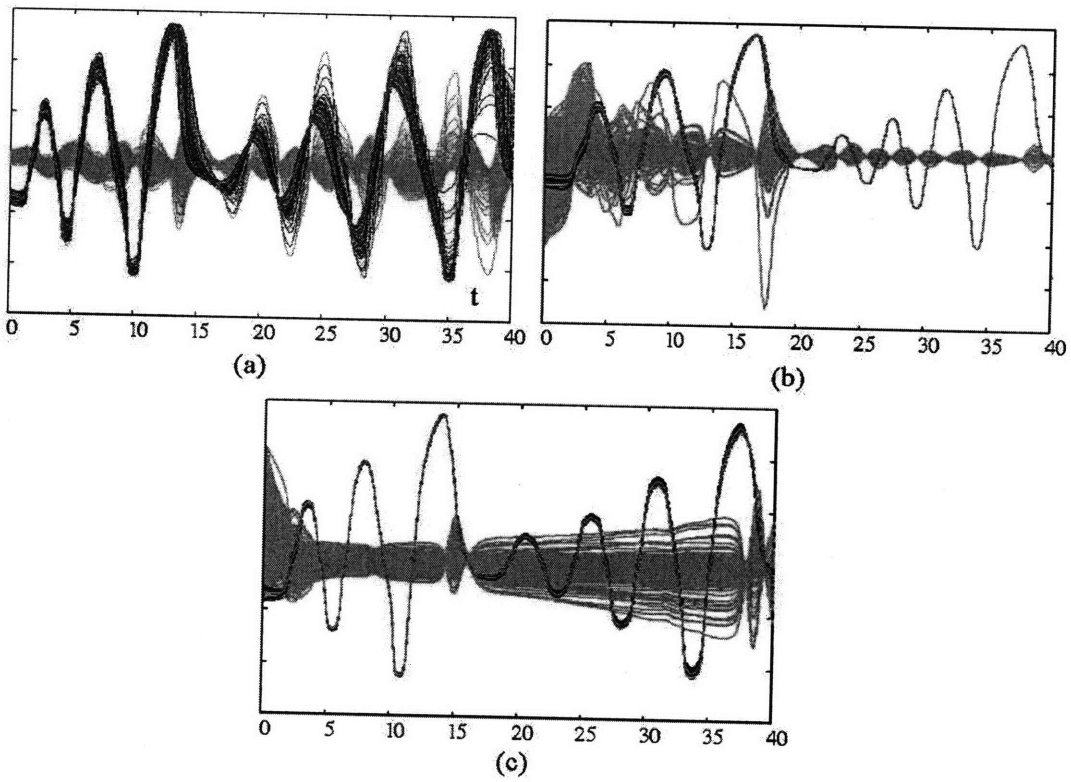

Figure 7-3: Plots of the evolution of the network of oscillators for several coupling strengths: (a) $\gamma = 0.01$ (unstable region), (b) $\gamma = 0.1$ (stable region), and (c) $\gamma = 0.35$ (unstable region). We superpose 200 plots representing the time evolution of all the x states and the errors between the x state of each oscillator and the one with the highest degree

7.2 Moment-Based Analysis of Laplacian Matrices

In this section, we study the spectral moments of the Laplacian matrix, $\mathcal{L}_G = I - D_G^{-1/2} A_G D_G^{-1/2}$, where A_G and D_G are the adjacency matrix and the diagonal matrix of degrees, respectively. (In order to avoid singularities in the Laplacian, we

consider graphs with no isolated nodes. Multiple components are allowed.) In the following subsection, we use algebraic graph theory to study low-order moments of the Laplacian matrix for any given graph. We apply our results to compute these Laplacian moments for a large subgraph of the Internet. In the subsection after that, we use our results to compute the low-order expected Laplacian moments of a random graph ensemble with a given expected degree sequence.

7.2.1 Algebraic Analysis of Low-Order Laplacian Moments

In this section, we derive closed-form expressions for the first three Laplacian moments for any graph. Our expressions are functions of locally-measurable topological properties of the graph, in particular, the joint-degree distribution and the distribution of triangles (as defined in Chapter 3).

Denote by $\{\lambda_i(\mathcal{L}_G)\}_{1\leq i\leq n}$ the set of eigenvalues of the Laplacian matrix $\mathcal{L}_G$. The following holds for the set of Laplacian eigenvalues:

$$\begin{aligned}\left\{\lambda_i(I - D_G^{-1/2}A_G D_G^{-1/2})\right\}_{1\leq i\leq n} &= \left\{1 - \lambda_i(D_G^{-1/2}A_G D_G^{-1/2})\right\}_{1\leq i\leq n} \\ &= \left\{1 - \lambda_i(D_G^{-1}A_G)\right\}_{1\leq i\leq n}.\end{aligned}$$

Hence, the Laplacian moments satisfy:

$$\begin{aligned}m_k(\mathcal{L}_G) &= \frac{1}{n}\sum_{i=1}^{n}\lambda_i^k(\mathcal{L}_G) \\ &= \frac{1}{n}\sum_{i=1}^{n}\left(1 - \lambda_i\left(D^{-1}A\right)\right)^k\end{aligned}$$

We now apply Newton's binomial expansion of $(1-x)^k$ to obtain

$$\begin{aligned}m_k(\mathcal{L}_G) &= \sum_{r=0}^{k}(-1)^r\binom{k}{r}\frac{1}{n}\sum_{i=1}^{n}\lambda_i^r\left(D^{-1}A\right) \\ &= \sum_{r=0}^{k}(-1)^r\binom{k}{r}m_r\left(D^{-1}A\right), \qquad (7.9)\end{aligned}$$

Thus, we can compute the k-th Laplacian moment as a linear combination of the spectral moments of $D_G^{-1}A_G$. We now analyze the r-th spectral moments of $D_G^{-1}A_G$ for a given graph. Applying the method of moments to $D_G^{-1}A_G$, we can derive the following expression for the spectral moments of $D_G^{-1}A_G$:

$$\begin{aligned} m_r\left(D_G^{-1}A_G\right) &= \frac{1}{n}\mathrm{tr}\left(D_G^{-1}A_G\right)^r \\ &= \frac{1}{n}\sum_{i=1}^{n}\sum_{1\leq i_1,\ldots,i_{r-1}\leq n}\left(a_{i,i_1}a_{i_1i_2}\ldots a_{i_{r-1}i}\right)\left(d_id_{i_1}\ldots d_{i_{r-1}}\right)^{-1}. \end{aligned} \tag{7.10}$$

We now study the above expansion for $r = 1$, 2, and 3.

First, since we do not allow self-loops (i.e., $a_{j,j} = 0$ for all j), we have that the first moment $m_1\left(D^{-1}A\right) = 0$. For the second moment, we have that:

$$m_2\left(D_G^{-1}A_G\right) = \frac{1}{n}\sum_{i=1}^{n}\left(\sum_{i_1=1}^{n}a_{i,i_1}\left(d_id_{i_1}\right)^{-1}\right). \tag{7.11}$$

Denote by $\mathcal{D}_k$ the set of nodes with degree k, and by M the maximum degree in the graph. We can partition the set of nodes, $\{1,\ldots,n\}$, into groups having the same degree. Hence, we can rewrite Eqn. (7.11) as follows:

$$m_2\left(D_G^{-1}A_G\right) = \frac{1}{n}\sum_{k_1=1}^{M}\sum_{i\in\mathcal{D}_{k_1}}\left(\sum_{k_2=1}^{M}\sum_{i_1\in\mathcal{D}_{k_2}}a_{i,i_1}\left(d_id_{i_1}\right)^{-1}\right),$$

Re-ordering the summands in the above equation, we obtain:

$$m_2\left(D_G^{-1}A_G\right) = \frac{1}{n}\sum_{1\leq k_1,k_2\leq M}\left(k_1k_2\right)^{-1}\left(\sum_{i\in\mathcal{D}_{k_1}}\sum_{i_1\in\mathcal{D}_{k_2}}a_{i,i_1}\right),$$

where the term in the last parenthesis counts the number of edges between the sets of nodes with degree k_1 and degree k_2. In Chapter 3, we noted this number of edges by M_{k_1,k_2} (in the context of the joint-degree distribution, JDD). Thus, the second

moment of $D_G^{-1}A_G$ can be written as:

$$m_2\left(D_G^{-1}A_G\right) = \frac{1}{n}\sum_{1\leq k_1,k_2\leq M}\frac{M_{k_1,k_2}}{k_1k_2}. \tag{7.12}$$

Similarly, from Eqn. (7.10) we have that the third spectral moment of $D_G^{-1}A_G$ is:

$$\begin{aligned} m_3\left(D_G^{-1}A_G\right) &= \frac{1}{n}\sum_{1\leq i,i_1,i_2\leq n}\left(a_{i,i_1}a_{i_1i_2}a_{i_2i}\right)\left(d_id_{i_1}d_{i_2}\right)^{-1} \\ &= \frac{1}{n}\sum_{1\leq k_1,k_2,k_3\leq M}\left(k_1k_2k_3\right)^{-1}\left(\sum_{i\in\mathcal{D}_{k_1}}\sum_{i_1\in\mathcal{D}_{k_2}}\sum_{i_2\in\mathcal{D}_{k_3}}a_{i,i_1}a_{i_1i_2}a_{i_2i}\right), \end{aligned}$$

In the above equation, the last term in parenthesis counts the number of triangles with nodes having degrees k_1, k_2 and k_3. We denote this number of triangles by T_{k_1,k_2,k_3}. Thus, the third order spectral moment of $D_G^{-1}A_G$ becomes:

$$m_3\left(D_G^{-1}A_G\right) = \frac{1}{n}\sum_{1\leq k_1,k_2,k_3\leq M}\frac{T_{k_1,k_2,k_3}}{k_1k_2k_3}. \tag{7.13}$$

In conclusion, we can compute the first three spectral moments of $D_G^{-1}A_G$ from the local measurements M_{k_1,k_2} and T_{k_1,k_2,k_3}.

Once the first three moments of $D_G^{-1}A_G$ are computed, we combine them to obtain the first three Laplacian moments of any given graph. By substituting Eqns. (7.12) and (7.13) into (7.9) and performing simple algebraic simplifications, we derive the following expressions for the first three Laplacian moments:

$$m_k\left(\mathcal{L}_G\right) = \begin{cases} 1, & \text{for } k=1, \\ 1+n^{-1}\sum_{1\leq k_1,k_2\leq M}\left(k_1k_2\right)^{-1}M_{k_1,k_2}, & \text{for } k=2, \\ 1+3n^{-1}\sum_{1\leq k_1,k_2\leq M}\left(k_1k_2\right)^{-1}M_{k_1,k_2} & \\ \quad -n^{-1}\sum_{1\leq k_1,k_2,k_3\leq M}\left(k_1k_2k_3\right)^{-1}T_{k_1,k_2,k_3}, & \text{for } k=3. \end{cases} \tag{7.14}$$

We elaborate on these expressions in the following examples:

Example Consider the complete tripartite graph in Fig. 7-4. The groups of nodes have sizes n_1, n_2, and n_3. We compute the first three Laplacian moments of this graph without performing an explicit eigenvalue decomposition.

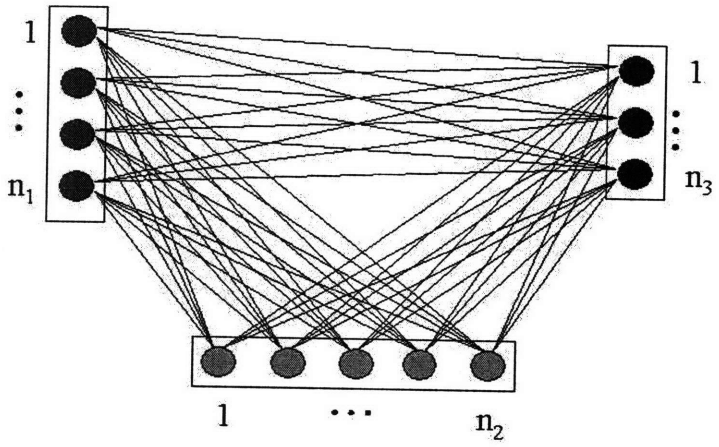

Figure 7-4: Tripartite graph with groups of nodes of sizes n_1, n_2, and n_3.

In order to apply Eqn. (7.14), we must determine M_{k_1,k_2} and T_{k_1,k_2,k_3}. These distributions are symmetric functions[1] taking the following values:

$$M_{k_1,k_2} = \begin{cases} n_1 n_2, & \text{for } k_1 = n_2 + n_3 \text{ and } k_2 = n_1 + n_3, \\ n_1 n_3, & \text{for } k_1 = n_2 + n_3 \text{ and } k_2 = n_1 + n_2, \\ n_2 n_3, & \text{for } k_1 = n_1 + n_3 \text{ and } k_2 = n_1 + n_2, \\ 0, & \text{otherwise,} \end{cases}$$

and

$$T_{k_1,k_2,k_3} = \begin{cases} n_1 n_2 n_3, & \text{for } k_1 = n_2 + n_3,\ k_2 = n_1 + n_3, \text{ and } k_3 = n_1 + n_2 \\ 0, & \text{otherwise.} \end{cases}$$

[1] Any permutation of their subscripts keeps the function unchanged.

Hence, we have that:

$$\begin{aligned}
\sum_{1\leq k_1,k_2\leq m} \frac{M_{k_1,k_2}}{k_1 k_2} &= 2\frac{n_1^2 n_2 + n_1 n_2^2 + n_1^2 n_3 + n_1 n_3^2 + n_2^2 n_3 + n_2 n_3^2}{(n_1+n_2)(n_2+n_3)(n_1+n_3)}, \\
\sum_{1\leq k_1,k_2,k_3\leq n} \frac{T_{k_1,k_2,k_3}}{k_1 k_2 k_3} &= 6\frac{n_1 n_2 n_3}{(n_1+n_2)(n_2+n_3)(n_1+n_3)}.
\end{aligned}$$

We can substitute the above expressions in Eqn. (7.14) to compute the Laplacian moments. For example, for the specific values: $n_1 = n_2 = n_3 = 10$, the first three Laplacian moments from Eqn. (7.14) are:

$$m_1(\mathcal{L}) = 1,\ m_2(\mathcal{L}) = 21/20,\ \text{and}\ m_3(\mathcal{L}) = 9/8.$$

One can validate that these values are exact by performing an explicit eigenvalue decomposition of the Laplacian of the tripartite graph: $\mathcal{L}_{tri} = I - D_{tri}^{-1/2} A_{tri} D_{tri}^{-1/2}$, with

$$\begin{aligned}
A_{tri} &= \begin{bmatrix} \mathbf{0}_{n_1,n_1} & \mathbf{K}_{n_1,n_2} & \mathbf{K}_{n_1,n_3} \\ \mathbf{K}_{n_2,n_1} & \mathbf{0}_{n_2,n_2} & \mathbf{K}_{n_2,n_3} \\ \mathbf{K}_{n_3,n_1} & \mathbf{K}_{n_3,n_2} & \mathbf{0}_{n_3,n_3} \end{bmatrix}, \\
D_{tri} &= \begin{bmatrix} (n_2+n_3)\,\mathbf{I}_{n_1} & \mathbf{0}_{n_1,n_2} & \mathbf{0}_{n_1,n_3} \\ \mathbf{0}_{n_2,n_1} & (n_1+n_3)\,\mathbf{I}_{n_2} & \mathbf{0}_{n_2,n_3} \\ \mathbf{0}_{n_3,n_1} & \mathbf{0}_{n_3,n_2} & (n_1+n_2)\,\mathbf{I}_{n_3} \end{bmatrix},
\end{aligned}$$

where $\mathbf{0}_{n_i,n_j}$, $\mathbf{I}_n$, and $\mathbf{K}_{n_i,n_j}$ are the all-zeroes, identity, and all-ones block matrices, respectively.

In this chapter we have derived closed-form expressions for the Laplacian and Kirchhoff first three low-order moments. Our expressions present the desirable feature of being dependent on locally measurable graph properties such as the joint-degree distribution and the distribution of triangles.

Chapter 8

Conclusions and Future Research

This thesis has been devoted to developing a better understanding of the spectral properties of large-scale complex networks. Spectral graph theory provides us with a framework in which to connect graph-theoretical properties to the behavior of dynamical processes taking place in networks. In this thesis, we have illustrated this relationship by studying the following three canonical processes:

(a) spreading processes (such as virus or rumor spreading);

(b) distributed consensus of autonomous agents;

(c) synchronization of nonlinear oscillators.

The dynamical behavior of these processes is closely related to the distribution of eigenvalues of the following matrices representing the network structure:

(1) Adjacency matrix (whose eigenvalues are related to spreading processes).

(2) Laplacian matrix (whose eigenvalues are related to distributed consensus).

(3) Kirchhoff matrices (whose eigenvalues are related to synchronization of oscillators).

With the connection between graph eigenvalues and dynamics established, we analyzed spectral distributions of large-scale complex networks. For this, we used

stochastic models of the graph structure to infer spectral information from a set of local measurements. We paid special attention to two popular classes of stochastic graph models:

(i) Static models (also called generalized Erdös-Rényi models, or off-line models). Models in this class aim to fit a set of measurements taken from a real-world network into a random graph ensemble with a fixed number of nodes n.

(ii) Dynamically evolving models (also called dynamic models, growing models, or on-line models): In these models, a network grows in time according to a set of stochastic growth rules aiming to replicate the generational process of a particular real network.

The core of this thesis is devoted to analyze spectral properties of these two classes of stochastic graph models. We extensively used the method of moments to derive closed-form expressions for the expected spectral moments of the adjacency, Laplacian, and Kirchhoff matrices for both static and dynamic stochastic graph models. We also introduced several techniques to extract spectral features from a truncated sequence of spectral moments. These features have interesting applications for the global dynamics of processes taking place in networks.

8.1 Additional Further Research

During the development of this thesis, we have found many other interesting potential avenues for extending the results developed in this dissertation. Of these problems, we find specially challenging the following:

1. *Proofs for several conjectures drawn in this thesis.* In particular, we have the following pending work: *(i)* prove that the eigenvector associated to the maximum eigenvalue of a Chung-Lu random graph concentrates around $\mathbf{w}$ under certain technical conditions, and *(ii)* prove that the BA dynamic network model behaves like if uncorrelated for asymptotically large networks.

2. *Design of large-scale networks from a spectral point of view.* Eigenvalue optimization is a fundamental problem with applications in many fields of science and technology. Optimization of a graph structure, on the other hand, is most often a hard combinatorial problem. In most cases, the objective function is nonlinear, nondifferentiable, and very sensitive to small perturbations of the graph structure. There are a few cases in which the graph optimization problem has been found to be specially tractable. Some of the recent advances in graph design are related to semidefinite optimization (SDP). Recently, an important set of papers casts several optimization problems involving Laplacian eigenvalues into an SDP formulation [41], [42].

3. *Spectral analysis of random directed networks.* Throughout this thesis, our focus has been on unweighted, undirected graph. Analysis of directed graphs is, arguably, the main open questions in the field of spectral graph theory [54]. In this case, the adjacency matrix is not symmetric anymore. Consequently, the eigenvalue distribution lies, in general, on the complex plane. Therefore, one would need to adjust the moment approach to hold for two-dimensional distributions.

4. *Development of more realistic stochastic models.* In this thesis we have focus our attention on stochastic models able to reproduce degree distributions. For many applications, reproducing a graphs degree distribution may not be enough to capture important properties of the network topology. The field of complex networks still lacks a systematic method to analyze and synthesize network topologies reproducing other structural properties.

5. *Study networks with geographical constrains.* In some real-world networks, nodes are embedded into a geographical area, and distances among connected nodes should be taken into account. Analysis and design of realistic large-scale stochastic models taking into account this ingredient is another relevant issue.

6. *Practical applications.* We have focused our attention on problems of theoretical

nature. One open interesting research line is to explore the applicability of our results in real engineering systems (such as on-line cyber-communities), or in physical applications (such as molecular dynamics).

We hope this work encourages further research on the emerging field of complex networks, their evolution, their application to artifical networks, and their connection with real-world large-scale networks.

Appendix A

Miscellanea of Notation

A.1 Asymptotic Notation

Many of the results in this thesis are of asymptotic nature (for very large graphs). We use the standard asymptotic notation [14]. For two functions f and g of the same argument (usually the graph size n for us), we write $f = O(g)$ if $f \leq c_1\, g + c_2$ for all possible values of the argument, where c_1 and c_2 are constants. We write $f = \Omega(g)$ if $g = O(f)$, and $f = \Theta(g)$ if $f = O(g)$ and $f = \Omega(g)$. If the limit of the ratio f/g tends to zero as the argument tend to infinity, we write $f = o(g)$. Finally, $f \approx g$ denotes that $f = (1 + o(1))g$, i.e., that f/g tends to 1 when the argument tend to infinity.

A.2 Kronecker Product

Given an $m \times n$ matrix A and a $p \times q$ matrix B, their Kronecker product $C = A \otimes B$ is defined component-wise as $c_{\alpha\beta} = a_{ij} b_{kl}$, where $\alpha := p\,(i-1)+k$ and $\beta := q\,(j-1)+l$. This can be written in block matrix form as

$$C = \begin{bmatrix} a_{11}B & a_{12}B & \dots \\ a_{21}B & a_{22}B & \\ \vdots & & \ddots \end{bmatrix}.$$

This product has many interesting properties, see [100]. In particular,

$$(A \otimes B)(C \otimes D) = (AC) \otimes (BD),$$

provided the dimensions of the matrices are commensurate.

Appendix B

Proof of Theorem 4.4.2

Theorem B.0.1 *Consider the random matrix ensemble $\mathcal{A}_n(\sigma)$ with $\sigma = (\sigma_1, \sigma_2, ..., \sigma_n)$ satisfying $n\,\sigma_{\max}^2 = o(1)$. Then, the odd expected spectral moments of $\tilde{A}_n \in \mathcal{A}_n(\sigma)$ are:*

$$\mathbb{E}_{\tilde{A}_n \in \mathcal{A}_n(\sigma)}[m_{2s+1}(\tilde{A}_n)] = o(1).$$

Proof We prove our claim by analyzing the terms $\mu_{2s+1,p}(\tilde{A}_n)$ in Eqn. (4.25) for different values of p.

First, for $p > s+1$, one can prove that every walk $\mathbf{c}_k \in C_{2s+1,p}^{(n)}$ have an edge with multiplicity one. This implies that, $\mathbb{E}[\tilde{\omega}(\mathbf{c}_k)] = 0$ for all $\mathbf{c}_k \in \widehat{C}_{2s+1,p}^{(n)}$. Thus, $\mu_{2s+1,p}(\tilde{A}_n) = 0$ for $p > s+1$.

Second, for $p \leq s+1$, we find in [58] the following bound $|\widehat{C}_{2s+1,p}^{(n)}| \leq c\,n^p$. Also, one can prove the following upper bound

$$\mathbb{E}[\tilde{\omega}(\mathbf{c}_k)] \leq K^{2s-2p+3}\sigma_{\max}^{2p-2},$$

which implies that $\mu_{2s+1,p}(\tilde{A}_n) \leq cK^{2s+3-2p}\left(n\,\sigma_{\max}^2\right)^{p-1}$. Thus, the odd spectral moments can be upper bounded as follows:

$$\mathbb{E}[m_{2s+1}(\tilde{A}_n)] \leq \sum_{p=1}^{s+1} cK^{2s+3-2p}\left(n\,\sigma_{\max}^2\right)^{p-1}.$$

Since c and K are constants, and $n\,\sigma_{\max}^2 = o\,(1)$, we have

$$\mathbb{E}[m_{2s+1}(\tilde{A}_n)] = o\,(1)\,.$$

Appendix C

Explicit Expressions for the Polynomials in Eqn. (4.10)

In this appendix we present an algorithm to efficiently compute an explicit representation of the symbolic polynomials in (4.10). Along with the algorithmic steps, we shall illustrate their use with a specific example: the 8-th order expected spectral moment ($s = 4$ in (4.10)).

The following is a description of the algorithmic steps:

1. Computation of the set of exponents associated to the set of monomials inside the summation in Eqn. (4.10). Note that this set is defined by the set of feasible sequences of non-negative integers $\mathcal{F}_s$. Those sequences $\mathbf{r} = (r_1, ..., r_s)$ fulfill $\sum_{j=1}^{s} j\, r_j = 2s$, and represent all the possible degree distributions of trees with $s + 1$ nodes. Hence, we can generate this set of possible degree distribution by generating the set of possible degree sequences (and transforming them into degree distributions). A feasible degree sequence $\mathbf{d} = (d_1, ..., d_{e+1})$ satisfy $\sum_{i=1}^{s+1} d_i = 2s$, for $d_i \geq 1$. We can generate the set of feasible degree sequences using the following steps:

   (a) Find the set of non-negative integer partitions of $s-1$, i.e., $(\delta_1, \delta_2, ...)$ such that $\sum_j \delta_j = s - 1$, $\delta_i \in \mathbb{N}$. (The number of positive integers in each

partition is less or equal to $s-1$.) For example, for $s=4$, the partitions are (3), $(2,1)$, and $(1,1,1)$.

(b) From each partition, we yield a sequence of $s+1$ nonnegative integers by filling up the sequence with zeroes. For example, for $s=4$, we obtain $(3,0,0,0,0)$, $(2,1,0,0,0)$ and $(1,1,1,0,0)$ (sequences of length 5).

(c) Construct the set of feasible *degree sequences* by summing 1 to each entry in the previous sequences. In our example, we obtain $(4,1,1,1,1)$, $(3,2,1,1,1)$ and $(2,2,2,1,1)$. One can prove that the resulting sequences fulfill the condition $\sum_{i=1}^{s+1} d_i = 2s$, for $d_i \geq 1$; thus, these sequences are the set of feasible degree sequences for trees with $s+1$ nodes.

(d) Construct the set of feasible *degree distributions* from the set of degree sequences. In our example, we obtain the following degree distributions from the above degree sequences: $(4,0,0,1)$, $(3,1,1,0)$, and $(2,3,0,0)$, respectively. (Note how these sequences, $(r_1, r_2, ..., r_s)$, satisfy $\sum_{j=1}^{s} j\, r_j = 2s$.)

2. Once the set of feasible degree distributions $(r_1, r_2, ..., r_s)$ are computed, we can compute the set of monomials

$$2\binom{s}{r_1, ..., r_s} W_1^{r_1} W_2^{r_2} ... W_s^{r_s},$$

and mount the final polynomial expression in (4.10). For $s=4$, the monomials take the form $2W_1^4W_2^0W_3^0W_4^1$, $8W_1^3W_2^1W_3^1W_4^0$, and $4W_1^2W_2^3W_3^0W_4^0$, and the final multivariate polynomial expression in (4.10) is

$$\mathbf{E}\left[m_8\left(A_n\right)\right] = \frac{\rho^4}{n}\left[2W_1^4W_4 + 8W_1^3W_2W_3 + 4W_1^2W_2^3\right].$$

Appendix D

Proof of Lemma 4.5.3

Lemma D.0.2 *Consider the random matrix ensemble $\mathcal{A}_n(\sigma)$. Then, for $\mu_{k,p}(\tilde{A}_n)$ defined in Eqn. (4.25), we have that:*

(i) $\mu_{2s,p}(\tilde{A}_n) = 0$, *for* $p > s+1$,

(ii) $\mu_{2s,s+1}(\tilde{A}_n) \geq n^s \frac{1}{s+1}\binom{2s}{s}\sigma_{\min}^{2s}$,

(iii) $\mu_{2s,p}(\tilde{A}_n) = o(1)\mu_{2s,s+1}(\tilde{A}_n)$, *for* $p < s+1$,

if the sequence $\sigma = (\sigma_1, \sigma_2, ..., \sigma_n)$ *satisfies:*

$$\frac{s^6}{\sigma_{\max}^2}\left(\frac{\sigma_{\max}}{\sigma_{\min}}\right)^{2s} = o(n).$$

Proof of Item (i) Assume $k = 2s$ and $p > s+1$. One can easily prove, using the Pigeonhole principle, that any closed walk $\mathbf{c}_k \in C_{2s,p}^{(n)}$ covering more than $s+1$ nodes cannot be in $\widehat{C}_{k,p}^{(n)}$. Thus, according to Lemma 4.5.1, we have that $\tilde{\omega}(\mathbf{c}_k) = 0$. Thus,

$$\mu_{2s,p}(\tilde{A}_n) = 0, \text{ for } p > s+1. \tag{D.1}$$

Proof of Item (ii) Assume $k = 2s$ and $p = s+1$. We prove that:

$$\mu_{2s,s+1}(\tilde{A}_n) \geq n^s \frac{1}{s+1}\binom{2s}{s}\sigma_{\min}^{2s}. \tag{D.2}$$

We prove this result using Eqn. (4.28) and following two steps:

(a) we count the number of closed paths in $\widehat{C}^{(n)}_{2s,s+1}$, and

(b) we bound the contribution of each walk in Eqn. (4.28), i.e., $\mathbb{E}[\tilde{\omega}(c_k)]$ for $\mathbf{c}_k \in \widehat{C}^{(n)}_{2s,s+1}$.

The counting problem in step *(a)* is solved by assigning a code to each walk $\mathbf{c}_k = \{i_1, i_2, ..., i_{2s}, i_1\}$, for $\mathbf{c}_k \in \widehat{C}^{(n)}_{2s,s+1}$, and counting the number of possible codes. In this thesis, we propose a coding scheme based on ordered rooted trees (ORT's). In particular, we codify a given walk, $\mathbf{c}_k \in \widehat{C}^{(n)}_{2s,s+1}$, following the next three steps:

C1. Determine the ordered set of $s+1$ nodes in $\mathcal{V}(\mathbf{c}_k)$. The nodes are ordered according to the order of appearance in the walk.

C2. Find a rooted tree $T_s(\mathbf{c}_k)$ with the following characteristics:

(i) it is rooted at i_1,

(ii) it spans the set of nodes $\mathcal{V}(\mathbf{c}_k)$, and

(iii) the branches of $T_s(\mathbf{c}_k)$ are chosen from the set of edges $\mathcal{E}(\mathbf{c}_k)$.

Since each undirected edge must appear at least twice in $\mathbf{c}_k$ ($m_{i,j} \geq 2$ in Eqn. (4.27)), one can easily prove that all the edges in $\mathcal{E}(\mathbf{c}_k)$ overlap with branches of $T_s(c_k)$.

C3. The order in which nodes appear for the first time in the walk $\mathbf{c}_k$, induces a total order on the set of nodes in the spanning tree $T_s(\mathbf{c}_k)$. Thus, a closed walk $\mathbf{c}_k \in \widehat{C}^{(n)}_{2s,s+1}$ uniquely defines an ORT on the set of nodes $\mathcal{V}(\mathbf{c}_k)$. Reciprocally, one can prove that an ORT spanning the set of nodes $\mathcal{V}(\mathbf{c}_k)$ uniquely defines a walk $\mathbf{c}_k \in \widehat{C}^{(n)}_{2s,s+1}$. In other words, there is a bijection between the set of closed walks in $\widehat{C}^{(n)}_{2s,s+1}$ and the set of ORT's spanning $s+1$ nodes.

Based on this bijection, we count the number of walks in $\widehat{C}^{(n)}_{2s,s+1}$ by counting the number of associated ORT's. We solve this counting problem in two steps:

(a) We first count the number of possible choices for the set of $s+1$ nodes $\mathcal{V}(\mathbf{c}_k)$. This number is equal to $n(n-1)...(n-s)$.

(b) We count the number of ORT's spanning $\mathcal{V}(\mathbf{c}_k)$. This number is given by the $2s$-th order Catalan number [188], defined as $C_{2s} = \frac{1}{s+1}\binom{2s}{s}$.

Therefore, the number of walks in $\widehat{C}_{2s,s+1}^{(n)}$ is:

$$|\widehat{C}_{2s,s+1}^{(n)}| = n\,(n-1)\,...\,(n-s)\,\frac{1}{s+1}\binom{2s}{s}. \tag{D.3}$$

We now lower-bound the contribution of each walk in Eqn. (4.28). According to this equation, the contribution associated to each walk is given by $\mathbb{E}[\tilde{\omega}\,(\mathbf{c}_k)]$. Since every edge in $\mathbf{c}_k \in \widehat{C}_{2s,s+1}^{(n)}$ satisfies that $m_{i,j} = 2$ in Eqn. (4.21), we have that:

$$\mathbb{E}[\tilde{\omega}\,(\mathbf{c}_k)] \geq \sigma_{\min}^{2s}, \tag{D.4}$$

where $\sigma_{\min} = \min_i \sigma_i$.

Finally, we use Eqns. (D.3) and (D.4) in Eqn. (4.25) to deduce the bound in Eqn. (D.2).

Proof of Item (iii) Assume $k = 2s$ and $p < s+1$. We show that, under the condition

$$\frac{s^6}{\sigma_{\max}^2}\left(\frac{\sigma_{\max}}{\sigma_{\min}}\right)^{2s} = o\,(n)\,,$$

we have that

$$\mu_{2s,p}(\tilde{A}_n) = o(1)\mu_{2s,s+1}(\tilde{A}_n), \text{ for } p < s+1. \tag{D.5}$$

We prove this result by following the methodology proposed in [84] (and refined in the more recent papers, [198], [58]). First, we derive an upper bound of $\mu_{2s,p}$ for $p < s+1$. We find this bound, from Eqn. (4.25), following the same two steps that we used in the proof of item **(ii)**, i.e.: *(a)* we bound the number of walks in $\widehat{C}_{2s,p}^{(n)}$ for $p < s+1$, and *(b)* we bound $\mathbb{E}[\tilde{\omega}(\mathbf{c}_k)]$ for $\mathbf{c}_k \in \widehat{C}_{2s,p}^{(n)}$. For step *(a)*, we use a refined version of the bound proved in [84] (see also [198]):

$$|\widehat{C}_{2s,p}^{(n)}| \leq n^p 4^{p-1}\binom{2s}{2p-2}p^{4(s-p+1)}, \text{ for } p < s+1. \tag{D.6}$$

For step *(b)*, we deduce a bound of $\mathbb{E}[\tilde{\omega}(\mathbf{c}_k)]$ using the methodology introduced in [84]:

$$\mathbb{E}[\tilde{\omega}(\mathbf{c}_k)] \leq \frac{\sigma_{\max}^{2p-2}}{K^{2p-2-2s}}. \tag{D.7}$$

Finally, we can use Eqns. (D.6) and (D.7) in Eqn. (4.25) to bound the value of $\mu_{2s,p}$ as follows:

$$\mu_{2s,p}(\tilde{A}_n) \leq n^{p-1}4^{p-1}\binom{2s}{2p-2}p^{4(s-p+1)}\frac{\sigma_{\max}^{2p-2}}{K^{2p-2-2s}}. \tag{D.8}$$

In order to prove Eqn. (D.5), we study the ratio between $\mu_{2s,s+1}$ and $\mu_{2s,p}$. Assume s is an arbitrarily large integer, then from Eqns. (D.2) and (D.8), we have:

$$\begin{aligned}\frac{\mu_{2s,s+1}(\tilde{A}_n)}{\mu_{2s,p}(\tilde{A}_n)} &\geq \frac{1}{2}\left(\frac{4n}{K^2p^4s^2}\right)^{s+1-p}\frac{\sigma_{\min}^{2s}}{\sigma_{\max}^{2p-2}} \\ &\geq \frac{2n\,\sigma_{\max}^2}{K^2s^6}\left(\frac{\sigma_{\min}}{\sigma_{\max}}\right)^{2s}.\end{aligned} \tag{D.9}$$

where, in the first inequality, we have used that:

$$\binom{2s}{2p-2} \leq \left(\frac{2s}{2s-2p+2}\right)^{2s-2p+2} \leq 2s^{2s-2p+2},$$

and, in the second inequality, we take into account that the greatest lower bound is achieved for $p = s$, [84]. In order for $\mu_{2s,s+1}$ to dominate the summation in Eqn. (4.26), we need the lower bound of the ratio in Eqn. (D.9) to be $\Omega(1)$, which is achieved for:

$$\frac{s^6}{\sigma_{\max}^2}\left(\frac{\sigma_{\max}}{\sigma_{\min}}\right)^{2s} = o(n). \tag{D.10}$$

Appendix E

Proofs of Lemma 4.5.5 and Corollary 4.5.6

Lemma E.0.3 *Let* $\mathbf{r}_T = \{r_1, ..., r_s\} \in \mathbb{N}^s$, *with* $\sum_i r_i = s+1$, *and* $\sum_i i\, r_i = 2s > 0$. *Then the number* $\nu(\mathbf{r}_T)$ *of ORT's (with* $s+1$ *nodes) presenting degree distribution* $\mathbf{r}_T$ *is given by:*

$$\nu(\mathbf{r}_T) = 2\binom{s}{r_1, r_2, ..., r_s}.$$

Proof Consider a ORF F on s nodes and t (ordered) components presenting a δ-degree distribution $\rho_F = \{\rho_F(0), \rho_F(1), ..., \rho_F(s-1)\} \in \mathbb{N}^{s-1}$. We can uniquely construct a ORT, T, by connecting the components of F to a root node i (see Fig. E-1). (Notice that this construction is unique because there is an order in the set of components of F). Since F has t components, the δ-degree of i is equal to t; thus, the δ-degree distribution of T is $\rho_T = \{\rho_T(0), \rho_T(1), ..., \rho_T(s)\}$ such that $\rho_T(k) = \rho_F(k)$ for $k \neq t$ and $\rho_T(t) = \rho_F(t) + 1$. Reciprocally, given T, we can uniquely reconstruct the ORF, F, by removing the root node r and associated edges. From this construction, we conclude that there is a bijection between the set of ORT's having both a root degree of t and a δ-degree distribution ρ_T, and the set of ORF's with s components and δ-degree distribution ρ_F. Therefore, based on lemma 4.5.4,

we can count the number of ORT's with root degree t and degree distribution ρ_T as:

$$\frac{t}{s}\binom{s}{\rho_F(0),...,\rho_F(t),...,\rho_F(m_F)}.$$

Summing over the possible degrees for the root (i.e., $t = 1,...,s$) we obtain the total number of ORT's with degree distribution ρ_T as:

$$\sum_{t=1}^{s}\frac{t}{s}\binom{s}{\rho_F(0),...,\rho_F(t),...,\rho_F(m_F)}.$$

Furthermore, the degree distribution of T can be written as $\mathbf{r}_T = \{r_T(1), r_T(2), ..., r_T(m_T+1)\}$ with $r_T(k) = \rho_F(k-1)+1$ for $k \neq t$ and $r_T(t) = \rho_F(t-1)+1$. Thus, the number of ORT's, $v(\mathbf{r}_T)$, with degree distribution $\mathbf{r}_T$ is given by:

$$\begin{aligned} v(\mathbf{r}_T) &:= \sum_{t=1}^{s}\frac{t}{s}\binom{s}{r_T(1),...,r_T(k)-1,...,r_T(s)} \\ &= \frac{1}{s}\binom{s}{r_T(1),...,r_T(k),...,r_T(s)}\sum_{t=1}^{m} t\, r_T(t) \\ &= 2\binom{s}{r_T(1),...,r_T(s)}, \end{aligned}$$

where, in the first equality, we multiply numerator and denominator by r_t, and in the second equality we use $\sum_t t\, r_T(t) = 2s$.

Corollary E.0.4 *Let* $\mathbf{r} = \{r_1,...,r_e\} \in \mathbb{N}^e$. *Then,*

$$\sum_{\mathbf{r}\in\mathcal{F}_s} 2\binom{s}{r_1,...,r_s} = \frac{1}{s+1}\binom{2s}{s},$$

where $\mathcal{F}_s$ *is the set of nonnegative integer sequences defined in (4.1).*

Proof In Lemma 4.5.5, we proved that the number of ORT's with degree distribution $\mathbf{r} = (r_1,...,r_s)$ is equal to $2\binom{s}{r_1,...,r_s}$. Since $\mathcal{F}_s$ represents the set of all possible degree distributions for trees with $s+1$ nodes, we have that $\sum_{\mathbf{r}\in\mathcal{F}_s} 2\binom{s}{r_1,...,r_s}$ counts the total

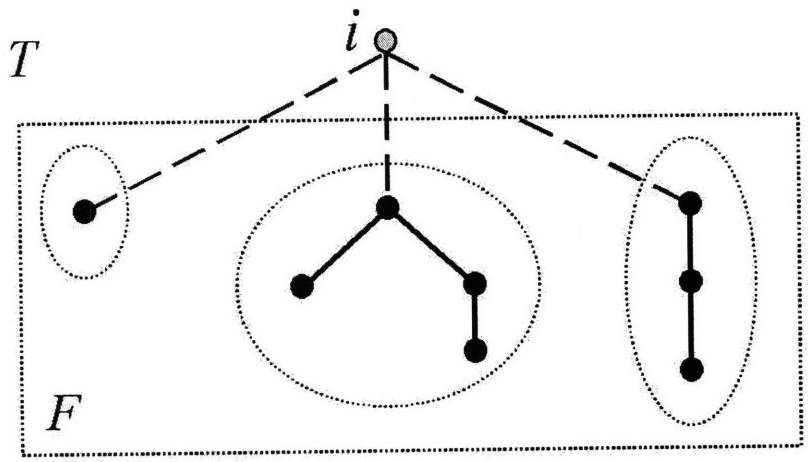

Figure E-1: In this Figure, we encircle by a dashed ellipse the isolated components of the forest F. The complete forest is inside the smaller dashed rectangle. Adding a root i, we can construct a tree T (inside the outer dashed rectangle). The subtrees of T are the components of F.

number of ORT's with $s+1$ nodes. The solution to this counting problem is known to be the Catalan number $C_s = \frac{1}{s+1}\binom{2s}{s}$, [188].

Appendix F

Proof of Theorem 4.7.1

Before we provide a proof of Theorem 4.7.1, we introduce notation and several useful results. First, according to the method of moments (Section 4.3), we can compute the spectral moments as:

$$\begin{aligned} m_k(\tilde{A}_n) &= \frac{1}{n}\mathrm{tr}\,\tilde{A}_n^k \\ &= \frac{1}{n}\sum_{1\le i_1,i_2,\ldots,i_k\le n} \tilde{a}_{i_1 i_2}\tilde{a}_{i_2 i_3}\ldots\tilde{a}_{i_{k-1} i_k}\tilde{a}_{i_k i_1}. \end{aligned} \tag{F.1}$$

Using the graph-theoretic nomenclature introduced in Subsection 4.3.2, we can rewrite Eqn. (F.1) as:

$$m_k(\tilde{A}_n) = \frac{1}{n}\sum_{\mathbf{c}_k\in C_k^{(n)}} \tilde{\omega}\left(\mathbf{c}_k\right), \tag{F.2}$$

where $\mathbf{c}_k$ represents a closed walk of length k, $\mathbf{c}_k = (i_1, i_2, ..., i_k, i_1)$, and $C_k^{(n)}$ is the set of possible closed walks of length k in the complete graph with n nodes, K_n. We also define the following function:

$$\tilde{\omega}\left(\mathbf{c}_k\right) = \tilde{a}_{i_1 i_2}\tilde{a}_{i_2 i_3}\ldots\tilde{a}_{i_{k-1} i_k}\tilde{a}_{i_k i_1}, \tag{F.3}$$

which, apart from closed walks, can take a graph as its argument. In particular, we are interested in using multigraphs[1] as the argument of $\tilde{\omega}(\cdot)$. For a given multigraph G, we denote by $\mathcal{E}(G)$ the set of different edges in G, and by m_{ij} the multiplicity of a particular edge $(i,j) \in \mathcal{E}(G)$ (where the multiplicity is defined as the number of edges connecting the same pair of nodes). Hence, we have

$$\tilde{\omega}(G) = \prod_{(i,j)\in\mathcal{E}(G)} \tilde{a}_{ij}^{m_{ij}}. \tag{F.4}$$

The above function presents the following property: For two multigraphs, G_1 and G_2, we have

$$\tilde{\omega}(G_1 \cup G_2) = \tilde{\omega}\left(\bar{G}_1\right) \tilde{\omega}\left(\bar{G}_2\right) \tilde{\omega}(G_1 \cap G_2), \tag{F.5}$$

where $\bar{G}_1$ and $\bar{G}_2$ are defined as: $G_1 - (G_1 \cap G_2)$ and $G_2 - (G_1 \cap G_2)$, respectively.

Apart from the above notation, we introduce the following useful results:

Lemma F.0.5 *Consider the centralized adjacency matrix $\tilde{A}_n$ associated to a Chung-Lu random graph $\mathcal{G}_n(\mathbf{w})$ with an uniformly bounded expected degree sequence, i.e., $1 \leq w_i \leq D < \infty$. Then,*

$$\mathbb{E}[\tilde{a}_{ij}^m] = \Theta\left(n^{-1}\right).$$

Proof The proof is a consequence of the definition of $\tilde{a}_{ij}$ in the Chung-Lu model. Since $\tilde{a}_{ij}$ are the entries of the centralized adjacency matrix, we have

$$a_{ij} = \begin{cases} 1 - p_{ij}, & \text{w.p. } p_{ij}, \\ -p_{ij}, & \text{w.p. } 1 - p_{ij}, \end{cases}$$

where $p_{ij} = \rho w_i w_j$, with $\rho = (\sum_i w_i)^{-1}$. From the condition $1 \leq w_i \leq D < \infty$, we

[1] A multigraph is a graph in which multiple edges are allowed to connect to the same pair of nodes at the same time.

have that $\rho = \Theta\left(n^{-1}\right)$, which implies $p_{ij} = \Theta\left(n^{-1}\right)$. Thus, we obtain

$$\mathbb{E}[\tilde{a}_{ij}^m] = p_{ij}\left(1 - p_{ij}\right)^m + \left(1 - p_{ij}\right)\left(-p_{ij}\right)^m = \Theta\left(n^{-1}\right).$$

Using the above lemma, we can prove the following corollaries:

Corollary F.0.6 *Consider the centralized adjacency matrix $\tilde{A}_n$ associated to a Chung-Lu random graph $\mathcal{G}_n(\mathbf{w})$ with an uniformly bounded expected degree sequence, $1 \leq w_i \leq D < \infty$. Then, for a multigraph, G, such that $m_{ij} \geq 2$ for all $(i,j) \in \mathcal{E}(G)$, we have*

$$\mathbb{E}[\tilde{\omega}(G)] = \Theta(n^{-|\mathcal{E}(G)|}).$$

Proof Using independence among different edges in a Chung-Lu graph, we have, from (F.4), that

$$\mathbb{E}[\tilde{\omega}(G)] = \prod_{(i,j)\in\mathcal{E}(G)} \mathbb{E}[\tilde{a}_{ij}^{m_{ij}}].$$

Hence, we conclude the proof by applying Lemma F.0.5 to the above equation.

Corollary F.0.7 *Consider the centralized adjacency matrix $\tilde{A}_n$ associated to a Chung-Lu random graph $\mathcal{G}_n(\mathbf{w})$ with an uniformly bounded expected degree sequence, $1 \leq w_i \leq D < \infty$. Then, for a multigraph G satisfying $m_{ij} \geq 2$ for all $(i,j) \in \mathcal{E}(G)$, we have*

$$Var[\tilde{\omega}(G)] = \Theta\left(n^{-|\mathcal{E}(G)|}\right) \tag{F.6}$$

Proof First, we expand (F.6) as

$$Var[\tilde{\omega}(G)] = \mathbb{E}[\tilde{\omega}^2(G)] - \mathbb{E}^2[\tilde{\omega}(G)]$$

Using independence among different edges in a Chung-Lu graph, and Lemma F.0.5, we derive:

$$\begin{aligned}\mathbb{E}[\tilde{\omega}^2(G)] &= \prod_{(i,j)\in\mathcal{E}(G)} \mathbb{E}[\tilde{a}_{ij}^{2m_{ij}}] = \Theta\left(n^{-|\mathcal{E}(G)|}\right), \\ \mathbb{E}^2[\tilde{\omega}(G)] &= \left(\prod_{(i,j)\in\mathcal{E}(G)} \mathbb{E}[\tilde{a}_{ij}^{m_{ij}}]\right)^2 = \Theta\left(n^{-2|\mathcal{E}(G)|}\right),\end{aligned}$$

which proves our statement.

After introducing the above nomenclature and results, we now provide a proof of Theorem 4.7.1:

Proof of Theorem 4.7.1 Using the notation introduced in Eqns. (F.2) and (F.3), we can write the variance of the k-th spectral moment of $\tilde{A}_n$ as:

$$Var[m_k(\tilde{A}_n)] = n^{-2} \sum_{\mathbf{c}_1\in C_k^{(n)}} \sum_{\mathbf{c}_2\in C_k^{(n)}} \mathbb{E}[\tilde{\omega}(\mathbf{c}_1)\,\tilde{\omega}(\mathbf{c}_2)] - \mathbb{E}[\tilde{\omega}(\mathbf{c}_1)]\,\mathbb{E}[\tilde{\omega}(\mathbf{c}_2)], \qquad \text{(F.7)}$$

where $\mathbf{c}_1$ and $\mathbf{c}_2$ represents two closed walks of length k, and $C_k^{(n)}$ denotes the set of closed walks of length k in the complete graph with n nodes, K_n. In a slight abuse of notation, we denote by $\mathbf{c}_1$ and $\mathbf{c}_2$ the undirected multigraphs associated to the closed walks of the same name.

We define the following subgraphs:

$$\mathbf{c}_\cap := \mathbf{c}_1 \cap \mathbf{c}_2, \qquad \bar{\mathbf{c}}_1 := \mathbf{c}_1 - \mathbf{c}_\cap, \qquad \bar{\mathbf{c}}_2 := \mathbf{c}_2 - \mathbf{c}_\cap.$$

Since $\mathbf{c}_1 = \bar{\mathbf{c}}_1 \cup \mathbf{c}_\cap$ and $\mathbf{c}_2 = \bar{\mathbf{c}}_2 \cup \mathbf{c}_\cap$, we can use (F.5) to derive:

$$\begin{aligned}\mathbb{E}[\tilde{\omega}(\mathbf{c}_1)\,\tilde{\omega}(\mathbf{c}_2)] &= \mathbb{E}[\tilde{\omega}(\bar{\mathbf{c}}_1)]\,\mathbb{E}[\tilde{\omega}(\bar{\mathbf{c}}_2)]\,\mathbb{E}\left[\tilde{\omega}^2(\mathbf{c}_\cap)\right], \text{ and} \\ \mathbb{E}[\tilde{\omega}(\mathbf{c}_1)]\,\mathbb{E}[\tilde{\omega}(\mathbf{c}_2)] &= \mathbb{E}[\tilde{\omega}(\bar{\mathbf{c}}_1)]\,\mathbb{E}[\tilde{\omega}(\bar{\mathbf{c}}_2)]\,\mathbb{E}^2[\tilde{\omega}(\mathbf{c}_\cap)].\end{aligned}$$

Substituting the above expressions in Eqn. (F.7), we derive the following expression

for the variance:

$$\begin{aligned} Var[m_k(\tilde{A}_n)] &= n^{-2} \sum_{\mathbf{c}_1,\mathbf{c}_2 \in C_k^{(n)}} \mathbb{E}[\tilde{\omega}(\bar{\mathbf{c}}_1)]\,\mathbb{E}[\tilde{\omega}(\bar{\mathbf{c}}_2)]\,\left(\mathbb{E}\left[\tilde{\omega}^2(\mathbf{c}_\cap)\right] - \mathbb{E}^2\left[\tilde{\omega}(\mathbf{c}_\cap)\right]\right) \\ &= n^{-2} \sum_{\mathbf{c}_1,\mathbf{c}_2 \in C_k^{(n)}} \mathbb{E}[\tilde{\omega}(\bar{\mathbf{c}}_1)]\,\mathbb{E}[\tilde{\omega}(\bar{\mathbf{c}}_2)]\; Var\left[\tilde{\omega}(\mathbf{c}_\cap)\right]. \end{aligned} \tag{F.8}$$

Notice that applying Corollaries F.0.6 and F.0.7, we can derive the following orders of magnitude for the factors involved in (F.8):

$$\begin{aligned} \mathbb{E}[\tilde{\omega}(\bar{c}_1)] &= \Theta(n^{-|\mathcal{E}(\bar{\mathbf{c}}_1)|}), \\ \mathbb{E}[\tilde{\omega}(\bar{c}_2)] &= \Theta(n^{-|\mathcal{E}(\bar{\mathbf{c}}_2)|}), \\ Var\left[\tilde{\omega}(c_\cap)\right] &= \Theta(n^{-|\mathcal{E}(\mathbf{c}_\cap)|}). \end{aligned}$$

Hence, the term inside the double summation in (F.8) satisfies:

$$\begin{aligned} \mathbb{E}[\tilde{\omega}(\bar{\mathbf{c}}_1)]\,\mathbb{E}[\tilde{\omega}(\bar{\mathbf{c}}_2)]\; Var\left[\tilde{\omega}(\mathbf{c}_\cap)\right] &= \Theta\left(n^{-(|\mathcal{E}(\bar{\mathbf{c}}_1)|+|\mathcal{E}(\bar{\mathbf{c}}_2)|+|\mathcal{E}(\mathbf{c}_\cap)|)}\right) \\ &= \Theta\left(n^{-|\mathcal{E}(\mathbf{c}_1 \cup \mathbf{c}_2)|}\right). \end{aligned} \tag{F.9}$$

We now analyze conditions under which the term inside the double summation in Eqn. (F.8) becomes zero. This occurs when any of the three factors inside the double summation becomes zero. There are two possible conditions under which this can happen:

(Z1) The factor $\mathbb{E}[\tilde{\omega}(\bar{c}_1)]$ (or $\mathbb{E}[\tilde{\omega}(\bar{c}_2)]$) is zero if there is an edge with multiplicity one (i.e., $m_{ij} = 1$) in $\bar{c}_1$ (or $\bar{c}_2$).

(Z2) The factor $Var\left[\tilde{\omega}(c_\cap)\right]$ becomes zero if $\mathbf{c}_1$ and $\mathbf{c}_2$ have no common edges.

Hence, for the term inside the double summation in (F.8) to be non-zero, the following conditions must be simultaneously satisfied:

(C1) The closed walks $\mathbf{c}_1$ and $\mathbf{c}_2$ must have at least one common edge.

(C2) The complementary closed walks $\bar{\mathbf{c}}_1$ and $\bar{\mathbf{c}}_2$ must have edges of multiplicity greater or equal than 2.

In the following, we use conditions **(C1)** and **(C2)** to upper bound the order of magnitude of the double summation in Eqn. (F.8). First, from **(C1)** and **(C2)**, we deduce that all the edges in the union graph, $\mathbf{c}_1 \cup \mathbf{c}_2$, must have multiplicity at least 2. Hence, since both $\mathbf{c}_1$ and $\mathbf{c}_2$ are closed walks of length k, the maximum number of edges that can be covered by $\mathbf{c}_1 \cup \mathbf{c}_2$, satisfying **(C1)** and **(C2)**, is equal to k. Therefore, defining the set:

$$D_{k,p}^{(n)} = \{(\mathbf{c}_1, \mathbf{c}_2) \in (C_k^{(n)})^2 \text{ s.t. } |\mathcal{E}(\mathbf{c}_1 \cup \mathbf{c}_2)| = p\},$$

we can rewrite Eqn. (F.8) as:

$$Var[m_k(\tilde{A}_n)] = n^{-2} \sum_{p=1}^{k} \sum_{(\mathbf{c}_1,\mathbf{c}_2) \in D_{k,p}^{(n)}} \mathbb{E}[\tilde{\omega}(\bar{\mathbf{c}}_1)]\, \mathbb{E}[\tilde{\omega}(\bar{\mathbf{c}}_2)]\, Var[\tilde{\omega}(\mathbf{c}_\cap)], \tag{F.10}$$

where p denotes the number of edges covered by the union of $\mathbf{c}_1$ and $\mathbf{c}_2$. For a given p, we can apply Eqn. (F.9) to compute the order of magnitude of the term inside the double summation in Eqn. (F.10) as follows:

$$\mathbb{E}[\tilde{\omega}(\bar{\mathbf{c}}_1)]\, \mathbb{E}[\tilde{\omega}(\bar{\mathbf{c}}_2)]\, Var[\tilde{\omega}(\mathbf{c}_\cap)] = \Theta\left(n^{-p}\right). \tag{F.11}$$

Furthermore, we can also apply the constrains **(C1)** and **(C2)** to upper bound the order of magnitude of the number of non-zero terms in the rightmost summation in (F.10), i.e., $\left|D_{k,p}^{(n)}\right|$. This is achieved by bounding the maximum number of nodes that the union graph $\mathbf{c}_1 \cup \mathbf{c}_2$ can span under the constrains **(C1)** and **(C2)**. One can prove that $\mathbf{c}_1 \cup \mathbf{c}_2$ span a maximal number of nodes when the following two conditions are satisfied:

(M1) Both $\bar{\mathbf{c}}_1$ and $\bar{\mathbf{c}}_2$ are composed by multiedges of multiplicity greater or equal than 2 arranged in a tree structure.

(M2) The intersection subgraph, $c_\cap$, is composed by multiedges arranged in a cycle.

Thus, the maximum number of nodes spanned by $\mathbf{c}_1 \cup \mathbf{c}_2$, such that $|\mathcal{E}(\mathbf{c}_1 \cup \mathbf{c}_2)| = p$

(and satisfying **(C1)** and **(C2)**), is equal to p. Since each node in $\mathbf{c}_1 \cup \mathbf{c}_2$ can be a member of $\{1, ..., n\}$, we have that

$$\left| D_{k,p}^{(n)} \right| = O\left(n^p\right). \tag{F.12}$$

Finally, we apply Eqns. (F.11) and (F.12) in (F.10) to upper bound the asymptotic behavior of the variance as follows:

$$\begin{aligned} Var[m_k(\tilde{A}_n)] &= n^{-2} \sum_{p=1}^{k} \sum_{(\mathbf{c}_1, \mathbf{c}_2) \in D_{k,p}^{(n)}} \Theta\left(n^{-p}\right) \\ &= n^{-2} \sum_{p=1}^{k} O\left(n^p\right) \Theta\left(n^{-p}\right) = O\left(n^{-2}\right). \end{aligned}$$

This concludes our proof.

Bibliography

[1] M. Abramowitz, and I.A. Stegun, I. A. (Eds.), *Handbook of Mathematical Functions with Formulas, Graphs, and Mathematical Tables*, 9th printing. New York: Dover, 1972.

[2] Y.Y. Ahn, S. Han, H. Kwak, S. Moon, and H. Jeong, "Analysis of Topological Characteristics of Huge Online Social Networking Services," in *Proc. of the 16^{th} International Conference on World Wide Web*, 2007.

[3] W. Aiello, F. Chung, and L. Lu, "A Random Graph Model for Massive Graphs," in *Proc. of the 32^{nd} ACM Symp. on Theory of Computing*, pp. 171-180, 2000.

[4] W. Aiello, F. Chung, and L. Lu, "Random Evolution in Massive Graphs," in *Handbook of Massive Data Sets*, pp. 97-122, 2002.

[5] N. I. Akhiezer, *The Classical Moment Problem and some Related Questions in Analysis*, Hafner Publishing Co., 1965.

[6] R. Albert, H. Jeong, A.L. Barabási, "The Diameter of the World Wide Web," *Nature*, vol. 401, pp. 130-131, 1999

[7] R. Albert, A.L. Barabási, "Statistical Mechanics of Complex Networks," *Reviews of Modern Physics*, vol. 74, pp. 47-97, 2002.

[8] D. Aldous, "Some Inequalities for Reversible Markov Chains," *Journal of the London Mathematical Society*, pp. 564-576, 1982.

[9] D. Aldous, "Random Walks on Finite Groups and Rapidly Mixing Markov Chains," *Séminaire de probabilités de Strasbourg*, vol. 17, pp. 243-297, 1983.

[10] J.A. Almendral and A. Díaz-Guilera, "Dynamical and Spectral Properties of Complex Networks," *New J. Phys.*, vol. 9, 187, 2007.

[11] N. Alon, "Eigenvalues and Expanders," *Combinatorica*, vol. 6, 83-96, 1986.

[12] N. Alon, "Spectral Techniques in Graph Algorithms," *Lecture Notes in Computer Science*, vol. 1380, pp. 206-215. Springer-Verlag, 1998.

[13] N. Alon, A. Coja-Oghlan, H. Hàn, M. Kang, V. Rödl, and M. Schacht, "Quasi-Randomness and Algorithmic Regularity for Graphs with General Degree Distributions," *Lecture Notes in Computer Science*, vol. 4596, pp.789-800, 2007.

[14] N. Alon and J.H. Spencer, *The Probabilistic Method*, 2^{nd} Edition. Wiley-Interscience, 2000.

[15] N. Alon, M. Krivelevich, and V. Vu, "On the Concentration of Eigenvalues of Random Symmetric Matrices," *Israel J. Math.*, vol. 131, pp. 259-267, 2002.

[16] H. Andersson, "Epidemic Models and Social Networks," *Math. Scientist,* vol. 24, pp. 128-147, 1999.

[17] G. Andrews and K. Eriksson, *Integer Partitions*, Cambridge University Press, 2004.

[18] E.A.G. Armour and W.B. Brown, "The Stability of Three-Body Atomic and Molecular Ions," *Acc. Chem. Res.*, vol. 26, pp. 168-173, 1993.

[19] L. Arnold, "On the Asymptotic Distribution of the Eigenvalues of Random Matrices," *J. Math. Analysis and Appl.*, vol. 20, pp. 262-268, 1967.

[20] F.M. Atay, T. Biyikoglu, and J. Jost, "Synchronization of Networks with Prescribed Degree Distributions," *IEEE Trans. Circ. Syst. I*, vol. 53, no.1, 2006.

[21] B. Ayazifar, *Graph Spectra and Modal Dynamics of Oscillatory Networks*, MIT Thesis, 2002.

[22] Y. Azar, A. Fiat, A. Karlin, F. McSherry, and J. Saia, "Spectral Analysis of Data," in *Proc. 33rd ACM Symp. on Theory of Computing*, pp. 619–626, 2001.

[23] Z.D. Bai, "Methodologies in Spectral Analysis of Large Dimensional Random Matrices," *Statistica Sinica*, vol. 9, pp. 611-677, 1999.

[24] A.L. Barabási, and R. Albert, "Emergence of Scaling in Random Networks," *Science*, vol. 285, pp. 509-512, 1999.

[25] A.L. Barabási, R. Albert, and H. Jeong, "Scale-Free Characteristics of Random Networks: The Topology of the World-Wide Web," *Physica A*, vol. 281, pp. 69–77, 2000.

[26] M. Barahona, L.M. Pecora, "Synchronization in Small-World Systems," Physical Review Letters, vol. 89, 054101, 2002

[27] M. Beeler, R.W. Gosper, and R. Schroeppel, "HAKMEM," *MIT AI Memo*, vol. 239, 1972.

[28] E.A. Bender and E.R. Canfield, "The Asymptotic Number of Labelled Graphs with Given Degree Sequences," *J. Combin. Theory Ser. A*, no. 24, pp. 296-307, 1978.

[29] D. Bertismas and I. Popescu, "Optimal Inequalities in Probability Theory: A Convex Optimization Approach," *SIAM J. Optim.*, vol. 15, no. 3, pp.780-804, 2005.

[30] G. Berkolaiko, R. Carlson, S.A. Fulling, P. Kuchment, *Quantum Graphs and Their Applications*. AMS, 2006.

[31] G. Bianconi, "Spectral Properties of Complex Networks," *arXiv*:0804.1744v1 [cond-mat.dis-nn], 2008.

[32] N. Biggs, *Algebraic Graph Theory*, 2^{nd} Edition. Cambridge University Press, 1993.

[33] V.D. Blondel, J.M. Hendrickx, A. Olshevsky, and J.N. Tsitsiklis, "Convergence in Multiagent Coordination, Consensus, and Flocking," in *Proc. 44th IEEE Conf. on Decision and Control*, pp. 2996- 3000, 2005.

[34] S. Boccaletti S., V. Latora, Y. Moreno, M. Chavez, and D.-H. Hwang, "Complex Networks: Structure and Dynamics," *Physics Reports*, vol. 424, no. 4-5, pp. 175-308, 2006.

[35] M. Boguñá and R. Pastor-Satorras, "Epidemic Spreading in Correlated Complex Networks," *Physical Review E*, vol. 66, 047104, 2002.

[36] B. Bollobás, "Martingales, Isoperimetric Inequalities and Random Graphs," in *Combinatorics*, pp. 113-139, North-Holland, 1988.

[37] B. Bollobás, *Random Graphs*, 2nd Edition. Cambridge University Press, 2001.

[38] B. Bollobás, O. M. Riordan, J. Spencer, and G. Tusnady, "The Degree Sequence of a Scale-Free Random Graph Process," *Random Structures and Algorithms*, vol. 18 , pp. 279-290, 2001.

[39] B. Bollobás and O. Riordan, "Robustness and Vulnerability of Scale-Free Random Graphs," *Internet Mathematics*, vol. 1, pp. 1-35, 2003.

[40] R.B. Boppana, "Eigenvalues and Graph Bisection: An Average-Case Analysis," *IEEE Symp. on Foundations of Computer Science*, pp. 280-285, 1987.

[41] S. Boyd, "Convex Optimization of Graph Laplacian Eigenvalues," in *Proc. International Congress of Mathematicians*, 2006.

[42] S. Boyd, P. Diaconis, and L. Xiao, "Fastest Mixing Markov Chain on a Graph," *SIAM Review*, vol. 47, pp. 667-689, 2004.

[43] S. Boyd, A. Ghosh, B. Prabhakar, and D. Shah, "Gossip Algorithms: Design, Analysis and Applications," in *Proc. INFOCOM*, vol. 3, pp. 1653-1664, 2005.

[44] A. Broder, R. Kumar, F. Maghoul, P. Raghavan, R. Statac, A. Tomkinsb, and J. Wiener, "Graph Structure in the Web," *Computer Networks*, vol. 33, pp. 309-320, 2000.

[45] T.A. Brody, J. Flores, J.B. French, P.A. Mello, A. Pandey, S.S.M. Wong, "Random-Matrix Physics: Spectrum and Strength Fluctuations," *Rev. Mod. Phys.*, vol. 53, pp. 385-479, 1981.

[46] W. Bryc, A. Dembo, and T. Jiang, "Spectral Measure of Large Random Hankel, Markov and Toeplitz Matrices," *Ann. Probab.*, vol. 34, pp. 1-38, 2006.

[47] http://www.caida.org/data/active/as-relationships/

[48] http://www.caida.org/research/topology/

[49] http://www.caida.org/home/about/annualreports/1998/

[50] Z. Cai, Y. Gu, and W. Zhong, "A New Approach of Computing Floquet Transition Matrix", *Computers and Structures*, vol. 79, pp. 631-635, 2001.

[51] M. Cha, H. Kwak, P. Rodriguez, Y.-Y. Ahn, and Sue Moon, "I Tube, You Tube, Everybody Tubes: Analyzing the World's Largest User Generated Content Video System," *Proc. 7^{th} ACM SIGCOMM Conf. on Internet Measurement*, pp. 1-14, 2007.

[52] P. Checcoa, M. Bieya, and L. Kocarev, "Synchronization in Random Networks with Given Expected Degree Sequences," *Chaos, Solitons & Fractals*, vol. 35, pp. 562-577, 2008.

[53] F.R.K. Chung, "Diameters and Eigenvalues," *J. Amer. Math. Soc.*, vol. 2, pp. 187-196, 1989.

[54] F.K.R. Chung, *Spectral Graph Theory*, American Mathematical Society, 1997.

[55] F.K.R. Chung and L. Lu, "The Diameter of Sparse Random Graphs," *Advances in Applied Mathematics*, vol. 26, pp. 257-279, 2002.

[56] F.K.R. Chung and L. Lu, "Connected Components in Random Graph with Given Degree Sequences," *Annals of Combinatorics*, vol. 6, pp. 125-145, 2002.

[57] F.R.K. Chung and L. Lu, "The Average Distance in a Random Graph with Given Expected Degrees," *Internet Mathematics*, vol. 1, pp. 91-114, 2003.

[58] F.K.R. Chung, L. Lu, and V. Vu, "The Spectra of Random Graphs with Given Expected Degrees," *Proc. Nat. Acad. Sci.*, vol. 100, no. 11, pp. 6313-6318, 2003.

[59] F.K.R. Chung and L. Lu, *Complex Graphs and Networks*, American Mathematical Society, 2006.

[60] A. Coja-Oghlan, "On the Laplacian Eigenvalues of G(n,p)," *Combinatorics, Probability and Computing*, vol. 16, pp. 923-946, 2007.

[61] V. Colizza, A. Flammini, M.A. Serrano, and A. Vespignani, "Detecting Rich-Club Ordering in Complex Networks", *Nature Physics*, vol. 2, pp. 110-115, 2006.

[62] C. Cooper and A.M. Frieze, "A General Model of Web Graphs," *Random Structures and Algorithms*, vol. 22, pp. 311-335, 2001.

[63] T.H. Cormen, C.E. Leiserson, R.L. Rivest, and C. Stein, *Introduction to Algorithms*, Second Edition. MIT Press and McGraw-Hill, 2001.

[64] R.E. Curto, and L.A. Fialkow, "The Truncated Complex K-Moment Problem," *Trans. Amer. Math. Soc.*, vol. 352, pp. 2825-2855, 2000.

[65] D. Cvetkovic, M. Doob, H. Sachs, *Spectra of graphs: Theory and application*, Academic Press, 1980.

[66] http://cdg.columbia.edu/cdg/datasets

[67] R. Diestel, *Graph Theory*, 3^{rd} Edition. Springer-Verlag, 2005.

[68] S.N. Dorogovtsev and J.F.F. Mendes, "Accelerated Growth of Networks", in *Handbook of Graphs and Networks*. Wiley Interscience, 2002.

[69] S.N. Dorogovtsev and J.F.F. Mendes, "Evolution of Networks with Aging of Sites", *Physical Review E*, vol. 62, pp. 1842-1845, 2000.

[70] S.N. Dorogovtsev and J.F.F. Mendes, *Evolution of Networks: From Biological Nets to the Internet and WWW.* Oxford University Press, 2003.

[71] P.G. Doyle, J.L. Snell, *Random Walks and Electric Networks.* Mathematical Association of America, Washington, DC, 1984.

[72] R. Durrett, *Random Graph Dynamics.* Cambridge University Press, 2006.

[73] J.-P. Eckman and D. Ruelle, "Ergodic Theory of Chaos and Strange Attractors," *Review of Modern Physics*, vol. 57, pp. 617-656, 1985.

[74] P. Erdös and A. Rényi, "On Random Graphs," *Publicationes Mathematicae*, vol. 6, pp. 290-297, 1959.

[75] P. Erdös and A. Rényi, "On the Evolution of Random Graphs," *Bulletin of the Institute of International Statistics*, vol. 5, pp. 17-61, 1961.

[76] M. Faloutsos, P. Faloutsos, and C. Faloutsos, "On Power-Law Relationship of the Internet Topology," *Comput. Commun. Rev.*, vol. 29, pp. 251-263, 1999.

[77] M. Farkas, *Periodic Motion.* AMS Publishing, 1994.

[78] I.J. Farkas, I. Derenyi, A.L. Barabási, and T. Vicsek, "Spectra of Real World Graphs: Beyond the Semicircle Law," *Phys. Rev. E.*, vol. 64, 2001.

[79] J.A. Fax and R.M. Murray, "Information Flow and Cooperative Control of Vehicle Formations," *IEEE Transactions on Automatic Control*, vol. 49, no. 9, pp. 1465-1476, 2004.

[80] U Feige and E Ofek, "Spectral Techniques Applied to Sparse Random Graphs," Random Structures and Algorithms, 2005

[81] M. Fiedler, "Algebraic Connectivity of Graphs", *Czech. Math. J.*, vol. 23, pp. 298-305, 1973.

[82] M. Fiedler, "A Property of Eigenvectors of Nonnegative Symmetric Matrices and its Applications to Graph Theory," *Czechoslovak Mathematical Journal*, vol. 25, pp. 619–633, 1975.

[83] G. Finke, R.E. Burkard, and F. Rendl, "Quadratic Assignment Problem," *Ann. Discrete Math.*, vol. 31, pp. 61-82, 1987.

[84] Z. Füredi and J. Komlós, "The Eigenvalues of Random Symmetric Matrices," *Combinatorica*, vol. 1, pp. 233-241, 1981.

[85] A.J. Ganesh, L. Massoulié, D.F. Towsley, "The Effect of Network Topology on the Spread of Epidemics," *INFOCOM*, pp. 1455-1466, 2005.

[86] M.T. Gastner and M.E.J. Newman, "Optimal Design of Spatial Distribution Networks," *Physical Review E*, vol. 74, 2006.

[87] V. Gazi and K. M. Passino, "Stability Analysis of Swarms," *IEEE Trans. Autom. Control*, vol. 48, no. 4, pp. 692-697, 2003.

[88] C. Gkantsidis, M. Mihail, and A. Saberi, "Conductance and Congestion in Power-Law Graphs," *SIGMETRICS*, 2003.

[89] P.M. Gleiss, P.F. Stadler, A. Wagner, and D.A. Fell, "Relevant Cycles in Chemical Reaction Networks," *Adv. Complex Syst.*, vol. 4, 207, 2001.

[90] M.X. Goemans and D.P. Williamson, "Improved Approximation Algorithms for Maximum Cut and Satisfiability Problems using Semidefinite Programming," *Journal of the ACM*, vol. 42, pp. 1115-1145, 1995.

[91] C.D. Godsil and G. Royle, *Algebraic Graph Theory*. Springer, 2001.

[92] G. Goldztein and S. H. Strogatz, "Stability of Synchronization in Networks of Digital Phase-Locked Loops," *Int. J. Bifurcations Chaos Appl. Sci. Eng.*, vol. 5, pp. 983-990, 1995.

[93] M.C. González and A.L. Barabási, "Complex Networks: From Data to Models," *Nature Physics*, vol. 3, pp. 224-225, 2007.

[94] G. Grimmett and D. Stirzaker, *Probability and Random Processes*, 3^{rd} Edition. Oxford University Press, 2001.

[95] I. Gupta, A.-M. Kermarrec, A.J. Ganesh, "Efficient and Adaptive Epidemic-Style Protocols for Reliable and Scalable Multicast," *IEEE Trans. Parallel Distrib. Syst.*, vol. 17, pp. 593-605, 2006.

[96] A. Gut, *Probability: A Graduate Course*. Springer, 2005.

[97] Y. Hatano and M. Mesbahi, "Agreement Over Random Networks," *IEEE Transactions on Automatic Control*, vol. 50, pp. 1867-1872, 2005.

[98] J.F. Heagy, L.M. Pecora, and T.L. Carroll, "Short Wavelength Bifurcations and Size Instabilities in Coupled Oscillator Systems," *Phys. Rev. Lett.*, vol. 74, no. 21, 1995.

[99] R.A. Horn and C.R. Johnson, *Matrix Analysis*. Cambridge University Press, 1990.

[100] R.A. Horn and C.R. Johnson, *Topics in Matrix Analysis*. Cambridge University Press, 1994.

[101] Y. Ijiri and H.A. Simon, *Skew Distributions and the Sizes of Business Firms*. North Holland, Amsterdam, 1977.

[102] A. Jadbabaie, J. Lin, and A.S. Morse, "Coordination of Groups of Mobile Autonomous Agents Using Nearest Neighbor Rules," *IEEE Trans. Autom. Control*, vol. 48, pp. 988-1001, 2003.

[103] S. Janson, T. Luczak, and A. Rucinski, *Random Graphs*. Wiley, 2000.

[104] H. Jeong, B. Tombor, R. Albert, Z.N. Oltvai, A.L. Barabási, "The Large-Scale Organization of Metabolic Networks," *Nature*, vol. 407, pp. 651-654, 2000.

[105] J. Jia and C. Chen, "GMT: A Geometry-based Model on BitTorrent-like Topology," *IEEE Int. Conf. on Signal Processing*, vol. 4, pp. 16-20, 2006.

[106] C. Jin, Q. Chen, and S. Jamin, "Inet: Internet Topology Generator," University of Michigan Technical Report CSE-TR-433-00, 2000.

[107] F. Juhasz, "On the Spectrum of a Random Graph," in *Algebraic Methods in Graph Theory*, 1978.

[108] T. Kailath, *Linear Systems.* Prentice-Hall, 1979.

[109] A.F. Karr, *Probability.* Springer-Verlag, 1993.

[110] D. Kempe and F. McSherry, "A Decentralized Algorithm For Spectral Analysis," *Journal of Computer and System Sciences*, vol. 74, pp. 70-83, 2007.

[111] D.-H. Kim, A.E. Motter, "Ensemble Averageability in Network Spectra," *Phys. Rev. Lett.*, vol. 98, 248701, 2007.

[112] G. Kirchhoff, "Über die Auflösung der Gleichungen, auf welche man bei der untersuchung der linearen verteilung galvanischer Ströme geführt wird," *Ann. Phys. Chem.*, vol. 72, pp. 497-508, 1847.

[113] J. Kleinberg, S. R. Kumar, P. Raphavan, S. Rajagopalan, and A. Tomkins, "The Web as a Graph: Measurements, Models and Methods," *Proc. Int. Conf. Combinatorics and Computing*, pp. 26-28, 1999.

[114] P.L. Krapivsky, S. Redner, and F. Leyvraz, "Connectivity of Growing Random Networks," *Physical Review Letters*, vol. 85, pp. 4629-4632, 2000.

[115] D. Krioukov, K. Fall, and X. Yang, "Compact Routing on Internet-like Graphs," in *Proc. INFOCOM*, 2004.

[116] M. Krivelevich and B. Sudakov, "The Largest Eigenvalue of Sparse Random Graphs," *Combinatorics, Probability and Computing*, vol. 12, pp. 61-72, 2003.

[117] R. Kumar, J. Novak, and A. Tomkins, "The Structure and Evolution of Online Social Networks," *Proc. ACM SIGKDD*, pp. 611-617, 2006.

[118] R. Lambiotte, "Activity ageing in growing networks," *Journal of Statistical Mechanics: Theory and Experiment*, pp. 02020, 2007.

[119] S. Lang, *Algebra*, Springer-Verlag, 2004

[120] J. B. Lasserre, "Bounds on Measures Satisfying Moment Conditions," *Annals Appl. Prob.*, vol 12, pp. 1114-1137, 2002.

[121] E.L. Lehmann, *Elements of Large-Sample Theory*, Springer-Verlag, 1999.

[122] F. Leighton and S. Rao, "Multicommodity Max-flow Min-cut Theorems and their Use in Designing Approximation Algorithms," *Journal of the ACM*, vol. 46, pp. 787-832, 1999.

[123] L. Li, D. Alderson, J.C. Doyle, W. Willinger, "Towards a Theory of Scale-Free Graphs: Definition, Properties, and Implications," *Internet Mathematics*, vol. 2, pp. 431-523, 2005.

[124] X. Li and G. Chen, "A Time-Varying Complex Dynamical Network Model and Its Controlled Synchronization Criteria," *IEEE Trans. Automatic Control*, vol. 50, no.1, 2005.

[125] http://www.limewire.org

[126] N. Linial, E. London, and Rabinovich, "The Geometry of Graphs and Some of Its Algorithmic Applications," *Combinatorica*, vol. 15, pp. 215-245, 1995.

[127] J. Lu and D.W.C. Ho, "Local and Global Synchronization in General Complex Dynamical Networks with Delay Coupling", *Chaos, Solitons and Fractals*, vol. 37, pp. 1497-1510, 2008.

[128] N. Madras and G. Slade, *The Self-Avoiding Walk*. Birkhäuser Boston, 1996.

[129] P. Mahadevan, D. Krioukov, K. Fall, and A. Vahdat, "Systematic Topology Analysis and Generation Using Degree Correlations," in *Proc. SIGCOMM*, vol. 36, pp. 135-146, 2006.

[130] F. McSherry, "Spectral Partitioning of Random Graphs," in *Proc. 42nd IEEE Symp. on Foundations of Computer Science*, pp. 529–537, 2001.

[131] A. Medina, A. Lakhina, I. Matta, and J. Byers, "BRITE: An Approach to Universal Topology Generation," in *Proc. MASCOTS*, pp. 346-353, 2001.

[132] M.L. Mehta, *Random Matrices.* Academic Press, 2004.

[133] J.F.F. Mendes and S.N. Dorogovtsev, *Evolution of Networks: From Biological Nets to the Internet and WWW*, Oxford University Press, 2003.

[134] R. Merris,"A Note on Laplacian Graph Eigenvalues," *Linear Algebra Appl.*, vol. 285, 1988.

[135] R.K. Merton,"The Matthew Effect in Science," *Science*, vol. 5, 1968.

[136] M. Mesbahi, "On Maximizing the Second Smallest Eigenvalue of a State-Dependent Graph Laplacian," *IEEE Transactions on Automatic Control*, vol. 51, no.1, pp. 116-120, 2006.

[137] S. Meyn, *Control Techniques for Complex Networks*, Cambridge University Press, 2007.

[138] R.E. Mirollo and S.H. Strogatz, "Synchronization of Pulse-Coupled Biological Oscillators," *SIAM Journal on Applied Mathematics*, vol. 50, pp. 1645-1662, 1990.

[139] M. Mitzenmacher, "A Brief History of Generative Models for Power Law and Lognormal Distributions," *Internet Mathematics*, vol. 1, pp. 226-251, 2003.

[140] B. Mohar and S. Poljak, "Eigenvalues in Combinatorial Optimization," in *Combinatorial and Graph-Theoretical Problems in Linear Algebra*, IMA Volumes in Mathematics and Its Applications, vol. 50, pp. 107-151, Springer-Verlag, 1993.

[141] B. Mohar, "The Laplacian Spectrum of Graphs," in *Graph Theory, Combinatorics, and Applications*, vol. 2, pp. 871–898, 1991.

[142] M. Molloy and B. Reed, "A Critical Point for Random Graphs with a Given Degree Sequence," *Random Structures and Algorithms*, vol. 6, pp. 161-179, 1995.

[143] M. Molloy, and B. Reed, "The Size of the Giant Component of a Random Graph with a Given Degree Sequence," *Combinatorics, Probability and Computing*, vol. 7, pp. 295-305, 1998.

[144] C. Moore and M.E.J. Newman, "Epidemics and Percolation in Small World Networks," *Phys. Rev. E*, vol. 61, 5678-5682, 2000.

[145] A.E. Motter, C. Zhou, and J. Kurths, "Network Synchronization, Diffusion, and the Paradox of Heterogeneity," *Phys. Rev. E*, vol. 71, 016116, 2005.

[146] T. Nagao and G.J. Rodgers, "Spectral Density of Complex Networks with a Finite Mean Degree," *J. Phys. A: Math. Theor.*, vol. 41, 265002, 2008.

[147] M.E.J. Newman, "Scientific Collaboration Networks I. Network Construction and Fundamental Results," *Phys. Rev. E*, vol. 64, 016131, 2001.

[148] M.E.J. Newman, "Models of the Small World," *Journal of Statistical Physics*, vol. 101, pp. 819-841, 2000.

[149] M.E.J. Newman, "Assortative Mixing in Networks," *Phys. Rev. Lett.*, vol. 89, 208701, 2002.

[150] M.E.J. Newman, "The Structure and Function of Complex Networks," *SIAM Review*, vol. 45, pp. 167-256, 2003.

[151] M.E.J. Newman, A.-L. Barabasi, and D.J. Watts, *The Structure and Function of Complex Networks*, Princeton University Press, 2006.

[152] M.E.J. Newman, S.H. Strogatz, and J. Watts, "Random Graphs with Arbitrary Degree Distributions and Their Applications," *Phys. Rev. E*, vol. 64, 026118, 2001.

[153] R. Olfati-Saber and R. M. Murray, "Distributed Cooperative Control of Multiple Vehicle Formations Using Structural Potential Functions," in *Proc. 15th IFAC World Congress*, June 2002.

[154] R. Olfati-Saber, "Consensus Problems in Networks of Agents with Switching Topology and Time-Delays," *IEEE Trans. Autom. Control*, vol. 49, pp. 1520-1533, 2004.

[155] R. Olfati-Saber, "Flocking for Multi-Agent Dynamic Systems: Algorithms and Theory," *IEEE Trans. on Automatic Control*, vol. 51, pp. 401-420, 2006.

[156] F. Paganini, J. Doyle, and S. Low, "Scalable Laws for Stable Network Congestion Control," in *Proc of IEEE Conference on Decision and Control*, vol. 1, pp. 185-190, 2001.

[157] A. Papoulis and S.U. Pillai, *Probability, Random Variables and Stochastic Processses,* 4^{th} ed. McGraw-Hill, 2002.

[158] P.A. Parrilo, *Structured Semidefinite Programs and Semialgebraic Geometry Methods in Robustness and Optimization*, Ph.D. Thesis, California Institute of Technology, May 2000.

[159] R. Pastor-Satorrás, A. Vázquez, and A. Vespignani, "Dynamical and Correlation Properties of the Internet," *Phys. Rev. Lett.*, vol. 87, 258701, 2001.

[160] L.M. Pecora and T.L. Carroll, "Master Stability Functions for Synchronized Coupled Systems," *Phys. Rev. Lett.*, vol. 80, pp. 2109-2112, 1998.

[161] L.M. Pecora and M. Barahona, "Synchronization of Oscillators in Complex Networks," *New Research on Chaos and Complexity* (Eds. F. Orsucci and N. Sala), Nova Science Publishers, 2005.

[162] I. Popescu, "A Semidefinite Programming Approach to Optimal Moment Bounds for Convex Classes of Distributions," *Mathematics of Operation Research*, Vol. 30, no. 3, 2005.

[163] S. Prajna, A. Papachristodoulou, and P. A. Parrilo, "SOSTOOLS: Sum of Squares Optimization Toolbox for MATLAB – User's Guide," *Control and Dynamical Systems, California Institute of Technology*, 2002.

[164] V.M. Preciado and G.C. Verghese, "Suppression of Homoclinic Chaos using Multiharmonic Inputs: Melnikov Analysis and Root-Locus Design," in Proc. *IFAC Nonlinear Control Systems*, vol. 2, pp. 843-848, 2004.

[165] V.M. Preciado and G.C. Verghese, "Synchronization in Generalized Erdös-Rényi Networks of Nonlinear Oscillators," *Proc. of the 44^{th} Conference on Decision and Control,* pp. 4628 - 4633, 2005.

[166] V.M. Preciado, and G.C. Verghese, "Low-Order Spectral Analysis of Kirchhoff Matrices for a Probabilistic Graph With a Prescribed Expected Degree Sequence," *submitted for publication.*

[167] M. Putinar, "Positive Polynomials on Compact Semi-Algebraic Sets", *Indiana University Mathematics Journal*, vol. 42, pp. 969–984, 2003.

[168] E. Ravasz and A.L. Barabási, "Hierarchical Organization in Complex Networks," *Phys. Rev. E*, vol. 67, 026112, 2003.

[169] E. Ravasz, A.L. Somera, D.A. Mongru, Z.N. Oltvai, and A.-L. Barabási, "Hierarchical Organization of Modularity in Metabolic Networks," *Science*, vol. 297, pp. 1551-1555, 2002.

[170] C.W. Reynolds, "Flocks, Herds, and Schools: A Distributed Behavioral Model," in *Proc. ACM SIGGRAPH Computer Graphics*, vol. 21, pp. 25-34, 1987.

[171] M. Ripeanu, A. Iamnitchi, and I. Foster, "Mapping the Gnutella Network," *IEEE Internet Computing*, vol. 6, pp. 50-57, 2002.

[172] R.T. Rockafellar, *Convex Analysis*, Princeton University Press, 1970.

[173] O.E. Rössler, "An Equation for Continuous Chaos," *Phys. Lett. A*, vol. 57, pp. 397-398, 1976.

[174] http://www.cs.washington.edu/research/networking/rocketfuel/

[175] A.N. Samukhin, S.N. Dorogovtsev, and J.F.F. Mendes, "Laplacian Spectra of Complex Networks and Random Walks on Them: Are Scale-Free Architectures Really Important?," *Phys. Rev. E*, vol. 77, 036115, 2008.

[176] K. Schmüdgen, "The K-Moment Problem for Compact Semialgebraic Sets," *Math. Ann.*, vol. 289, pp. 203-206, 1991.

[177] F. Schweitzer and J.A. Holyst, "Modelling Collective Opinion Formation by Means of Active Brownian Particles," *The European Physical Journal B*, vol. 15, pp. 723-732, 2000.

[178] B. Schwikowski, P. Uetz, and S. Fields, "A Network of Protein-Protein Interactions in Yeast," *Nature Biotechnology*, vol. 18, pp. 1257 - 1261, 2000.

[179] A.J. Seary and W.D. Richards, "Partitioning Networks by Eigenvectors," in *Proc. of the Int. Conf. on Social Networks*, vol. 1, pp. 47-58, 1996.

[180] S. Shakkottai and R. Srikant, "Network Optimization and Control," *Foundations and Trends in Networking*, vol. 2, pp. 271-379, 2007.

[181] J.A. Shohat and J.D. Tamarkin, *The Problem of Moments*, Math. Surveys no. 1, Amer. Math. Soc., 1943.

[182] J.-J.E. Slotine and W. Wang, "A Study of Synchronization and Group Cooperation Using Partial Contraction Theory," *Lecture Notes in Control and Information Science*, vol. 309, Springer-Verlag, 2004.

[183] D.J. de Solla Price, "Networks of Scientific Papers," *Science*, vol. 149, pp. 510-515, 1965.

[184] J.C. Sommerer and E. Ott, "A Physical System With Qualitatively Uncertain Dynamics," *Nature*, vol. 365, pp.138, 1993.

[185] E. Sontag, *Mathematical Control Theory: Deterministic Finite Dimensional Systems*, Springer-Verlag, 1998.

[186] R. Speicher, "Free Probability Theory and Non-Crossing Partitions," *Séminaire Lotharingien de Combinatoire*, B39c, 1997.

[187] N. Spring, R. Mahajan, D. Wetherall, and T. Anderson, "Measuring ISP Topologies With Rocketfuel," *IEEE/ACM Transactions on Networking*, vol. 12, pp. 2-16, 2004.

[188] R. P. Stanley, *Enumerative Combinatorics*, Vol. 1 and 2, Cambridge University Press, 1999.

[189] S.H. Strogatz, "Exploring Complex Networks," *Nature*, vol. 410, pp. 268-276, 2001.

[190] S.H. Strogatz, *Sync: The Emerging Science of Spontaneous Order*, Hyperion, 2003.

[191] A. Tahbaz-Salehi and A. Jadbabaie, "A Necessary and Sufficient Condition for Consensus Over Random Networks," *IEEE Transactions on Automatic Control*, vol. 53, pp. 791-795, 2008.

[192] H. Tangmunarunkit, R. Govindan, S. Jamin, S. Shenker, and W. Willinger, "Network Topology Generators: Degree-Based vs. Structural," in *SIGCOMM*, vol. 32, pp. 147-159, 2002.

[193] A.H.Y. Tong, G. Lesage, G.D. Bader, H. Ding, H. Xu, and X. Xin, "Global Mapping of the Yeast Genetic Interaction Network," *Science*, vol. 303, pp. 808-813, 2004.

[194] J. Tsitsiklis, D. Bertsekas, and M. Athans, "Distributed Asynchronous Deterministic and Stochastic Gradient Optimization Algorithms," *IEEE Trans. Autom. Control*, vol. 31, pp. 803-812, 1986.

[195] J. Tsitsiklis and M. Athans, "Convergence and Asymptotic Agreement in Distributed Decision Problems," *IEEE Trans. Autom. Control*, vol. 29, pp. 42-50, 1984.

[196] F. Varela, J.P. Lachaux, E. Rodriguez, J. Martinerie, "The Brainweb: Phase Synchronization and Large-Scale Integration," *Nature Reviews Neuroscience*, vol. 2, 229-239, 2001.

[197] V. Vazirani. *Approximation Algorithms.* Springer-Verlag, 2001.

[198] V. Vu, "Spectral Norm of Random Matrices," in *Proc. of STOC*, pp. 423-430, 2005.

[199] X. Wang, X. Liu, and D. Loguinov, "Modeling the Evolution of Degree Correlation in Scale-Free Topology Generators," IEEE INFOCOM 2008, pp. 1094-1102, 2008.

[200] Y. Wang, D. Chakrabarti, C. Wang, and C. Faloutsos, "Epidemic Spreading in Real Networks: An Eigenvalue Viewpoint," in *Proc. Int. Symp. on Reliable Distributed Systems*, pp. 25-34, 2003.

[201] D.J. Watts and S. Strogatz, "Collective Dynamics of Small World Networks," *Nature,* vol 393, pp. 440-42, 1998.

[202] D.B. West, *Introduction to Graph Theory*, 2^{nd} Edition, Prentice Hall, 2001.

[203] E.P. Wigner, "On the Distribution of the Roots of Certain Symmetric Matrices," *The Annals of Mathematics*, vol. 67, pp. 325-327, 1958.

[204] E.P. Wigner, "Characteristic Vectors of Bordered Matrices With Infinite Dimensions," *The Annals of Mathematics*, vol. 62, pp. 548-564, 1955.

[205] H.S. Wilf, "The Eigenvalues of a Graph and Its Chromatic Number," *J. London Math. Soc.*, vol. 42, pp. 330-332, 1967.

[206] R.J. Wilson, *Introduction to Graph Theory*, Wiley, 1986.

[207] C.W. Wu, "Synchronization in Arrays of Coupled Nonlinear Systems: Passivity, Circle Criterion, and Observer Design," *IEEE Trans. Circ. Syst. I*, vol. 48, pp. 1257-1261, 2001.